KU Leuven
Biomedical Sciences Group
Faculty of Medicine
Department of Cellular and Molecular Medicine



THE ROLE OF TRP CHANNELS IN THE DEFENSE AGAINST BACTERIAL URINARY TRACT INFECIONS

Noémie LUYTS

Jury:
Supervisor: Prof. Wouter Everaerts
Co-supervisor: Prof. Thomas Voets
Chair examining committee: Prof. Kathleen Freson
Chair public defense: Prof. Jan Eggermont
Jury members: Prof. Guy Bogaert
Prof. Katrien Lagrou
Prof. Karel Everaert
Prof. John Heesakkers

Dissertation presented in partial fulfilment of the requirements for the degree of Doctor in Biomedical sciences

June, 2022

ACKNOWLEDGEMENTS

Dit is waarschijnlijk het enige hoofdstuk dat jij gaat lezen en dus het belangrijkste van mijn thesis. THE PRESSURE IS ON! Ik wil starten met jou te bedanken. Voor je aanwezigheid vanavond maar ook op andere momenten tijdens mijn PhD traject. Het was niet altijd even gemakkelijk maar met jou als deel van mijn achterban ben ik er geraakt. Ik ben blij dat jij in mijn team zit!

Ik wil graag mijn chair prof. Eggermont bedanken om deze avond in goede banen te leiden. Verder oprechte dank aan mijn interne juryleden prof. Bogaert en prof. Lagrou voor jullie opvolging en waardevolle commentaar doorheen de jaren. Het was fijn om mijn werk met jullie te kunnen delen en samen tot dit eindresultaat te komen. Bedankt ook aan mijn externe juryleden prof. Heesakkers en prof. Everaert om de tijd te nemen om mijn werk kritisch na te lezen en mij vandaag op de rooster te leggen.

Het avontuur is gestart dankzij Wouter. Tijdens het co-assistenschap heb je mijn interesse in onderzoek aangewakkerd en je enthousiasme bij de rondleiding in het LICR-labo werkte aanstekelijk. Toen ik thuis vertelde dat ik een doctoraat zou gaan doen, werd verbaasd gereageerd, een wetenschapper paste niet echt bij mijn fluo-gele karakter. Bedankt Wouter om mij een kans te gunnen om hierin te groeien. Je gaf me de vrijheid om een nieuw project op te starten en leerde me kritisch nadenken. Onze meetings waren altijd interessant, vaak op wetenschappelijk vlak, maar ik kon ook bij jou terecht om persoonlijk even te ventileren of om vakantietips voor Kroatië uit te wisselen. Je leerde mij veel op vlak van fundamenteel onderzoek, klinische studies en gaf me een blik achter de schermen in de urologie. Ik vond het fijn om deel uit te mogen maken van jouw team en neem al je tips en tricks mee!

Het avontuur is mede door Thomas tot een goed einde gebracht. De quote “mijn deur staat altijd open” heb je waar gemaakt. In het begin vond ik het wat intimiderend om bij het hoofd van het labo aan te kloppen. Zodra ik door had dat je eigenlijk graag gestoord wordt met wetenschappelijke vragen of om nog eens wat cellen te patchen, vond ik vaker de weg naar jou. Je hebt een ongelofelijk talent om over elk onderwerp de juiste vragen te stellen en meteen tot de essentie te komen. Bovendien ben je

enorm begaan met hoe iedereen zich voelt in het team. Je bent een uitzonderlijke PI op alle vlakken en ik wil je dan ook bedanken voor je input.

Vervolgens wil ik heel LICR bedanken. Jullie waren een hele fijne bende frollega's. Met aan het hoofd naast Thomas en Wouter ook Rudi, Joris en Karel. Bij jullie vond ik nog meer deuren die steeds open stonden voor een fijne babbel, over fietsen of pipi. Gracias!
Bedankt aan de vaste waarden die de hele LICR-boel rechthouden Annelies, Melissa, Silvia, Evy, Nele, Sara, Andi, Séraphina en ook Raf, Luc, Vivianne en Inge. Jullie aandeel in het labo is niet te onderschatten, elke visiting professor die ik heb rondgeleid was terecht onder de indruk van het fantastische team waarop we als PhD studenten kunnen rekenen. Bedankt allemaal voor alle praktische hulp, leuke babbels en lunch-runs en toffe momenten. Nog een speciale dikke dikke merci aan Annelies, om mee mijn project op te starten en mij zelfs in je gezin op te nemen. Zonder jouw vleugels was het niet hetzelfde geweest.
Bedankt aan alle toffe collega's Ana, Frone, Evelien, Lena, Alina, Pieter, Lotte, Jan, Martina, Alex, Davide, Angelique, Andy, Jean-Paul, Bahar, Hanne, Justyna en Aryane die op deze moment de LICR gang een leuke werkplek maken en ook alle oldies van LICR die een plekje in mijn hart hebben veroverd de afgelopen jaren zoals Laura, Lucia, Kathi, Koenraad en Brett (you back girl!) en uiteraard ook Yero met je super goed advies, zelfs vanuit Hasselt.

Special vermelding voor team culi-club, wetenschappers met een hart voor eten en soms een speciale dessert-maag. Bedankt voor de gezellige avonden en liters koffie. Merci Dorien voor al je sportief geweld en luisterend oor. Merci Caroline (x2) voor jullie gegibber dat een saaie dag beter maakt. Merci Marie voor je enthousiasme over wetenschap maar eigenlijk alles in het leven. Merci Leon om onze bureau gezellig te maken en mij overal bij te helpen. Merci Robbe om wie je bent, zo grappig en attent komt ge ze niet vaak tegen. Merci Charlotte om met uw gekke dansmoves en zotte verhalen, het was echt een zwart gat toen je vertrok uit het labo. Merci Katrien, een beetje mijn lab-mom en vat vol goed advies en knuffels op de juiste momenten. Matthias, bedankt voor je eeuwige 'alles komt goed' vibe, praktische hulp en advies. Liefste Laura, het labo is een zonnigere plek met u erbij. Meerdere keren per dag komt er een 'whajooo' gevolgd door een zot verhaal en krijg je iedereen aan het lachen. En

uiteraard wil ik Helene bedanken, omdat we dit avontuur samen gestart zijn, hebben we een vergelijkbaar traject gevolgd. Bij jou kon ik altijd terecht, voor ups en downs, om door het administratieve bos de bomen te zien en als congres roomie. Ik ben blij dat onze wegen nog even verder parallel blijven lopen!
Met jullie was het labo leven minder zeste en meer frieten.

Een ander team dat ik wil bedanken zijn mijn urologie PhD collega's. Uros, Thomas en Lisa, bedankt om mij de weg naar ON1 en het padelveld te tonen. Loic, Bram, Eduard, Laura, Andries merci om meermaals een week te breken, dit was bevorderlijk voor de mentale gezondheid.

Ook buiten Gasthuisberg kon ik rekenen op fantastische steun. Merci Joris om tijdens het grootste deel van dit avontuur mijn rots te zijn, we waren een topteam. Thanks Fredje ik weet dat jij op eender welk moment alles voor mij zou laten vallen. You're the best. Sofke, dikke merci om mijn gedachten altijd te weten verzetten met een nieuw sportief avontuur. Grand merci Jess & Maarten voor de gezellige buurtwerking. Thanks, Joren, Hannah, Astrid, Karel, Maarten & Yannic, voor jullie interesse en onze haardvuur avonturen. Merci aan alle veppers (Fredje, Christine, Aless, Lorrie, Carole, Nynke, Evie, Ellen, Nathan, Jojo, Oli, Anke, Melina, PJ, Thomas, Géza, Charlotte, Bas, Anthony, Laurens, Gaetan) die ook 10 jaar na afstuderen nog steeds een hechte groep vormen. Het was zo cool om te zien hoeveel moeite iedereen heeft gedaan om erbij te kunnen zijn vanavond, da's echte vriendschap. Ook mijn Sigi, Lars, Eliseke, Hanne, Goke, Liese, Lau, Mari, bedankt om jullie drukke agenda's gewoon te blokkeren om vanavond te kunnen klinken. Work hard, brunch harder en ik kijk al uit naar ons volgende (Italië) reisje.

Speciaal extra hard bedankt aan Laudine, Charlotte, Laurien, Lotteke en Eva om de laatste maanden mee op mijn rollercoaster te zitten. Jullie zorgden voor de perfecte afwisseling tussen girls nights, impulsieve trips en goed gevulde weekends. De perfecte achterban. Merci Charlie om mijn partner te zijn bij al mijn creatieve projecten (ja ook deze mooie cover), binnen Baroudeur en ook een beetje in het leven.

En last but not least mijn familie. Bedankt harde kern Magalie, Rens, Hannes, Tante Miriam en Luc om voor mij te supporteren bij elke stap van mijn traject. Nana en opa,

mijn favoriete plek op deze wereld is bij jullie in de bovenste schuif. Bedankt voor jullie steun, gevulde diepvries en levenslessen. En tot slot mams en not-the-mama, jullie hebben mij altijd de warmte en ruimte gegeven om elke uitdaging te durven aangaan. Bedankt voor jullie onvoorwaardelijke liefde en steun. Ik zou jullie elke keer opnieuw kiezen, us three & wij boom.

TABLE OF CONTENTS

I. INTRODUCTION 16

1. URINARY TRACT INFECTIONS 17
   1.1. Definitions of urinary tract infections and anatomy of the urinary tract 17
   1.2. Socio-economic impact and epidemiology of recurrent infections 19
   1.3. Treatment options for UTIs 20
2. THE HOST – URINARY TRACT & UROTHELIUM 21
   2.1. The urothelium, a unique epithelial barrier 22
   2.2. The sensor-transductor role of the urothelial cells 23
   2.3. Interaction with pathogens, host defenses at work 23
3. THE PATHOGEN - UROPATHOGENIC *ESCHERICHIA COLI* 26
   3.1. UPEC virulence factors 26
   3.2. The invasion and colonization of the urinary tract by UPEC 29
4. TRP CHANNELS AND CALCIUM SIGNALING 31
   4.1. Calcium signaling 31
   4.2. Introduction to TRP channels 32
   4.3. TRP channels in the urinary tract 32
   4.4. TRP related diseases of the LUT 34

II. OBJECTIVES 38

1. TO ESTABLISH A LONGITUDINAL MODEL TO FOLLOW-UP BACTERIAL LOAD IN MICE WITH UTIS. 38
2. TO CHARACTERIZE *IN VITRO* RESPONSES OF UROTHELIAL CELLS TO A BACTERIAL SUSPENSION. 38
3. TO STUDY TRP CHANNELS AS A POTENTIAL TARGET OF PHENAZOPYRIDINE 38

III. MATERIALS AND METHODS 42

1. CELL CULTURE 42
2. CALCIUM IMAGING 43
3. PATCH CLAMP 44
4. BACTERIAL CULTURE 44
5. EXPERIMENTAL MURINE UTI MODEL 45
6. BIOLUMINESCENCE IMAGING 45
7. STATISTICS 46

IV. RESULTS 48

1. LONGITUDINAL FOLLOW-UP OF URINARY TRACT INFECTIONS AND THEIR TREATMENT IN MICE USING BIOLUMINESCENCE IMAGING 50
2. UROTHELIAL CELLS RESPOND TO A VIABLE BACTERIAL SOLUTION WITH RELEASE OF CALCIUM FROM THE INTRACELLULAR STORES IN AN PLC-DEPENDENT MANNER 70
3. INHIBITION OF TRPM8 BY THE URINARY TRACT ANALGESIC DRUG PHENAZOPYRIDINE 88

V. GENERAL DISCUSSION 107

VI. CONCLUSION AND FUTURE STEPS 116

1. LONGITUDINAL FOLLOW-UP OF URINARY TRACT INFECTIONS AND THEIR TREATMENT IN MICE USING BIOLUMINESCENCE IMAGING 116
2. UROTHELIAL CELLS RESPOND TO A VIABLE BACTERIAL SOLUTION WITH RELEASE OF CALCIUM FROM THE INTRACELLULAR STORES IN AN PLC-DEPENDENT MANNER 116
3. INHIBITION OF TRPM8 BY THE URINARY TRACT ANALGESIC DRUG PHENAZOPYRIDINE 117

VII. ABSTRACT 121

VIII. DUTCH SUMMARY 125

IX. ACADEMIC CV 127

X. KEY TERMS 133

XI. SCIENTIFIC ACKNOWLEDGEMENTS & PERSONAL CONTRIBUTIONS 136

XII. CONFLICT OF INTEREST STATEMENT 137

XIII. REFERENCES 140

LIST OF ABBREVIATIONS

ACh	Acetylcholine
AITC	Allyl isothiocyanate
AMG	AMG517
AMP	Antimicrobial peptides
AMTB	*N*-(3-Aminopropyl)-2-[(3-methylphenyl)methoxy]-*N*-(2-thienylmethyl)benzamide hydrochloride
ASIC	Acid-sensing ion channels
ATP	Adenosine triphosphate
ATP	Adenosinetriphosphate
AUC	Area under the curve
BG	Background
BLI	Bioluminescence imaging
BPS	Bladder pain syndrome
C3H/HeJ	Murine genetic background
C57Bl/6	Murine genetic background
CAPS	Capsaicin
CCD	Charge-coupled device
CFU	Colony forming units
CGRP	Calcitonin gene-related peptide
CHO	Chinese hamster ovary cells
CI	Confidence interval
CNF-1	Cytotoxic necrotizing factor 1
DAG	Diacylglycerol
DAMP	Damage-associated molecular pattern
DC	Direct current
DRG	Dorsal root ganglion
E. coli	Escherichia coli
ENaC	Epithelial sodium channel
FOV	Field of view
Fura-2 AM	Fura-2 acetoxymethyl ester
GAG	Glycosaminoglycan

G-CSF	Granulocyte colony-stimulating factor
GFP	Green fluorescent protein
GSK	GSK1016790A
HC	HC-0674047
HEK293	Human embryonic kidney cells
HylA	α-Hemolysin
IBC	Intracellular bacterial community
IC_{50}	Half maximal inhibitory concentration
ICI	Intercontractile interval
IL	Interleukin
IP_3	Inositol triphosphate
ISO	Isosakuranetin
JoVE	Journal of Visualized experiments
Km	Kanamycin sulfate
KO	Knock out
LB	Luria-Bretani
LPS	Lipopolysaccharide
LUT	Lower urinary tract
MEM	Minimal essential medium
NF-kB	Nuclear factor kappa-light-chain enhancer of activated B cells
OAB	Overactive bladder
OD	Optical density
OMV	Outer membrane vesicle
P2X	Purinergic 2X receptor
P2Y	Purinergic 2Y receptor
PAMP	Pathogen-associated molecular pattern
PAR	Protease-activated receptor
PBS	Phosphate buffered saline
PIP_2	Phosphatidylinositol 4,5-bisphosphate
PLC	Phospholipase C
PMB	Polymyxin B
PS	Pregnenolone sulphate
QIR	Quiescent intracellular reservoir

ROI	Region of interest
ROS	Reactive oxygen species
RR	Relative risk
RR	Ruthenium red
rUTI	Recurrent UTI
SD	Standard deviation
SEM	Standard error of the mean
Thapsi	Thapsigargin
TLR	Toll-like receptor
TRP	Transient receptor potential
TRPA	Transient receptor potential ankyrin
TRPC	Transient receptor potential canonical
TRPM	Transient receptor potential melastatin
TRPMl	Transient receptor potential mucolipin
TRPP	Transient receptor potential polycystin
TRPV	Transient receptor potential vanilloid
UC	Urothelial cell
UP	Uroplakin
UPEC	Uropathogenic *Escherichia coli*
UTI	Urinary tract infection
VBNC	Viable but non culturable state

INTRODUCTION

I. Introduction

Bacterial infections of the urinary tract are amongst the most common infections in humans. They cause significant morbidity and impose a high burden on our healthcare system. Although patients can be treated with antibiotics, up to 25% of them will develop recurrent infections. Moreover, the bacteria causing urinary tract infections (UTIs) have become increasingly resistant to antibiotics over the last decades, making them more difficult to eradicate[1]. Other treatment modalities, such as vaccinations and behavioral therapies are being explored[2]. Importantly, a recent randomized trial demonstrated a reduction in number of UTIs in women who increased their fluid intake[3]. The relationship between the bladder function (how urine is stored and expelled) and the susceptibility to UTIs, however, is poorly understood.

In this context, a group of ion channels, called Transient Receptor Potential (TRP) channels, is of particular interest. These ion channels have the ability to respond to a variety of physical and chemical stimuli enabling them to detect changes in the environment of the cell[4]. Several members of the TRP channels family are expressed in sensory nerve fibers innervating the bladder and on the urothelial cells, where they play an essential role in sensing the bladder's content. These channels participate in the (patho)physiology of the lower urinary tract (LUT) and pharmacologic or genetic manipulation of TRP channels has been shown to alter bladder function[5].

TRP channels could therefore offer a novel therapeutic approach in patients with recurrent UTIs by improving bladder function. Moreover, a better understanding of the mechanisms of primary afferent sensitization during urinary tract infection may provide novel insights into the pathogenesis of bladder disorders such as overactive bladder (OAB) and bladder pain syndrome (BPS). However, the role of TRP channels in UTI susceptibility and hyperalgesia remains to be shown.

1. Urinary tract infections

1.1. Definitions of urinary tract infections and anatomy of the urinary tract

The urinary tract comprises the lower urinary tract with the urethra and bladder, and the upper urinary tract consisting of the ureters and kidneys (figure 1). Urinary tract infections occur when pathogens ascend through the urethra into the bladder, where they can adhere to and invade the urothelial cells. The invasion of the urinary tract gives rise to inflammation of the bladder wall. The host-pathogen interactions will alter the bladder function resulting in the classic UTI symptoms, such as frequency and urgency.

The diagnosis of a urinary tract infection is based on a combination of urinary symptoms and a urine culture, demonstrating the presence of bacteria in the urine above a certain threshold, usually 10^5 colony forming units (CFUs) /mL to distinguish between bacteriuria and contamination. However, for *Escherichia coli* this threshold has been shown to be as low as 10-10^2 CFU /mL[6,7]. If a patient presents with typical symptoms of an uncomplicated UTI (see below), a urine dipstick will suffice to confirm the diagnosis, as it has a high positive predictive value, and to start empirical antibiotics. In all other cases, a urine culture should be performed. However, there is a discrepancy as approximately 20% of women presenting with urinary symptoms have negative urine cultures[1]. In contrast, bacteria are found in the urine of asymptomatic individuals, which can indicate contamination of the urine sample or true asymptomatic bacteriuria. Only patients undergoing urological procedures breaching the mucosa and pregnant women require treatment for asymptomatic bacteriuria.

Figure 1. Anatomy of the urinary tract and classification of UTIs

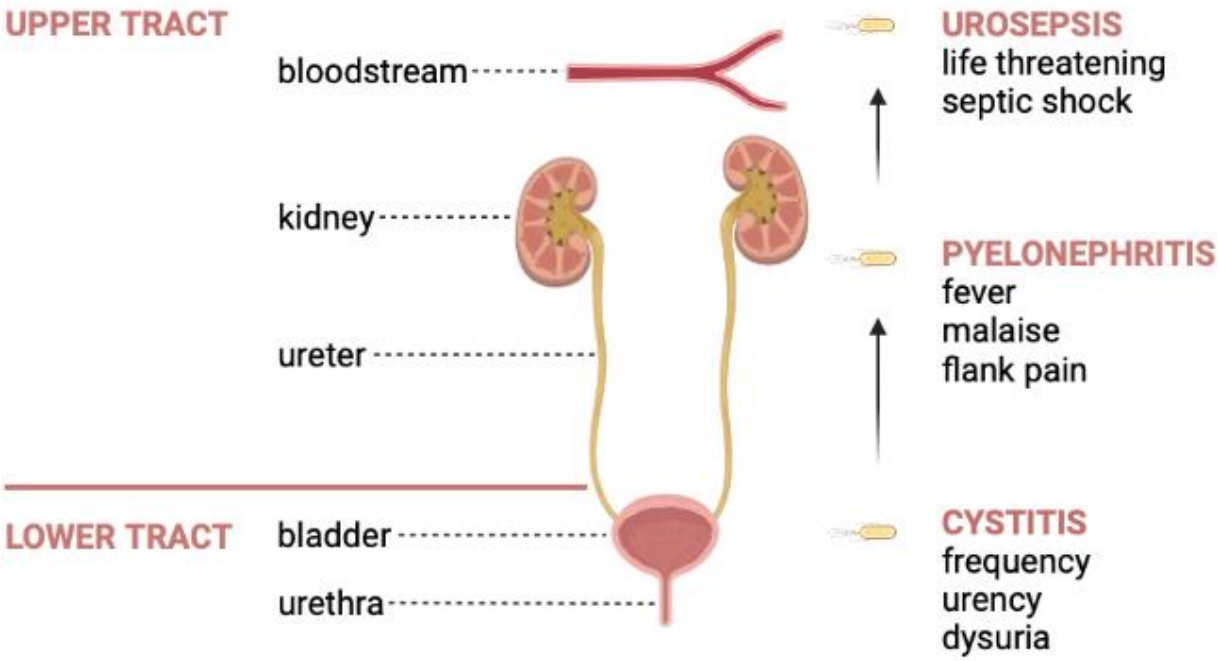

There are different types of classifications for UTIs. First, they can be classified based on the severity of the infection. This can range from asymptomatic bacteriuria to cystitis, pyelonephritis and even life threatening urosepsis. During a cystitis, patients often report a burning sensation (dysuria), frequency, and urgency. If the infection rises to the upper tract, patients will present with fever, general malaise, and flank pain. A urosepsis occurs when bacteria enter the bloodstream, this is a life-threatening situation that requires rapid treatment to prevent septic shock (figure 1)[8-11].

A second classification divides UTIs in uncomplicated or complicated cases. An uncomplicated UTI occurs in a host without anatomical or functional abnormalities or indwelling catheters. All other UTIs, thus in patients with abnormalities or catheters and in pregnant women, are considered as complicated[11]. These patients have an increased chance of a complicated course. Additionally, as the prostate is often involved, all UTIs in men are classified as complicated. Prostatitis ranges from a straightforward clinical entity in its acute form to a complex, debilitating condition when chronic[12].

The most common organism causing community acquired UTIs are uropathogenic *Escherichia coli* (UPEC), accounting for approximately 80% of these infections[1]. Other uropathogens include *Staphylococcus saprophyticus,* enterococci and other

enterobacterales such as *Klebsiella pneumoniae* and *Proteus mirabilis*, which are together responsible for the remaining 20% of the uncomplicated UTI cases[13]. In patients with indwelling catheters or hospitalized patients[1], the contribution of other pathogens such as *Pseudomonas aeruginosa* and staphylococci is higher compared to their contribution in community acquired infections.

1.2. Socio-economic impact and epidemiology of recurrent infections

Urinary tract infections pose a serious burden to health care systems, with societal costs of tens of billion US $ worldwide, as it is estimated that about 150 million people develop a UTI each year[1,9]. These costs comprise outpatient doctor visits, loss of productivity, hospitalizations, and medical expenses like the use of antibiotics.

Interestingly, the rate at which bacterial strains, such as *E. coli*, are becoming resistant to the vast majority of antibiotics is increasing worldwide[13-15]. Enterobacteriaceae, the family of Gram-negative bacteria to which E. coli are part of, harbor gene conferring resistance, and plasmids harboring these resistance determinants can be transferred between bacteria[14]. Antibiotic exposure is the most important risk factor for the selection of antimicrobial resistance[16,17]. Furthermore, antimicrobial resistance is more common in complicated UTIs[15]. This might be caused by frequent antibiotic exposure and hospitalization, foreign bodies and the atypical organisms that can harbor multidrug resistance genes causing the UTIs[17,18].

Increased resistance to antibiotics has resulted in an increase in the number of recurrent and chronic infections[9]. Approximately 25% of adult women with a UTI will experience a recurrence within 3 months, despite a correct treatment. When two or more infections occur within six months, or three or more infections occur within 12 months, the term recurrent UTI (rUTI) is used[11]. Chronic infections are defined by the detectable persistence of pathogens, whereas for recurrent infections the patients will relapse. Relapses are typically caused by the same bacterial species, as these bacteria can reside in the bladder epithelium and re-emerge periodically[19]. Alternatively, uropathogens can reside in the gut or periurethral region, resulting in recurrent infections once ascending into the LUT[10]. A third reservoir for UPEC was shown by Brannon et al. as they demonstrated that *E. coli* can invade and reside in vaginal epithelial cells[20]. The reason why some people suffer from these recurrences

whereas others do not, remains elusive. In patients with rUTIs, recurrent and sometimes long-term antimicrobial regimens are used. The excessive and often inappropriate use of antibiotics drives the evolution of multidrug-resistant microorganisms globally and complicates the treatment of UTIs in general[10]. Therefore, alternative treatment options (see below) and behavioral changes are being explored and recommended by both the European Association of Urology and the American Urological Association [11,21].

1.3. Treatment options for UTIs

Antibiotics are the mainstay of the treatment for UTIs. The choice of a particular antimicrobial treatment depends on the presumed or proven pathogen, local resistance patterns, patient's allergy history, availability etc[10,11,16]. For lower UTI the percentage of resistance against a certain antibiotic must be below 20%, for upper tract UTI this must be below 10%. In Europe, the oral treatment with fosfomycin (3 g single dose), nitrofurantoin (100 mg twice daily for five days) or pivmecillinam (400 mg three times a day for three to five days) should be considered as a first-line treatment for uncomplicated cystitis[11,13,22-24]. Based on the available resistance data in Belgium, aminopenicillins and trimethoprim-sulfamethoxazole are no longer recommended for complicated UTIs of the LUT or UTI of the upper tract. And due to the long term adverse reactions, stringent regulatory conditions have been implemented in 2019 regarding the long term use of fluoroquinolones[11,25]. Antibiotics will continue to be the cornerstone in the treatment of UTIs. However, growing resistance and side effects, such as the impact on the intestinal microbiota, fuel the search for alternative treatment options especially for patients with recurrent UTIs.

First, **behavioral changes** are being advocated to patients with recurrent UTIs to minimize the number of infections. Physicians have long been advising their patients to **increase water-intake** to prevent UTIs. Recently, a randomized controlled trial was performed that supports this dogma. Hooton et al. assigned 163 women with a low fluid intake (< 1.5L /day) to a water or control group. Women in the water group were advised to drink 1.5L in addition to their normal intake. Increased fluid intake in these women significantly improved the primary outcome of number of cystitis episodes during 12 months (1.7 vs 3.2 episodes respectively, $p < .001$)[3]. The effect of other

behavioral changes, such as **post-coital urination and personal hygiene** measures, remains elusive[11,26].

The search for **alternative pharmacological strategies** has focused on the development of vaccines or inhibition of adhesion, due to the increased understanding of the bacterial components responsible for the pathogenicity of UPEC[2]. One of the most promising and studied agents is the **vaccine OM-89** (Uro-Vacom®) which is a bacterial extract prepared from 18 strains of *E. coli* and based on the current knowledge about the O-antigen. In a meta-analysis, the oral vaccine OM-89 reduced the mean number of UTIs by half (RR 0.61, 95% CI 0.48-0.78) compared to placebo[27]. The inhibition of adhesion, by inhibiting the type 1 pilus adhesin FimH, remains one of the other main strategies[9]. To this end, **D-mannose** can be used as it has the capability to saturate FimH adhesin by occupying a binding pocket. In a small clinical study, D-mannose was found to be as effective as nitrofurantoin in preventing UTIs without any significant side effects[28]. The use of **cranberry** supplements to prevent recurrent UTI remains controversial. Proanthocyanidins and fructose in cranberries prevent *E. coli* from adhering to the urothelial cells by inhibiting P-fimbrial adhesion and type 1 adhesion, respectively[29]. However, a meta-analysis including 4.473 participants was unable to show a significant reduction in UTI episodes[29]. Similarly, the use of **oral estrogens, probiotics or vitamin D** lacks convincing proof of clinical efficacy[9,27,30]. In contrast to oral estrogens, **vaginal application of estrogens** has been shown to significantly reduce rUTIs in a meta-analysis including 1936 patients (relative risk, 0.42; 95% CI, 0.30-0.59)[31].

Thus, despite the emergence of many non-antimicrobial measures, only a few are supported by well-designed studies[27]. Therefore, it remains important to further characterize the interaction between the urothelium and the pathogens.

2. The host – urinary tract & urothelium

The bladder consists of three principal tissue layers, namely the mucosa (urothelium), the suburothelial connective tissue and the smooth muscle (detrusor). As these layers and their individual cells are in close proximity, these tissues are able to communicate[19].

2.1. The urothelium, a unique epithelial barrier

The urothelium is a complex, stratified epithelium that lines the luminal side of the urinary tract from the urethra to the renal pelvis[32,33]. It is a very dynamic structure with multiple functions. First, it forms an impermeable barrier to water, urine solutes and pathogens. This barrier remains intact despite accommodating to large changes in volume inherent to the filling and emptying of the bladder[34]. Second, urothelial cells can contribute to mechanosensation and chemosensation[35]. They can transmit information about the bladder's content to the underlying nervous, connective, and muscular tissues[5,33].

Figure 2. The bladder epithelium (adapted from[34])

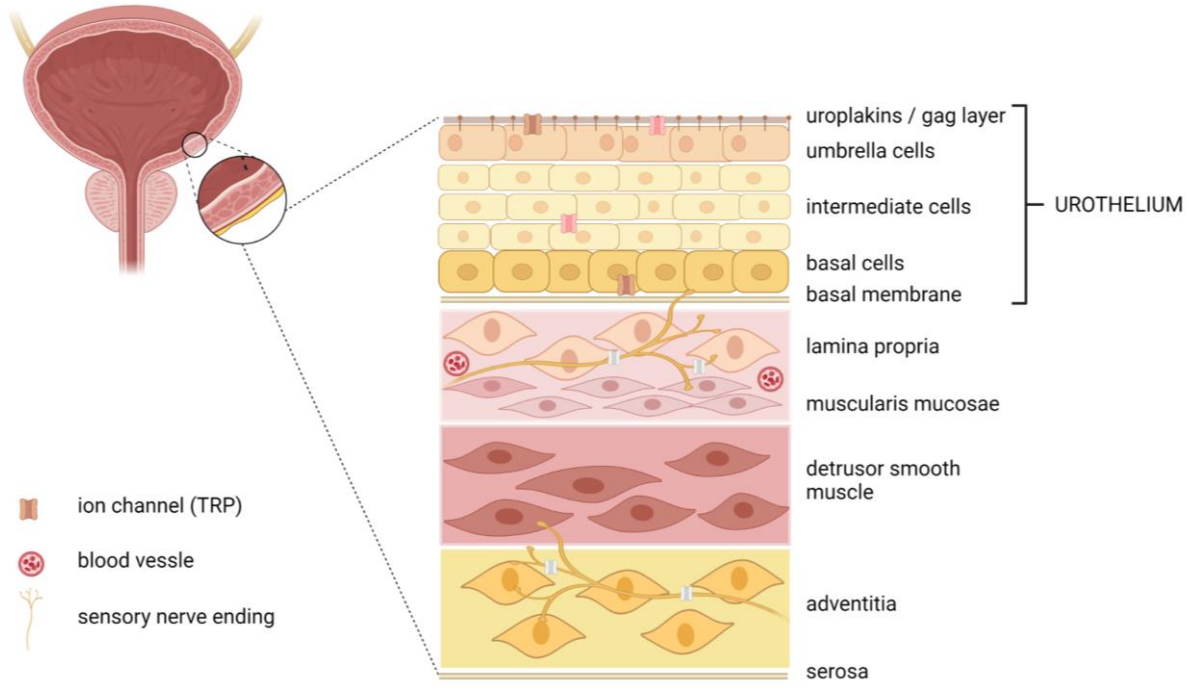

The urothelium contains a basal membrane and three layers of urothelial cells (a basal, intermediate and superficial layer)[33]. The superficial layer is composed of terminally differentiated, large hexagonal cells, termed umbrella cells. These umbrella cells play a prominent role in secreting antimicrobial substances, withstanding the forces of the urine flow and maintaining the tight barrier[36]. This impermeable barrier remains intact during bladder filling due to flattening of the umbrella cells, unfolding of the mucosal surface folds as well as exocytosis of fusiform vesicles with the apical membrane to

increase the mucosal surface area[32]. Importantly, the exocytosis and endocytosis of fusiform vesicles can be exploited by pathogens to invade the umbrella cells[37].

Umbrella cells have a highly specialized apical surface. The luminal side of the urothelial cells is covered with a glycosaminoglycan (GAG) layer, a mucus-like layer that prevents penetration of toxins and pathogens to the underlying epithelial cells. The natural constituents of the urothelial GAG layer include hyaluronic acid, heparan sulfate, heparin keratan sulfate, chondroitin sulfate and dermatane sulfate[38]. The GAG layer thus inhibits adherence of bacteria to the urothelial membrane[32]. In addition, the umbrella cells express uroplakins (UPs), mannosylated, transmembrane proteins on the apical surface, forming dense plaques with a lipid composition[37,39]. Together with the GAG layer, these UP contribute to the high-resistance barrier of umbrella cells and thus protect the underlying tissues from noxious components in the urine[37]. Besides their protective role, UP also play a role in UPEC pathogenesis by serving as a site for adhesion.

2.2. The sensor-transductor role of the urothelial cells

Urothelial cells express a wide variety of ion channels and receptors, including acid-sensing ion channels (ASIC), epithelial sodium channel (ENaC) and TRP channels and purinergic (P2Y and P2X), muscarinic, nicotinic, α and βadrenergic, cannabinoid, toll-like (TLR) and protease-activated (PAR) receptors[34,40,41]. This wide variety of receptors and channels enables the urothelium to respond to a myriad of stimuli including stretch, changes in pH, cytokines and neuroactive compounds[34]. In response to these stimuli, urothelial cells release molecules like adenosine triphosphate (ATP), acetylcholine (Ach), nitric oxide (NO), prostaglandins and nerve growth factor, enabling them to communicate with neighboring urothelial cells and/or underlying structures, like sensory nerve endings that lie in close proximity. Under pathological conditions, the urothelium can contribute to the development of hypersensitivity and -activity disorders[42].

2.3. Interaction with pathogens, host defenses at work

The highly specialized urothelium enables the bladder to respond to invading bacteria. As the first layer that interacts with the pathogens, the urothelium plays an important

role in the innate immune response. The resistance of the LUT to infections is mainly ascribed to the versatility of the innate immune defenses rather than adaptive immune responses, particularly if only the lower urinary tract is infected[19]. These immune responses need to be balanced to maintain the structural integrity of the barrier[19]. Severe acute inflammatory responses early in the infection predispose to chronic and recurrent infections in mice[43].

The interaction between the urothelium and the UPEC will result in the activation of many defense strategies that are summarized in figure 3. Not surprisingly, deviations in components of the host immune system can impact susceptibility to, or outcome of, infection[44].

Figure 3. Host responses to UPEC (adapted from[19])

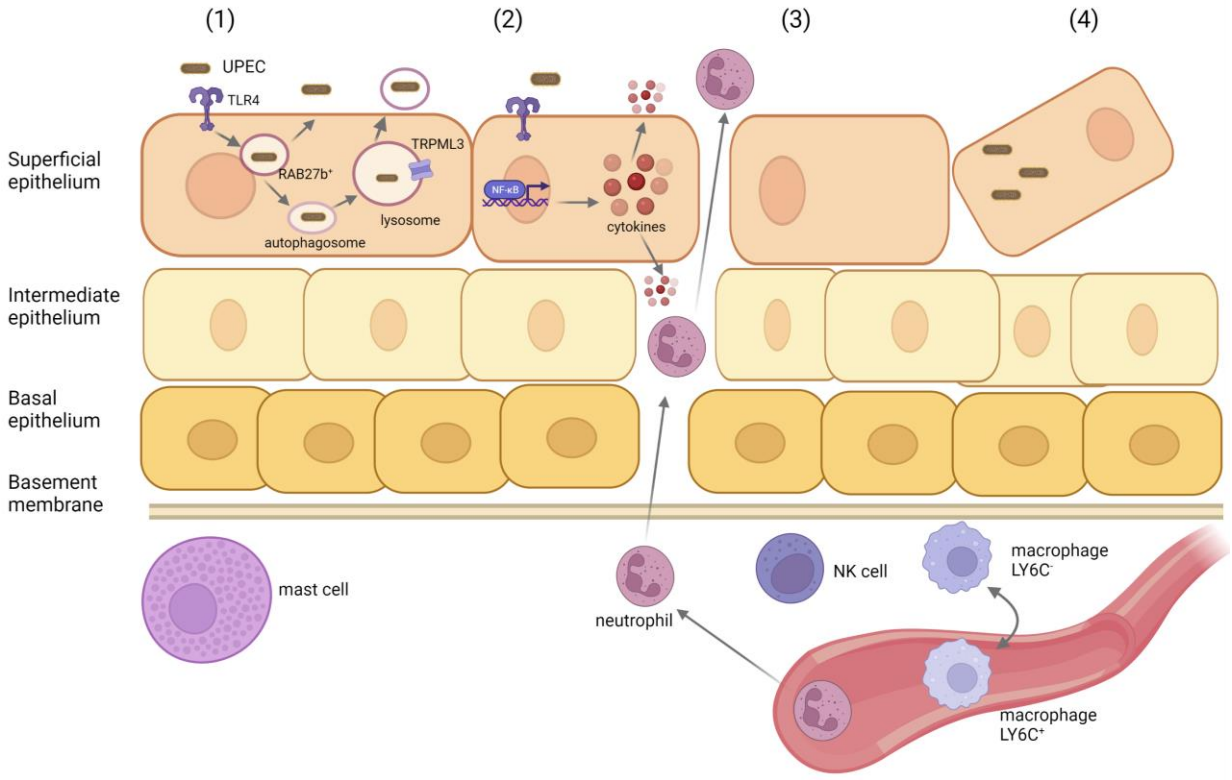

Upon invasion of UPEC in the urothelial cells (UC), the bacteria are **encapsulated (1)** in RAB27b$^+$ fusiform vesicles. These vesicles are expelled by the UC via multiple pathways, including a TLR4-dependent pathway. Bacteria that escape the exocytosis route are captured in lysosomes and undergo degradation. Some bacteria however can block the acidification of the lysosomes, hereby inhibiting autophagy. The high pH

of the malfunctioning lysosome is sensed by TRPML3, which triggers the exocytosis of the lysosome with the bacteria[19,45].

The recognition of intruding bacteria is of the utmost importance. Receptors on the urothelial cells such as the toll-like receptors (TLR2, TLR4, TLR5 and TLR11) play a critical role in the defense mechanisms of the urothelium against bacterial intrusion. TLRs can be engaged by multiple uropathogenic *E. coli* components, including lipopolysaccharide, flagella and both P and type 1 fimbriae[44]. Upon early recognition of pathogens, TLRs transduce the signal and induce nuclear translocation of nuclear factor kappa-light-chain enhancer of activated B cells (NF-kB) which results in the **transcription of pro-inflammatory compounds (2)**[19,39].

Subsequently, the urothelial cells **secrete soluble compounds (3)** such as pro-inflammatory cytokines (interleukins 1, 6 and 8) and antimicrobial peptides (AMPs: uromodulin, neutrophil gelatinase-associated lipocalin, ß-defensin 1, cathelicidin etc.). Besides their antibacterial properties, by disrupting bacterial membranes, these AMPs can have immune-modulatory effects such as promoting neutrophil infiltration[19].
The secreted solutes and the presence of infection can be sensed by the **resident immune cells (3)**, like macrophages ($LY6C^-$), natural killer cells and mast cells, which, in turn, will secrete various cytokines (eg. IL-8) to recruit immune cells (neutrophils and macrophages $LY6C^+$) from the bloodstream to clear the infection[19,44]. Multiple mechanisms are in place to prevent excessive responses, for example IL-10 production is considered to reduce the capacity of dendritic cells to function as antigen presenting cells. IL-10 thereby leads to a limited adaptive immune response, typical for infections of the lower urinary tract[19,46]. The activation of the immune responses is thus tightly regulated and currently still incompletely understood.

If UPEC are able to invade the cytoplasm of the UC, they will start to form intracellular bacterial communities (IBC, see below). The invasion into the cytoplasm can activate the last line of defense. The superficial layer will **exfoliate (4)**, and the bacteria infested UC will be cleared along with the urine. This last defense mechanism may seem very efficient; albeit it exposes the underlying tissue to toxic compounds in the urine and enables the UPEC to invade the deeper layers of the urothelium[19]. The restoring

capacity of the umbrella cells is high, so the exfoliation is followed by a rapid maturation of the deeper layers of the urothelium[35].

3. The pathogen - Uropathogenic *Escherichia coli*

Among the common bacterial uropathogens associated with UTI development, the primary causative bacteria are uropathogenic *E. coli* (UPEC). They account for approximately 80-90% of the community-acquired UTIs[1]. Their plethora of virulence factors, both structural and secreted, enable them to ascend into the LUT and adhere to the UC. The host-pathogen interactions will determine the severity of the infection.

3.1. UPEC virulence factors

A subset of *Escherichia coli* have the capacity to be uropathogenic as they have evolved a number of strategies to evade the innate immune responses, enabling the pathogens to more effectively colonize and persist in the urinary tract[47]. This uropathogenic capacity is attributed to specific virulence factors (figure 4). Virulence factors are bacteria associated molecules that contribute to pathogenic potential[48].

Figure 4. Virulence factors of uropathogenic E. coli (adapted from[9])

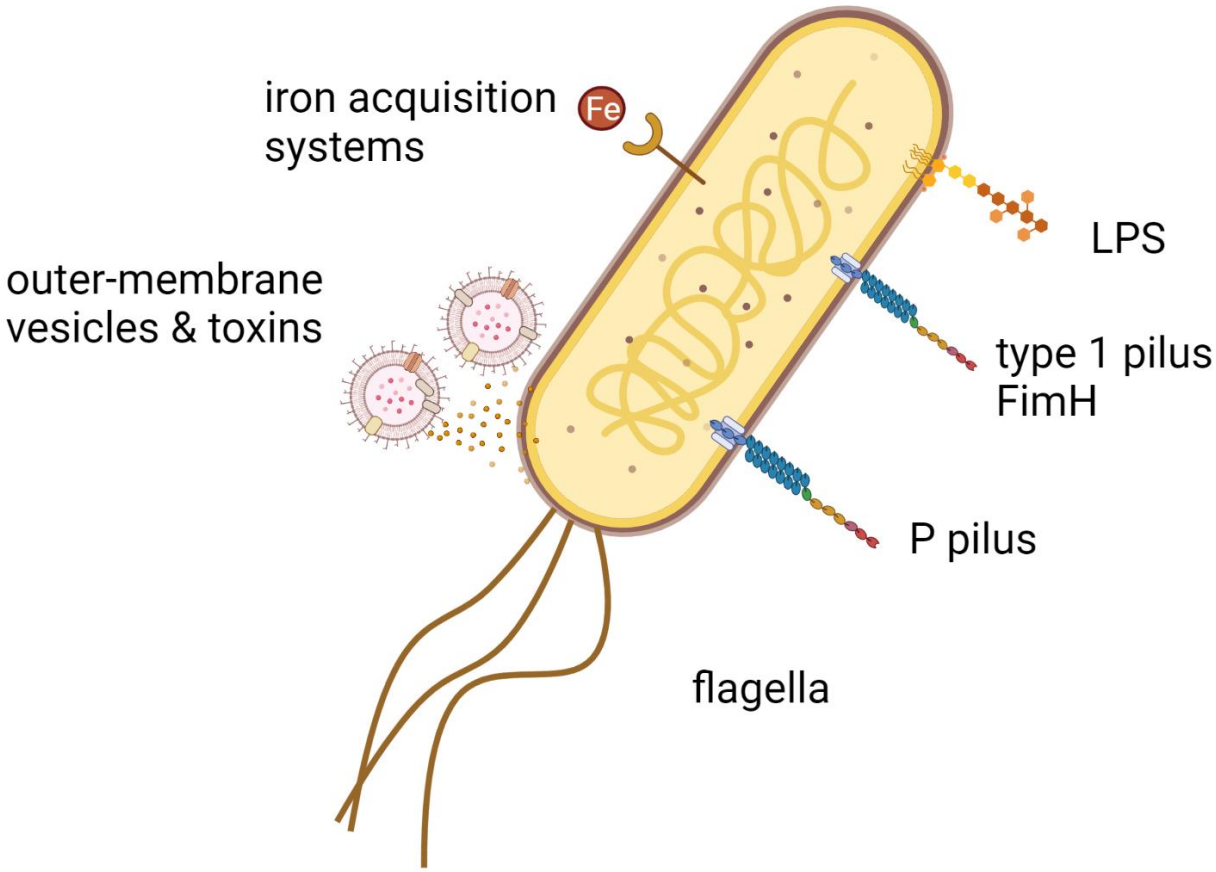

Lipopolysaccharide (LPS) is a structural component on the surface of gram-negative bacteria and is vital for bacterial cell integrity, viability, and defense against environmental stress[49]. These molecules consist of three regions: the lipophilic lipid A is linked to an oligosaccharide core, which is in turn bound to a long polysaccharide chain (the O antigen). In contrast to the highly variable O polysaccharide, the lipid A, which anchors LPS to the outer membrane, is well conserved among Gram-negative species. It is therefore recognized as a pathogen-associated molecular pattern (PAMP), by specific receptors including the toll-like receptors (TLR)[50]. Recently, TLR4-independent pathways have been shown to be able to sense LPS, such as TRP channels and Caspase-4/5 as a sensor in the membrane and cytoplasm, respectively[49].

Other structural components are type 1 and P-type pili. The **type 1 pilus** is a well characterized UPEC virulence factor as it promotes binding to the host tissues, which considered one of the paramount factors for establishing infection[47]. The type 1 pilus

adhesin, FimH, is expressed at the distal end of the tip. The attachment to host cells is mediated by FimH, as it can bind to mannosylated proteins, like uroplakins. Thus, FimH is involved in the initial attachment of UPEC to the urinary tract mucosa[37] and following attachment it will promote bacterial invasion[51]. Piliated phase variants were more effective in colonizing the urothelium compared to nonpiliated variants[52]. The understanding of the adhesion of UPEC to the UC has important implications for the development of novel UTI strategies[47], as stated above. **P-type pili** are associated with UPEC strains that are able to cause upper urinary tract infections and trigger a mucosal response to infection in humans. Their role in the murine UTI model is more subtle and thus less investigated[44].

Flagella-mediated motility contributes to the fitness of UPEC[44]. Nakamura et al. recently discovered that flagellum-mediated motility plays a role in adherence, maturation and dispersal[53]. Besides conferring adhesive and invasive properties, these organelles play a key role in the dynamics of biofilms.

Next, UPEC can secrete **toxins** that play different pathogenic roles during the infection. These toxins are not only released as soluble molecules but can be associated with outer-membrane vesicles (OMV), which protect them and ensure the delivery in the host cells. One of the toxins is **α-hemolysin** (HylA) which is implicated in invasion, stimulates pro-inflammatory cytokine production, and leads to an inflammatory response. It helps colonization by causing epithelial damage and cell death, thus promoting the release of nutrients such as iron[44,54] and exfoliation of the UC[55]. Furthermore, it was found to induce Ca^{2+}-oscillations in renal tubular epithelial cells, which can trigger ascension and colonization of the upper urinary tract[56]. Another important toxin is **cytotoxic necrotizing factor 1** (CNF1), which promotes invasion of UPEC into the host cells[54].

Iron is an essential nutrient of all living things, acting as a co-factor for some vital enzymes. Iron concentrations in the urine are low as the host has sequestered it. **Iron acquisition systems** are therefore contributing to the fitness of the UPEC, however due to redundancy in different acquisition systems, no single system is indispensable for virulence. The siderophore enterobactin represents one well investigated mechanism of iron acquisition[44].

In conclusion, UPEC are able to colonize the host, damage the surrounding tissue and avoid host immune responses[44]. To successfully do this, UPEC must overcome host defenses mediated by the innate and adaptive immune system as stated above.

3.2. The invasion and colonization of the urinary tract by UPEC

The first step of the infection is the ascension of the bacteria into the lower urinary tract. Subsequently UPEC will try to invade the urothelial cells and colonize the bladder (figure 5). Invasion into the urothelium will benefit the UPEC, as they are able to withstand expulsion caused by flushing and are protected from antibiotics and antimicrobial compounds.

Figure 5. Invasion and colonization of the urothelium (adapted from[57])

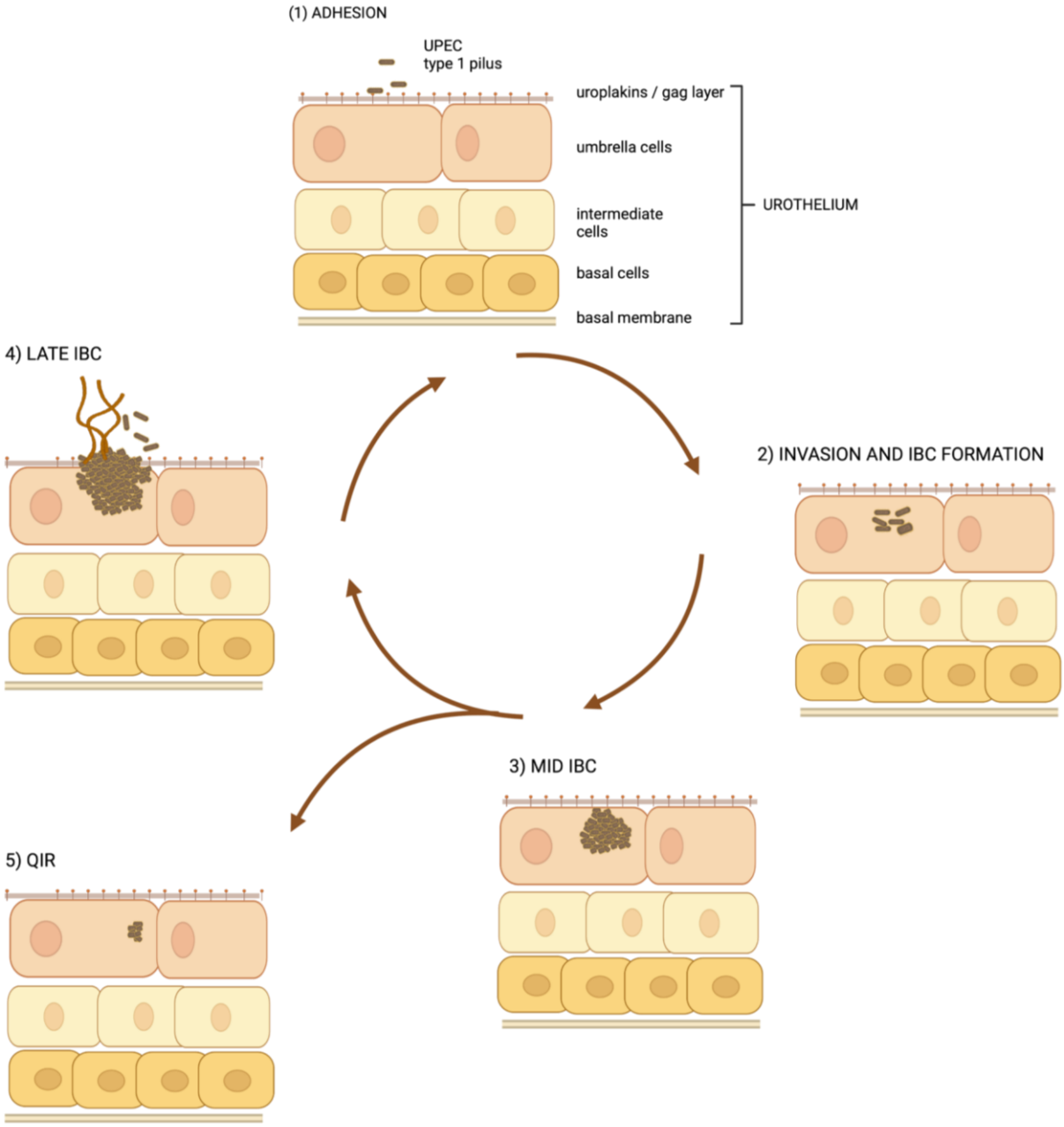

Adhesion (1) to the urothelium is mediated by the interaction of specialized bacterial fimbriae with the uroplakins, in a type 1 pilus-dependent manner[10]. Subsequently, UPEC enter into the UC, which can have different possible outcomes. The bacteria can be exocytosed in a TLR4-dependent process via the lysosome or exfoliation[58], as discussed previously. Alternatively, they can break out of the phagocytic vacuoles and escape into the host cell cytoplasm[59]. How the UPEC are able to break out of the vacuole remains unknown[39]. Once in the cytoplasm, they replicate rapidly and form intracellular bacterial communities (IBC). At this **early IBC (2)** stage, they can multiply

whilst evading host immune responses. Subsequently, the bacteria will become coccoid-shaped as they continue to divide without increasing in length and will become very organized and tightly packed to form the **mid IBC (3)**. The IBC will continue to grow and take up most of the cytoplasm, a new morphological change will occur and bacteria on the edge will convert back to rod-like or even filamentous forms and flux out of the urothelial cell, a stage called the **late IBC (4)**[59,60]. As the bacteria flux out of the host cell, back into the lumen of the bladder, the cycle of invasion starts over. Alternatively, bacteria in IBCs can undergo morphological changes and form **quiescent intracellular reservoirs (5)** (QIRs)[61-63]. These QIRs consist of less than 15 bacteria that persist in a dormant state, which is different from the large number of bacteria in the transient IBCs[43]. The bacteria are protected from antibiotics or antibacterial compounds released by the bladder. The high rate of recurrence and antibiotic resistance is being attributed to IBCs and QIRs[9,64], as the reservoirs have biofilm-like properties. The formation of IBC and QIRs was first observed in murine UTI models. Analysis of human urine specimens during acute cystitis confirmed the presence in human UC[57].

4. TRP channels and calcium signaling

4.1. Calcium signaling

Calcium is one of the most universal secondary messengers. Due to the low intracellular Ca^{2+} levels, cells are highly responsive to acute Ca^{2+} surges. Cells possess a wide range of tools to maintain these low intracellular levels, such as specialized Ca^{2+} pumps, binding proteins, exchangers and channels[65]. This toolkit can be activated by factors in the cellular microenvironment, thereby allowing the cell to integrate information and respond to it. The downstream effects of these cytosolic Ca^{2+} changes differ amongst cell types.

Calcium signaling has been implicated in several steps of bacterial infections. An increase in free cytosolic Ca^{2+} can be induced by toxins. This can induce toxin-mediated effects or cytoskeletal rearrangements that are necessary for the binding and invasion of the pathogen. On the other hand, the UPEC induced release of ATP, which is considered a Ca^{2+} agonist, can expand the signaling and its consequences by a paracrine or autocrine route[66].

4.2. Introduction to TRP channels

As described previously, calcium channels have an important role in maintaining low intracellular calcium levels. In this context, a group of ion channels, called Transient Receptor Potential (TRP) channels, is of particular interest. TRP channels have the ability to respond to a variety of physical and chemical stimuli enabling them to detect changes in the cell's environment[65,67]. Furthermore, the channels contribute to changes in intracellular free calcium by acting directly as Ca^{2+}-entry channels in the plasma membrane, by changing membrane potentials or by providing an intracellular pathway for Ca^{2+}-release[65,68]. Thus, modulating TRP channel activity provides an important way to regulate intracellular calcium levels[69].

TRP channels share a basic tetrameric architecture, forming homo- or heteromeric channels. Each monomer consists of six transmembrane segments (S1-S6) and a cytosolic amino- and carboxy-terminal tail[4]. In mammals, 28 different TRP members have been identified, based on structural homology they can be divided into six subfamilies: TRPA (ankyrin), TRPC (canonical), TRPM (melastatin), TRPML (mucolipin), TRPP (polycystin) and TRPV (vanilloid). These TRP channels respond to various endo- and exogenous ligands as well as changes in pH, osmolarity, stretch and temperature. As such, the TRP channel members are involved in the detection of environmental stimuli and they are of the utmost importance in a plethora of physiological and pathological sensory processes[65].

4.3. TRP channels in the urinary tract

Several members of the TRP channels family are expressed in sensory nerve fibers innervating the bladder (TRPV1, TRPM3, TRPA1, TRPM8, TRPC4) and on the urothelial cells (TRPV4, TRPV2, TRPM7, TRPM4), where they play an essential role in sensing the bladder's content (figure 2). These channels participate in the (patho)physiology of the lower urinary tract (LUT) and pharmacologic or genetic manipulation of TRP channels has been shown to alter bladder function[5,65,67].

The most investigated channel in the lower urinary tract is presumably TRP vanilloid 1 **(TRPV1)**. It is a non-selective cation channel that can be activated by capsaicin, noxious stimuli, heat, protons, and low pH. TRPV1 is predominantly expressed in the

DRG neurons that innervate the bladder[42]. The contribution of TRPV1 to normal bladder function remains controversial, in contrast to its well-established role in the pathophysiology and treatment of neurogenic detrusor overactivity[69,70].

TRP ankyrin 1 **(TRPA1)** is characterized by a promiscuity towards activating agents, as it is sensitive to plant derived agonists (cinnamaldehyde, allicin, mustard oil) and potentially harming stimuli such as hydrogen sulfide[71]. The channel is known to be predominantly present on sensory neurons, especially in a subset of capsaicin-sensitive neurons[69]. Upon activation of the channel, protective reflexes, pain behavior and local release of neurotransmitters have been observed[68].

TRP melastatin 8 **(TRPM8)** is a non-selective cation channel that is sensitive to cool temperatures and cooling agents such as menthol, eucalyptol or icilin. In the urinary tract, TRPM8 is present in a subset of bladder innervating DRG neurons[5] and it is considered a thermoreceptor involved in the bladder cooling reflex[72,73]. Furthermore, TRPM8 has been proposed as a promising therapeutic target for hypersensitive bladder disorders[74,75,76]. On the contrary, the physiological role of TRPM8 in the LUT remains unclear, as mice with genetic disruption of *Trpm8* have a normal bladder phenotype[72].

The TRP vanilloid 4 **(TRPV4)** channel is a nonselective cation channel that can be activated by various mechanical and chemical stimuli, such as hypotonicity, shear stress, acid and GSK1016790A. It has been proposed as a candidate for mediating the urethra-to-bladder reflex and for mediating bladder afferent signaling[68]. Mechanical stimulus-dependent activation of TRPV4 on urothelial cells is thought to be a key event for ATP signaling in the micturition reflex pathway[69,77,78]. Deletion of the *Trpv4* gene in rodents had an impact on the micturition pattern; a longer inter-contractile interval with an increased number of non-void contractions were observed[79]. Pharmacological manipulation of TRPV4 improved bladder function in rodents both in pathological conditions of over- and underactivity[80,81].

4.4. TRP related diseases of the LUT

TRP channels in the lower urinary tract contribute to the generation of normal and abnormal bladder sensations through a variety of mechanisms and have demonstrated potential as targets for the treatment of LUTS in functional disorders of the lower urinary tract[5].

The role of TRP channels in **inflammatory responses** is increasingly being acknowledged[82]. During inflammation, there is an enhanced production or release of inflammatory mediators such as adenosine triphosphate (ATP), bradykinin, prostaglandins, nerve growth factor and protons[83]. These chemical mediators activate the channels such as TRPV1, TRPA1, purinergic receptors (P2X) and acid-sensing ion channels (ASIC) on nociceptors[83]. TRPA1 has been investigated and indicated as a target on the afferent fibers for reactive oxygen species (ROS) and H_20_2[84-86]. TRPV1 was found to be essential for the generation of bladder overactivity and noxious bladder input associated with experimental cystitis in an LPS-induced inflammation model[87]. Furthermore, TRPV1 can be sensitized by chemokines, thus enabling the integration of multiple noxious stimuli and playing a key role in neurogenic inflammation[65]. Co-administration of a TRPV1 and TRPV4 antagonist reversed the hyperactivity caused by LPS-induced cystitis in rats[88].

Besides the alterations of the sensitivity of TRP channels in nociceptors during inflammation, TRPs contribute to inflammatory processes in various ways, as they are expressed on cells of **the immune system**. For example, TRPM2 is highly expressed in granulocytes, neutrophils and macrophages[89]. The activation of the TRPM2 channel in these cells by ROS-induced Ca^{2+} entry is thought to lead to a positive feedback mechanism, producing more ROS[65]. Inhibition of TRPM2 was postulated to be an interesting strategy for treating inflammatory diseases[71]. Furthermore, TRPC1 is involved in antibody recognition in B lymphocytes and TRPC3 is considered to play a role in the T-cell receptor activation-induced Ca^{2+} entry in lymphocytes[90]. Interestingly, the role of TRPV4 in macrophages is being increasingly recognized. It was shown that macrophage activation functions such as phagocytosis and cytokine secretion are regulated through calcium. In a murine lung inflammation model, Sherega et al. have shown that TRPV4 is necessary for phagocytosis and anti-inflammatory cytokine

profile in a stiffness-dependent manner, thus connecting mechanosensation to immunity[91,92].

As stated previously, upon **infection** and invasion of UPEC in the urothelial cells (UC), bacteria are normally expulsed, however when this malfunctions, TRPML3 will trigger the exocytosis of the non-acidifying lysosome[19,45]. Additionally, in airway and urothelial cells, LPS from gram-negative bacteria has been shown to trigger protective responses, such as NO production, upon activation of TRPV4 in a TLR4-independent manner[93,94]. Besides TLR4 and TRPV4, extracellular LPS can be sensed by TRPA1 in neuronal cells. Here, LPS was shown to drive neurogenic inflammation, resulting in hyperalgesia, tissue swelling, calcitonin gene-related peptide (CGRP) release and arterial dilatation in mice[82,95]. In a study with *Trpa1* deficient mice, an attenuated response was seen upon LPS stimulation even though the animals had a similar inflammatory signature[96].
Furthermore, Rosen et al. have found that TRPV1 mediates inflammatory pain initiation[97]. Inflammation itself and the interaction between LPS and TLR4 can enhance nociceptive action based on sensitization of TRPV1[82]. Additionally, the O-antigen status of LPS is thought to define the pain phenotype of the *E. coli*[35,98]. These pain responses were independent of the severity of the inflammation[97]. In summary, LPS triggers the sensory nerves by the activating the TRP channels. This activation leads to the generation of an action potential and pain, as well as the release of neuropeptides. They can in their turn lead to neurogenic inflammation and if chronic, lead to hypersensitivity syndromes[82].

One of these hypersensitivity syndromes is **bladder pain syndrome** (BPS). It is defined as “the complaint of suprapubic pain related to bladder filling, accompanied by other symptoms such as increased daytime and night- time frequency, in the absence of proven urinary infection or other obvious pathology”[99]. The underlying disease mechanism remains elusive, however the involvement of TRP channels expressed in nociceptive afferent nerves is being proposed. Pain arising in the bladder and urethra is conveyed via nociceptor sensory neurons from the DRGs that express the sensory TRP channels TRPV1, TRPA1, TRPM3 and TRPM8[100]. Both the expression of TRPM8 and TRPV1 on the nerve fibers and the density of those fibers has been shown to be increased in biopsies of patients with BPS[101-104]. Intravesical instillations with a TRPV1

agonist, have been used to desensitize the sensory neurons of the bladder with contrasting results[105]. TRPA1 antagonists significantly decreased mechanical hyperalgesia induced by cyclophosphamide without interfering with locomotor activity[106]. As for BPS, the pathophysiology of **overactive bladder syndrome** (OAB) is multifactorial and poorly understood[70]. Multiple TRP channels have been proposed to play a role in the pathophysiology or to be druggable targets. TRPV1 has gotten the most attention, especially for the treatment of neurogenic detrusor overactivity[70,107].

In conclusion, the therapeutic potential of some of these channels, including TRPV1, TRPV4, TRPM8, TRPA1, for treatment of bladder inflammation, over- and underactivity and bladder pain disorders has been suggested and supported by preclinical and clinical information. Vanneste et al. stated that “targeted inhibition or activation of well-chosen TRP channels in the LUT could result in disease modification rather than merely treatment of symptoms”[5]. However, the translation of this information to clinical application has been slow[108].

OBJECTIVES

II. Objectives

UTIs are amongst the most common bacterial infections in humans, requiring millions of antibiotic prescriptions annually. Available therapies have not evolved significantly in recent years, do not prevent recurrences, and are challenged by rising antibiotic resistance. The field lacks a thorough understanding of the protective host immunity and the impact of bladder function on UTI susceptibility[39]. As such, there is an urgent need for novel strategies for the treatment and prevention of UTIs[10].

The general aim of this dissertation is to obtain a better understanding of the interaction between the host and the pathogen, the urothelium and UPEC. We hypothesized that TRP channels in the bladder wall can modulate bladder function in response to UTI infections and that these alterations in bladder function will stimulate resolution of the UTIs.

To test this hypothesis, the dissertation focusses on 3 specific objectives:

1. To establish a longitudinal model to follow-up bacterial load in mice with UTIs.

The first objective is to optimize a murine UTI model and validate bioluminescent imaging as a technique to longitudinally follow-up the bacterial load. Having a longitudinal *in vivo* model at hand, allows future research of UTI susceptibility.

2. To characterize *In vitro* responses of urothelial cells to a bacterial suspension.

Previous research has demonstrated a rise in intracellular Ca^{2+} concentrations in urothelial cells exposed to bacterial toxins. Here, we investigate the hypothesis that a suspension of viable uropathogenic *E. coli* induces Ca^{2+} responses through pathways similar to those identified for the bacterial toxins. Specific objectives are (1) to determine responses of UC to a bacterial suspension and (2) to investigate the molecular pathways involved in these responses.

3. To study TRP channels as a potential target of phenazopyridine

Phenazopyridine hydrochloride (PAP) is an over-the-counter drug, which is broadly used to provide symptomatic relief of bladder pain in conditions such as cystitis or bladder pain syndrome[109]. Whereas the analgesic effect of PAP has been attributed to a local effect on the mucosa of the lower urinary tract, the molecular targets of PAP

responsible for the observed pain relief remains unknown. Here, we investigated the effect of PAP on pain related TRP channels expressed in sensory neurons that innervate the bladder wall. Specific objectives are (1) to explore the response of TRP channels to PAP and (2) to investigate a possible role for TRP channels in PAP-induced analgesia.

MATERIALS AND METHODS

III. Materials and methods

All animal experiments were conducted in accordance with the European Union Community Council guidelines and were approved by the Animal Ethics Committee of KU Leuven (P158/2018).

1. Cell culture

Urothelial cells

The protocol used to establish primary urothelial cells (UC) was described earlier[42]. Briefly, mice were euthanized, and their bladders were removed, cut open, and stretched out on a Sylgard-coated dish containing MEM (Invitrogen) with 2.5 mg/ml Dispase (Invitrogen) for 2 h at room temperature. Next, the urothelium was gently scraped from the underlying tissue, treated with trypsin-EDTA (Invitrogen) for 15 min, and resuspended in defined keratinocyte serum-free medium (Invitrogen). The cell suspension was plated on type IV collagen-coated coverslips and incubated overnight to ensure attachment. Cells were kept at 37°C in 5% CO_2 and used in experiments the next day.

HEK293 and CHO cells

Human embryonic Kidney 293 (HEK293) cells were obtained in 2007 from Dr. Stephen Roper (Miami school of medicine). The HEK293 cells were transiently transfected with 2 μg of TRP cDNA construct, linked to green fluorescent protein (GFP), using TransIT transfection reagents (BioMirus) 24h before the measurement. The transfected cells were visualized by GFP expression. Chinese Hamster Ovary cells (CHO, gifted by prof. Paul Vanveldhoven, laboratory of pharmacology KU Leuven) were stably expressing TRPA1. All cells were cultured in DMEM high glucose (Thermo fisher) supplemented with 50 mL foetal bovine serum (Gibco), 10 mL penicillin/streptomycin (Gibco), 10 mL glutamax (Thermo fisher) and 5 mL non-essential-amino-acids (Thermo fisher). In addition to this, 1 mL hydromycin and 500 µL blasticidin were added to the culture medium of the CHO cells. Cells were kept at 37°C in 10% (HEK293 cells) or 5% (CHO cells) CO_2.

DRG

Bilateral L5-S1 DRGs were isolated from mice as described previously[110]. In brief, the spinal column was isolated, cleaned, and split sagittal. The spinal cord, meninges covering the DRG, and the distal axon bundles were removed. DRGs were washed in neurobasal A medium (Invitrogen) supplemented with 10% fetal calf serum (basal medium), and then incubated for 1 h at 37°C in a mix of 1.5 mg /mL collagenase and 2.5 mg /mL dispase (Gibco). Digested ganglia were gently washed twice with basal medium and subsequently washed twice in neurobasal A medium supplemented with B27 (Invitrogen), 2 ng /mL GDNF (Invitrogen), 10 ng /mL NT4 (Peprotech), 1% (v/v) Glutamax (Gibco) and penicillin 50 units /mL—streptomycin 50 µg /mL (Gibco) (complete medium). 1 mL of complete medium plus 1 mL of bovine serum albumin (BSA) solution (16% w/v in PBS) were added to the ganglia. Cells were mechanically dissociated by passage through syringes fitted with increasing needle gauges. The cell suspension was added on top of a 3 mL BSA solution (16% w/v in PBS) and centrifuged at 500 × g for 6 min. The supernatant was discarded and the pellet was resuspended in complete medium. Neurons were seeded on poly-L-lysine/laminin coated glass-bottom chambers (Fluorodish, WPI) and cultured overnight at 37°C in 5% CO2 in complete medium.

2. Calcium imaging

For intracellular Ca^{2+} measurements, cells were incubated with 2 µM Fura-2 acetoxymethyl (AM) ester for 30 min at 37°C. The intracellular Ca^{2+} concentration ($[Ca^{2+}]_i$) was monitored through the ratio of fluorescence measured upon alternating illumination at 340 and 380 nm, using an MT-10 illumination system and cell^M software (Olympus). Absolute calcium concentrations were calculated from the ratio of the fluorescence signals at both wavelengths (F_{340}/F_{380}) after correction for the individual background fluorescence signals, using the Grynkiewicz equation[111]

$$[\mathrm{Ca}^{2+}] = K_{eff}\,\frac{R - R_0}{R_1 - R}$$

where the calibration constants R_0, R_1 and K_{eff} were determined from *in vitro* calibrations using droplets of Fura-2AM-containing solution with known calcium concentrations.

The cells were perfused using a gravity-based perfusion system with solutions containing (in mM) 150 NaCl, 6 KCl, 2 $CaCl_2$, 1.5 $MgCl_2$, 10 HEPES, and 10 Glucose and titrated to pH 7.4 with NaOH. Calcium free solution contained (in mM) 150 NaCl,

6 KCl, 1.5 $MgCl_2$, 10 HEPES, 10 Glucose and 1 EGTA. All compounds were obtained from Sigma-Aldrich and were dissolved in the bath solution containing 0 or 2 mM Ca^{2+} as indicated in the individual experiments.

3. Patch clamp

Membrane currents were measured in the whole-cell mode of the patch-clamp technique using an EPC-10 amplifier and Patchmaster software(HEKA Elektronik). Patch electrodes had a direct current (DC) resistance between 2 and 4 MΩ when filled with intracellular solution. Currents were sampled at 20 kHz and digitally filtered at 2.9 kHz. Between 50 and 70% of the series resistance was electronically compensated to minimize voltage errors. The holding potential in all experiments was 0 mV. A ramp protocol was applied consisting of 500-ms linear voltage ramps, applied at 0.5 Hz, from -100 mV to +100 mV (TRPM8), -100 mV to +150 mV (TRPM3), or -100 mV to +160 mV (TRPV1). For TRPM8, we also used a voltage step protocol, consisting of 100-ms steps to voltages ranging from -120 to +160 mV, followed by a 50-ms step to +60 mV. The standard extracellular solution for electrophysiological measurements contained (in mM) 150 NaCl, 1 $MgCl_2$ 10 HEPES (pH 7.4 with NaOH). Depending on the type of investigated channel, the pipette solution was composed of (in mM) 100 CsAsp, 45 CsCl, 10 EGTA, 10 HEPES, 1 $MgCl_2$ (pH 7.2 with CsOH) (TRPM3), 150 NaCl, 1 $MgCl_2$, 10 HEPES, 5 EGTA (pH 7.2 with NaOH) (TRPV1), or 150 NaCl, 5 $MgCl_2$, 5 EGTA, 10 HEPES (pH 7.2 with NaOH) (TRPM8). All measurements were carried out at room temperature (22–25°C).

4. Bacterial culture

The clinical cystitis isolate ‘UTI89’, a uropathogenic *E. coli* strain, was selected to establish the infections, due to its pathogenic capacity in both humans and rodents and common use in murine UTI models. The bioluminescent isogenic strain ‘UTI89-*lux’*, carrying the complete *lux* operon (LUXCDABE), was used for all imaging experiments[112].

The bioluminescent UPEC strain, UTI89-*lux,* was cultured statically overnight at 37°C in an incubator, in Luria-Bretani (LB) broth supplemented with 50 µg/mL kanamycin sulfate, before being diluted 1/100 into fresh LB broth without antibiotics and grown statically for an additional 24h at 37°C. Subsequently, cultures were centrifuged, and

the bacterial pellet was resuspended until a concentration of 4 x 10^8 CFU per mL was reached. For each experiment, a fresh bacterial culture was obtained.

5. Experimental murine UTI model

The experimental murine UTI model[59] was established and adapted to enable bioluminescence imaging (BLI). Briefly, 10-12-week-old female C57Bl/6J mice were anesthetized using Isoflurane and residual urine was expelled by gentle compression of the suprapubic region. A Hamilton syringe (100 µL) with a sterile 24-gauge angiocatheter (Insyte Autoguard BC Winged 24G) was used for transurethral catheterization and slow (5 µL/s) instillation of the bacterial inoculum (50 µL UTI89-*lux*).

The murine model is the predominantly used animal model as it allows researchers to investigate UTIs in a mammalian urinary tract. However, the catheterization of the rodents leads to bypassing of the urethra and thus the ascension. On the downside, large inoculi are needed to infect these mice that do not have spontaneous UTIs[113]. Marked differences exist in the UTI susceptibility between several murine strains. For example, C3H/HeJ mice are LPS non-responsive due to a mutation in the *Tlr4* gene, this makes them useful to study the role of TLR4 in UTI pathogenesis when compared to the C3H/HeN mice, without this mutation[114]. The strain used in the experiments in this dissertation was C56BL/6, which are intermediately susceptible to acute UTIs and have only rarely infections of the upper tract[114]. The advantage of this mouse strain is the availability of several mutants including *Trp*-knock out lines.

6. Bioluminescence imaging

All images were acquired using the IVIS Spectrum® system (Perkin Elmer, Waltham, USA) with an exposure time of approximately 30-60 seconds, F/stop of 1, field of view D, medium binning and a subject height of 1 cm. The exposure time was reduced when image saturation occurred. Images were acquired in triplicate. For *in vivo* assays, anesthetized and shaved mice were placed in the IVIS spectrum in supine position and were imaged before instillation, immediately after instillation and various hours or days post-infection. The total photon flux (photons/s/cm^2/sr) in defined regions of interest was quantified using the Living Image software package (Xenogen) and was used as a read-out for the bacterial load.

The advantages and limitations of the use of bioluminescence imaging for the evaluation of bacterial load in UTIs are discussed in the result section, chapter 1.

7. Statistics

Statistical analysis and graphing were performed in OriginPro 9.0. Results were considered significant if the two-sided p-value was smaller than 0.05. Specific statistical tests were stated in figure legends. All summary data are reported as mean ± SEM.

RESULTS

IV. Results

CHAPTER 1

Longitudinal Follow-up of Urinary Tract Infections and Their Treatment in Mice using Bioluminescence Imaging

Noémie Luyts, Greetje Vande Velde, Matthias Vanneste, Helene De Bruyn, Annelies Janssens, Natalie Verstraeten, Thomas Voets, Wouter Everaerts

Published in JoVE, June 2021

jove

Longitudinal Follow-Up of Urinary Tract Infections and Their Treatment in Mice using Bioluminescence Imaging

Noémie Luyts[1], **Greetje Vande Velde**[2], **Matthias Vanneste**[1], **Helene De Bruyn**[1], **Annelies Janssens**[1], **Natalie Verstraeten**[3], **Thomas Voets**[1], **Wouter Everaerts**[4]

[1] Laboratory of Ion Channel Research (LICR), VIB-KU Leuven Center for Brain & Disease Research, Leuven, Belgium & Department of Cellular and Molecular Medicine, KU Leuven [2] Biomedical MRI, Department of Imaging & Pathology, KU Leuven [3] Belgium & KU Leuven Centre of Microbial and Plant Genetics, VIB-KU Leuven Center for Microbiology, Leuven [4] Laboratory of Experimental Urology, Department of Development and Regeneration, KU Leuven

Corresponding Author:
Wouter Everaerts (wouter.everaerts@kuleuven.be)

Email addresses of Co-Authors:
Noémie Luyts (noemie.luyts@kuleuven.be)
Greetje Vande Velde (greetje.vandevelde@kuleuven.be)
Matthias Vanneste (matthias.vanneste@kuleuven.be)
Helene De Bruyn (helene.debruyn@kuleuven.be)
Annelies Janssens (annelies.janssens@kuleuven.be)
Natalie Verstraeten (natalie.verstraeten@kuleuven.be)
Thomas Voets (thomas.voets@kuleuven.be)
Wouter Everaerts (wouter.everaerts@kuleuven.be)

Date Published : June 14, 2021
DOI : 10.3791/62614
URL : jove.com/video/62614

KEYWORDS:
bioluminescence imaging, urinary tract infections, bacterial infection, uropathogenic E. coli, murine model, lux operon, photons

SUMMARY

This manuscript describes the intravesical administration of uropathogenic bacteria with a lux operon to induce a urinary tract infection in mice and subsequent longitudinal in vivo analysis of the bacterial load using bioluminescence imaging.

ABSTRACT

Urinary tract infections (UTI) rank among the most common bacterial infections in humans and are routinely treated with empirical antibiotics. However, due to increasing microbial resistance, the efficacy of the most used antibiotics has declined. To find alternative treatment options, there is a great need for a better understanding of the UTI pathogenesis and the mechanisms that determine UTI susceptibility. In order to investigate this in an animal model, a reproducible, non-invasive assay to study the course of UTI is indispensable.

For years, the gold standard for the enumeration of bacterial load has been the determination of Colony Forming Units (CFU) for a particular sample volume. This technique requires post-mortem organ homogenates and serial dilutions, limiting data output and reproducibility. As an alternative, bioluminescence imaging (BLI) is gaining popularity to determine the bacterial load. Labeling pathogens with a lux operon allow for the sensitive detection and quantification in a non-invasive manner, thereby enabling longitudinal follow-up. So far, the adoption of BLI in UTI research remains limited.

This manuscript describes the practical implementation of BLI in a mouse urinary tract infection model. Here, a step-by-step guide for culturing bacteria, intravesical instillation and imaging is provided. The in vivo correlation with CFU is examined and a proof-of-concept is provided by comparing the bacterial load of untreated infected animals with antibiotic-treated animals. Furthermore, the advantages, limitations, and considerations specific to the implementation of BLI in an in vivo UTI model are discussed. The implementation of BLI in the UTI research field will greatly facilitate research on the pathogenesis of UTI and the discovery of new ways to prevent and treat UTI.

INTRODUCTION

Urinary tract infections (UTI) are among the most common bacterial infections in humans. Almost half of all women will experience a symptomatic UTI during their lifetime[8]. Infections limited to the bladder can give rise to urinary symptoms such as increase in urinary frequency, urgency, hematuria, incontinence, and pain. When the infection ascends to the upper urinary tract, patients develop pyelonephritis, with malaise, fever, chills, and back pain. Furthermore, up to 20% of patients with UTI suffer from recurrent infections resulting in a dramatic decrease in antibiotic sensitivity[1,2,44]. In recent years, there has been a growing interest in novel therapies for the treatment and prevention of recurrent UTI. Despite a better understanding of the innate and adaptive immunity of the lower urinary tract and of the bacterial virulence factors necessary for invasion and colonization, no radical changes in the treatment regime have been translated to the daily urological practice[2]. In order to study UTI pathogenesis and susceptibility *in vivo*, a reproducible and non-invasive assay is indispensable.

Multiple animal UTI models have been described ranging from nematodes to primates, but the murine model is predominantly used[113,114]. This model consists of transurethral catheterization of (female) mice and subsequent instillation of a bacterial suspension, most commonly uropathogenic *Escherichia coli* (UPEC), directly into the bladder lumen[59]. After inoculation, the bacterial load has traditionally been quantified by determining colony forming units (CFU). This technique requires sacrificing animals to obtain *post-mortem* organ homogenates and serial dilutions, limiting data output and reproducibility. Moreover, longitudinal follow-up of the bacterial load in individual animals is not possible using this technique.

In 1995, Contag et al. suggested the use of bioluminescent-tagged pathogens to monitor disease processes in living animals[115,116]. Since then, bioluminescence imaging (BLI) has been applied to numerous infection models such as meningitis, endocarditis, osteomyelitis, skin, and soft tissue infections, etc.[117-119]. In the murine UTI model, a UPEC strain with the complete *lux* operon (*luxCDABE*) from *Photorhabdus luminescens* can be used[112]. An enzymatic reaction is catalyzed by the

bacterial luciferase which is dependent on the oxidation of long-chain aldehydes reacting with reduced flavin mononucleotide in the presence of oxygen, yielding the oxidized flavin, a long-chain fatty acid and light[119]. The *lux* operon encodes for the luciferase and other enzymes required for the synthesis of the substrates. Therefore, all metabolically active bacteria will continuously emit blue green (490 nm) light without the need for the injection of an exogenous substrate[119]. Photons emitted by *lux*-tagged bacteria can be captured using highly sensitive, cooled charge-coupled device (CCD) cameras.

The use of bioluminescent bacteria in a model for UTI allows for the longitudinal, non-invasive quantification of the bacterial load, omitting the need for sacrificing animals at fixed time points during the follow-up for CFU determination. Despite the wide range of possibilities, accumulating evidence for the robustness of this BLI technique in other fields and its advantages over classic models of UTI, it has not been widely implemented in the UTI research. The protocol presented here provides a detailed step-by-step guide and highlights the advantages of BLI for all future UTI research.

PROTOCOL

All animal experiments were conducted in accordance with the European Union Community Council guidelines and were approved by the Animal Ethics Committee of KU Leuven (P158/2018).

1. Culturing bacteria (adapted[59,112,120])

1.1. Preparation

1.1.1. Choose a luminescent UPEC strain that best fits the experimental needs.

NOTE: Here, the clinical cystitis isolate, UTI89 (E. coli), was selected because of its uropathogenic capacity in both humans and rodents, and its common use in murine UTI models[59,63,114]. The bioluminescent isogenic strain carrying the complete lux operon (luxCDABE) is further referred to as UTI89-*lux*. This operon also carries kanamycin sulfate (Km) resistance genes. Therefore, Km can be used to select bioluminescent colonies[112].

1.1.2. Make a correlation curve for the CFU and optical density at 600 nanometers (OD 600 nm) for the chosen bacterial strain[59].

1.1.2.1. To do this, culture bacteria (using the protocol below) and make 8 different dilutions in phosphate buffered saline (PBS). Measure the OD at 600 nm for all these dilutions and plate them on Luria-Bertani (LB) plates to determine the CFU.

1.1.2.2. Plot the OD 600 nm values and the CFU values to determine the correlation and to obtain a standard curve.

NOTE: For future experiments, measure the OD at 600 nm and use this standard curve to get an instant estimation of the CFU in a bacterial solution.

CAUTION: UPEC are pathogenic bacteria, ensure rooms are properly equipped and use personal protective equipment.

1.2. Three days before the instillation

1.2.1. Obtain single colonies by streaking out the glycerol stock of bacteria, using an inoculation loop, on LB plates supplemented with 50 µg/mL Km and culture overnight at 37 °C. Seal these plates with a paraffin film to store at 4 °C up to 1 week.

1.3. Two days before the instillation

1.3.1. Fill a sterile 14 mL polystyrene round bottom tube with dual-position snap caps with 5 mL of LB broth supplemented with 50 µg/mL Km. Pick a single bacterial colony with an inoculation loop and add this to the LB broth. Vortex for 10 s to ensure proper mixing.

1.3.2. Culture statically with the snap cap in the open position at 37 °C overnight.

NOTE: Static growth of E. coli promotes the expression of type 1-pili, which are critical for the adherence to and invasion of urinary epithelial cells.

1.3.3. Prepare a sterile Erlenmeyer or culture flask.

1.4. One day before the instillation

1.4.1. After the incubation, vortex the tube for 10 s to ensure proper homogenization of the bacterial culture. Make a sub-culture in the Erlenmeyer by adding 25 µL of the bacterial suspension to 25 mL of fresh LB medium without antibiotics.

1.4.2. Close the Erlenmeyer and culture statically at 37 °C overnight.

1.5. On the day of instillation

1.5.1. Vortex the Erlenmeyer for 10 s to ensure proper mixing.

1.5.2. Pour the culture from the Erlenmeyer into a 50 mL culture tube and centrifuge at 3,000 x g and 4 °C for 5 min. Decant the supernatant and resuspend the bacterial pellet in 10 mL of sterile PBS and vortex again for 10 s.

1.5.3. Choose the experimental concentration of the inoculum (CFU) and use the standard curve obtained in step 1.1.2 to determine the corresponding OD 600 nm.

1.5.4. Add 1 mL of the resuspended bacterial culture into 9 mL of sterile PBS and check the OD at 600 nm. Adjust further by adding either sterile PBS or concentrated bacterial solution, until the desired OD 600 nm is reached[47].

NOTE: For example, for UTI89-lux adjust the culture by adding PBS until the OD 600 nm reaches 0.45, corresponding to 2 x 10^7 CFU/ 50 µL. To verify the number of viable CFUs, make 10-fold serial dilutions and plate 50 µL of the fifth and sixth 10-fold dilutions on LB plates in triplicate to obtain less than 300 colonies. Count the obtained colonies the next day after overnight incubation at 37 °C. OD 600 nm gives an instant read-out but use CFU as quality control.

2. Inoculation of the animals (adapted from[47,121])

2.1. Preparation of the animals

2.1.1. Choose the desired mouse strain(s) depending on the research question and availability of knock-out lines, experimental details, and differences in UTI susceptibility[114,122]. Keep in mind that transurethral catheterization is easier in female mice. Do not use animals younger than 8 weeks, as they are immunologically immature. Here, 12-week-old female C57Bl/6J mice were used.

2.1.2. Order animals well in advance and let them acclimate, ideally for 7 days. Group house animals in individually ventilated cages, under standard 12 h light/dark conditions.

2.1.3. Shave the abdominal region of the animals to limit the loss of signal. Do not use hair removal cream, as it can burn the skin of the animals quickly. Restrain the animal by tightly holding the scruff and hind limbs with the non-dominant hand while shaving with the dominant hand. Alternatively, shave under isoflurane anesthesia.

NOTE: Animals were shaved 2 days prior to imaging, considering the animals will groom the shaved area even further.

2.1.4. Provide water and standard food ad libitum throughout the experiment. However, deprive animals from water 2 h prior to instillation to minimize the bladder volume during instillation.

2.1.5. Mount a sterile 24 G angiocatheter tip on a 100 µL syringe and fill the syringe with the bacterial solution prepared in step 1.5.3.

NOTE: To determine the background luminescence, obtain a baseline image prior to the instillation (see step 3, below).

2.2. Instillation of the animals

2.2.1. Place the animals in an induction chamber and anesthetize them using inhalation of isoflurane with pure oxygen as a carrier gas (induction at 3% and maintenance at 1.5%).

2.2.2. Place one animal on a working surface in the supine position and maintain a stable isoflurane anesthesia using a nose cone during the instillation. Apply the eye-ointment.

2.2.3. Expel the residual urine by applying gentle compression and making circular movements on the suprapubic region. Clean the lower abdomen with 70% ethanol prior to instillation.

2.2.4. Lubricate the catheter tip with normal saline. Put the index finger of the non-dominant hand on the abdomen and push it gently upwards. Start the catheterization of the urethra in a 90° angle (vertically) and once resistance is encountered, tilt it horizontally before inserting it further (0.5 cm).

NOTE: Never forcefully push the catheter, as this will cause harm to the urethra. Gentle turning motions can be helpful in catheter insertion. On the other hand, a lack of resistance usually indicates erroneous insertion into the vagina.

2.2.5. Perform a slow (5 µL/s) instillation of 50 µL of the bacterial inoculum (2×10^7 CFU).

NOTE: Higher volumes or faster instillation might cause reflux to the kidneys. During practice of the technique, blue ink can be used to evaluate reflux.

2.2.6. After the instillation, keep the syringe and catheter in place for a few more seconds and then slowly retract to prevent leakage. Record any irregularities such as a high amount of leakage or a bloody meatus and exclude animals, if necessary.

2.2.7. Position the animal in supine position at the nose cone of the imaging chamber and repeat the preceding steps 2.1.1–2.1.6 for all the remaining animals. Use one catheter per experimental group. Ensure anesthesia is continued and minimize the time between the first and the last animal.

2.2.8. If necessary, administer antibiotics or experimental drugs, prior to or after the imaging (step 3). For example, to administer enrofloxacin, add 40 µL of the enrofloxacin (100 mg/mL) solution to 3.96 mL of physiological saline to obtain a 1/100 dilution. Inject 100 µL/10 g subcutaneously at 9 am and 5 pm to administer 10 mg/kg of enrofloxacin twice daily for 3 days.

3. Bioluminescence imaging

3.1. Preparation and selection of imaging parameters

3.1.1. Open the BLI acquisition software (see Table of Materials) and click on Initialize in the imaging device (see Table of Materials) to test the camera and stage controller system and to cool the CCD camera to -90 °C.

NOTE: During this process, the door is locked, and the progress of the initialization can be followed on the control panel. A green light indicates that the temperature of -90 °C is reached. A warning will appear if imaging is attempted before completion of the initialization.

3.1.2. Ensure data is saved automatically: Click on acquisition Auto-save to and select the correct folder.

3.1.3. Select Luminescence and Photograph. Check the default luminescence settings: Set excitation filter to Block and emission filter to Open.

3.1.4. Set the exposure time to Auto when taking the first image, especially when expecting a dim signal to ensure an adequate number of photon counts. For in vivo measurements and bright signals, set the Exposure Time to ~30 s. If the image is saturated, a warning will appear. If this happens, reduce the exposure time.

3.1.5. Select the medium Binning, F/stop 1 and choose the correct field of view (FOV) (D for 5 animals).

3.1.6. Set the subject height to 1 cm when imaging mice.

3.1.7. Click on Add three times in the Acquisition Control Panel to obtain a sequence of three images, as technical replicates.

3.2. Imaging

3.2.1. Place mice in the imaging chamber in the supine position and use the manifold nose cone to maintain anesthesia (isoflurane 1.5%) throughout the experiment. Image up to 5 mice simultaneously and separate the animals using the light baffle to prevent reflection.

3.2.2. Close the door and click on Acquire to start the imaging sequence.

3.2.3. Fill in detailed information about the experiment (wild type and knockout animals, treatments, day of imaging, etc.). The imaging settings, such as exposure time, are saved automatically.

3.2.4. Remove mice from the imaging chamber and return them to their cage. Check for the full recovery after anesthesia. Within minutes, the animals should be fully awake and explorative. Do not provide analgesia as this might interfere with the UTI course.

3.2.5. Return the cages to the ventilated racks until the next imaging cycle. After completion of the experiment, euthanize the animals by CO2 asphyxiation or cervical dislocation. Do this before the recovery of isoflurane anesthesia to minimize distress.

3.3. Analysis of the images

3.3.1. Start the imaging software and load the experimental file by clicking on Browse.

3.3.2. Use the Tool Palette to adjust the color scale of the image. Standardize the visual aspect of the results by using the same settings for all the images, i.e., use a logarithmic scale with a minimum of 10^4 to a maximum of 10^7 photons. These adjustments do not affect the raw data but only the graphical presentation.

3.3.3. Use the ROI tools to draw a region of interest (ROI) on the image. Ensure the ROI is large enough to cover the complete area and use the same dimensions for all the images. Here, a square ROI of 3.5 cm x 4.5 cm was placed over the lower abdomen.

3.3.4. Click on ROI measurement to quantify the light intensity (counts or total photon flux). Export these data and use the average of the technical replicates.

NOTE: Counts represent the number of photons detected by the camera and should only be used for the image quality control. To report data, use total photon flux. Total photon flux is more physiologically relevant as it represents the light emitted from the surface and it is a calibrated unit, which is corrected for the exposure time (per second).

REPRESENTATIVE RESULTS

In vivo BLI correlates with CFU of the inoculum at time of instillation.

To evaluate the detection limit of BLI in vivo and the correlation with CFU of the inoculum, mice were infected with different concentrations of UTI89-*lux* and PBS as a negative control. Before instillation, uninfected animals were scanned to determine the background luminescence. Subsequent images were obtained immediately post-instillation (Figure 1A). After the instillation of UTI89-lux, bioluminescence was robustly detectable above 2 x 10^4 CFU and a linear correlation between the CFU of the inoculum and the bioluminescence was established (Figure 1B). In contrast, total photon flux was comparable to background signals for animals instilled with PBS and at the lowest bacterial concentration of 2 x 10^3 CFU.

BLI as a tool for longitudinal follow-up during treatment

To determine whether the curative effect of a validated antibiotic treatment can be demonstrated using longitudinal BLI, 20 animals were infected with an inoculum of 2 x 10^7 CFU/50 µL, and 10 of these animals were treated with enrofloxacin 10 mg/kg subcutaneously twice daily during the first 3 days post-infection. Both the natural evolution in the infected but untreated control group and the effect of antibiotic treatment on the infection kinetics in the treated group could be visualized in detail (Figure 2). An immediate decrease in bacterial load, as measured by total photon flux, was seen after the first dose of enrofloxacin. None of the treated animals had a subsequent rise in bacterial load. The inter-subject variability in the infected but untreated control group was higher and the decrease in bacterial load was slower. At day 10, 8 out of 10 animals of the control group had returned to a BLI signal comparable to their pre-instillation background. The overall bacterial load for each animal was calculated using the area under the curve (AUC) of the log-transformed total photon flux. A significant difference was observed between animals treated with enrofloxacin and untreated animals over the time course of 10 days. These results

demonstrate that BLI is a powerful tool to evaluate the effect of a potential treatment on the disease course of a UTI.

FIGURE AND TABLE LEGENDS

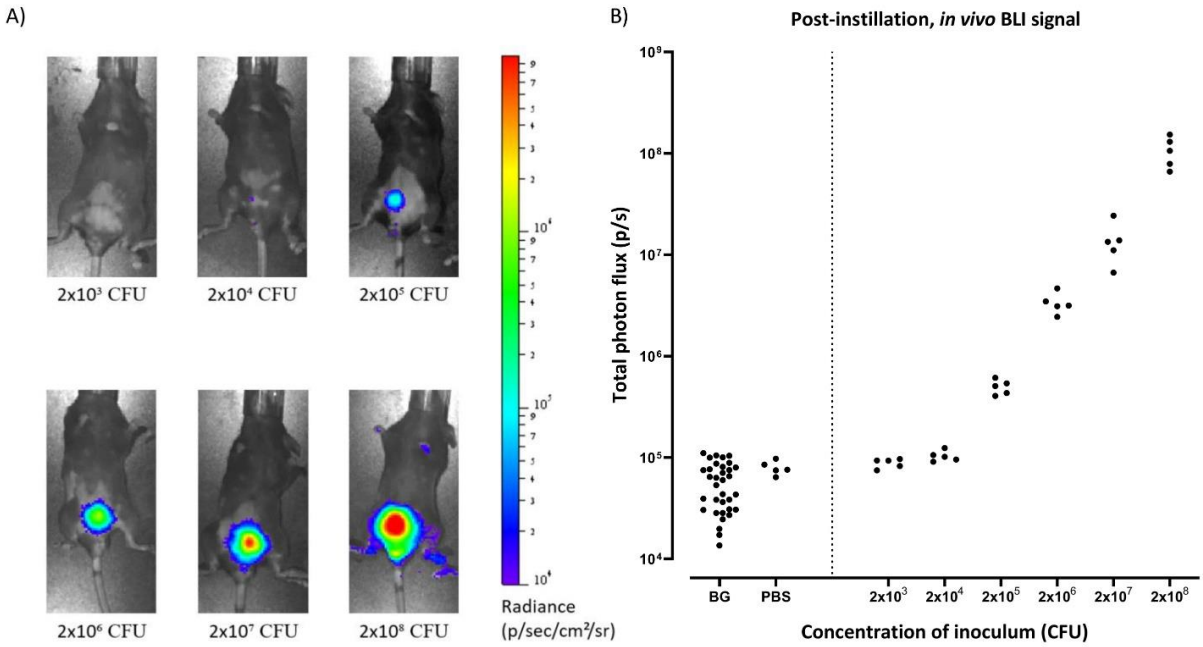

Figure 1: In vivo BLI correlates with CFU of the inoculum at the time of instillation. (a) *Representative images obtained with in vivo BLI of mice infected with increasing concentrations of inoculum (2 x 10^3–2 x 10^8 CFU) imaged immediately after bacterial instillation in the bladder. CFU = Colony Forming Units.* ***(b)*** *Quantification of bioluminescence emitted over the bladder region (total photon flux) compared to the concentration of the inoculum (CFU). BLI signal was robustly detected above 2 x 10^4 CFU ($p = 0.0002$ compared to background and $p = 0.015$ compared to the PBS control, unpaired t-test). Pearson correlation for the inoculi ranging from 2 x 10^3–2 x 10^8 CFU was $r = 0.9995$ ($p < 0.0001$). BG = background, PBS = Phosphate Buffered Saline, CFU = Colony Forming Units.*

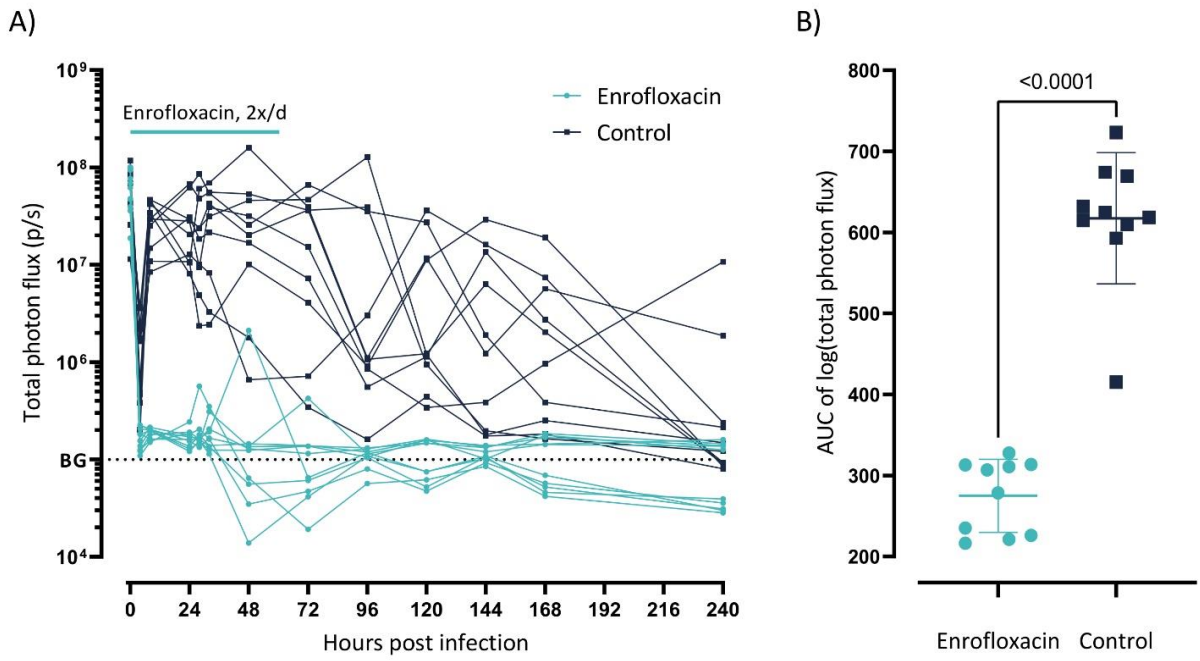

***Figure 2: BLI as a tool for longitudinal follow-up during treatment**. **(a)** Individual traces of the total photon flux for animals infected with 2 x 10^7 CFU of UTI89-lux and treated with enrofloxacin 10 mg/kg twice daily for 3 days (blue) versus an untreated control group (black), n = 10 per group. BG = background. **(b)** Analysis of traces from animals shown in panel a, reporting the AUC of log-transformed total photon flux for both the enrofloxacin (blue) and control group (black). N = 10 per group, mean ± SD, unpaired t-test p < 0.0001. AUC = Area under the curve.*

DISCUSSION

Advantages of BLI compared to CFU counts

Longitudinal data

A major disadvantage of the traditional method of counting CFU to quantify microbial burden is the requirement of post-mortem organ homogenates, providing only one cross-sectional data point per animal. Conversely, BLI enables non-invasive longitudinal follow-up of infected animals. The animals can be imaged 2 to 3 times a day, providing detailed insight into the kinetics of the infection. Additionally, repeated measures of the same animal drastically reduce the number of animals needed for adequately powered experiments. Furthermore, researchers can focus on the inter-individual variability and prior to examining or treating animals with a novel agent, they

can select animals with prespecified bacterial loads by using the real-time data. On the other hand, using the AUC of an experiment allows researchers to focus on the overall bacterial load and not on a single cross-sectional value. The added value of longitudinal and real-time data in the UTI setting cannot be overestimated.

Identification of dissemination of the infection

The spatial resolution of the images obtained with BLI is adequate to identify other sites that are colonized by *lux*- or *FLuc*-tagged pathogens[123]. For UTI, ascending infections to the kidneys or dissemination to the blood are highly relevant findings. In this experimental setting, any spread of infections induced by UTI89-*lux* beyond the lower urinary tract was not observed. This was expected considering this strain predominantly causes cystitis.

Data reproducibility and comparison

The reproducibility of experiments is higher when using BLI compared to CFU counts. Classically, triplicates of serial 10-fold dilutions of homogenates are plated and only those plates with 30 to 300 CFU are then counted to calculate the total number of CFU. This method is cumbersome, prone to high variability, results in many futile plates, and is extremely prone to human errors. Furthermore, there is no consensus on how to report the CFU, namely, per gram bladder tissue, per bladder, or per 1 mL homogenate. This renders the comparison of the results of different groups extremely difficult and could be ameliorated by the use of BLI and total photon flux.

Considerations and limitations of the method

Besides the classical considerations related to BLI *in vivo* such as absorption of photons by fur or hemoglobin, there are some considerations to be made when correlating BLI and CFU counts at the time of sacrifice.

First, discrepancies between both methods at the time of sacrifice are encountered[124], especially when antibiotic therapies are used. Therefore, the correlation between BLI and CFU counts at the time of sacrifice can be suboptimal and is not necessarily relevant. For BLI, the total photon flux can be lower than expected, because challenged bacteria can redirect their metabolism toward recovery and repair processes, rather than light emission. Additionally, the BLI measurement captures a snapshot of the

bacteria and their metabolism in real-time *in vivo*, resulting in lower BLI signals if bacteria are in a dormant or elongated state at the time of imaging. On the other hand, for CFU determination, drug-challenged bacteria react in an all-or-nothing manner after being removed from their infectious habitat (i.e., a biofilm) and plated. Once plated onto agar, the challenged bacteria may be irretrievably injured and unable to develop into observable colonies, resulting in lower CFU counts[125]. Additionally, challenged bacteria can enter a viable but non culturable state (VBNC). They remain metabolically active and viable but are no longer culturable on standard laboratory media. Bacteria that enter the VBNC state or that are organized in biofilms can be detected easily with BLI, while enumeration of CFU requires additional processing[125-127]. In conclusion, bioluminescence and viable counts measure different aspects of cell physiology and neither should be regarded as the definitive indicator of cell viability[125].

Moreover, the definition of bacterial load as measured by BLI or CFU counts is different due to differences in sample processing. When using CFU counts, only bacteria that reside within the bladder wall are included in the homogenate and counted. By contrast, BLI also captures photons emitted by bacteria in the urine and the urethra. In our opinion, the latter is a physiologically more correct representation of the total bacterial load as it includes all anatomically relevant compartments (bladder, urine, and urethra).

In contrast to CFU counts, BLI requires the generation of genetically altered luminescent bacteria. Depending on the insertion site, it is plausible that the introduction of the *lux* operon in the genome can alter the virulence potential of the bacterial strain. Therefore, when developing a new bioluminescent strain, its virulence and growth characteristics should be compared to the parental strain[112,117]. However, recent advances in genome editing allow for efficient and scarless tagging of all major bacterial pathogens, thereby limiting the impact on virulence or treatment responses. Moreover, genetic engineering opens possibilities toward conditional expression of bioluminescence reporter genes and, therefore, *in vivo* measuring of relevant bacterial subpopulations, gene expression, etc[128,129].

Finally, access to the advanced imaging device and acquisition software for *in vivo* BLI might be a limiting factor compared to the basic equipment required for CFU

enumeration. However, collaborations with imaging cores can minimize the expenses and investments necessary for BLI.

Considerations specific to the implementation of BLI in an *in vivo* UTI model

Animal model

The advantages of a murine UTI model are three-fold: It allows monitoring of disease progression in a mammalian urinary tract, the animals and their maintenance are relatively inexpensive, and mutant lines are available. On the other hand, induction of the infection usually entails transurethral catheterization and subsequent instillation of a high dosage of bacteria directly into the bladder lumen, thereby bypassing the natural process of ascension via the urethra[113,114].

Animal housing

Animals can be group housed during the experiment. We have examined the occurrence of transmission between animals of the same cage, by introducing sentinel animals into cages with infected animals. None of the sentinel animals had a detectable bacterial load, measured with both CFU and BLI.

Bladder volume

When combining the murine UTI model with BLI, researchers should keep the unique anatomical properties of the bladder in mind. The bladder is a hollow organ that contains a varying volume of urine. During UTI, the presence of bacteria-infested urine could theoretically influence the total photon count depending on the degree of bladder filling. However, standardization of the bladder volume is impractical and could intervene with the experimental design. Furthermore, in our experience, differences in bladder volume do not result in statistically significant differences in total photon flux.

Sample temperature

In vitro BLI (or as a simpler and cheaper alternative, measuring bioluminescence in a luminometer) can also be used to determine bacterial load on homogenates, urine, or bacterial suspensions containing UTI89-*lux*. However, the temperature of the sample is important as the emission of photons results from an enzymatic reaction and thus requires metabolic activity and the presence of oxygen. Drastic changes in

temperature during organ harvesting should be avoided by allowing the sample to calibrate on the heated (37 °C) stage 5 min prior to imaging.

Potential applications and importance

In summary, the cumbersome method of enumeration of CFU was limiting the reproducibility and efficacy of research in the UTI field. The experimental setup with BLI will advance in vivo UTI research on bladder physiology, UTI pathogenesis, and susceptibility by enabling longitudinal follow-up, while reducing the number of animals needed for these types of studies.

ACKNOWLEDGMENTS

This work was supported by grants from the Research Foundation — Flanders (FWO Vlaanderen; G0A6113N), the Research Council of KU Leuven (C1-TRPLe; T.V. and W.E.) and the VIB (to T.V.). W.E. is a senior clinical researcher of the Research Foundation — Flanders (FWO Vlaanderen). The strain UTI89-lux was a generous gift from Prof. Seed's laboratory.

DISCLOSURES

The authors declare no conflicts of interest.

CHAPTER 2

Urothelial cells respond to a viable bacterial solution with release of calcium from the intracellular stores in an PLC-dependent manner

Noémie Luyts, Brett Boonen, Annelies Janssens, Silvia Pinto, Thomas Voets, Wouter Everaerts

2. Urothelial cells respond to a viable bacterial solution with release of calcium from the intracellular stores in an PLC-dependent manner

ABSTRACT

Background and purpose: Bacterial infections of the urinary tract are amongst the most common infections in humans. The bacteria causing urinary tract infections (UTIs) have become increasingly resistant to antibiotics, making them more difficult to eradicate. Previous research has demonstrated a rise in intracellular Ca^{2+} concentrations in UC exposed to bacterial toxins. Here, we investigated if the exposure to viable uropathogenic *Escherichia coli* (UPEC) induces Ca^{2+} responses in UC and which molecular pathways were involved.

Experimental approach: The effect of UPEC (UTI89-*lux*, 4 x 10^8 CFU /mL) on urothelial cells was investigated using Fura-2-based calcium measurements. Potential mechanisms underlying UPEC-induced calcium responses were examined using genetic ablation of the known endotoxin receptors TLR4 and TRPV4 and pharmacological modulation of key calcium signaling components. The time course of UTI onset and resolution were examined using bioluminescence imaging (BLI).

Key results: Urothelial cells exposed to UPEC demonstrated a rapid increase in intracellular Ca^{2+} levels. In *Tlr4*- and *Trpv4*-deficient UC and mice, the calcium responses and bacterial clearance were preserved. A significant increase in intracellular Ca^{2+} concentration was observed upon UPEC stimulation in a calcium-free environment, indicating the involvement of Ca^{2+} release from the intracellular stores. Responses were abrogated upon application of Thapsigargin and U73122, agents known to deplete intracellular Ca^{2+} stores and inhibit phospholipase C (PLC) respectively.

Conclusion and implications: We have demonstrated that UPEC trigger calcium responses in UC. These responses are independent of the TRPV4 and TLR4 pathway and depend on PLC-dependent calcium release from intracellular stores. These observations indicate that intravesical bacteria can trigger a rapid response in the urothelial cell layer via yet unidentified PLC-coupled membrane receptors.

INTRODUCTION

Bacterial infections of the urinary tract are amongst the most common infections in humans. Community acquired UTIs are predominantly caused by uropathogenic *Escherichia coli* (UPEC), accounting for approximately 80% of these infections[1]. Antibiotics are the cornerstone in the treatment of UTIs, but their excessive use is thought to cause the evolution of multidrug-resistant microorganisms globally and to complicate the treatment of UTIs in general[10]. A better understanding of the host-pathogen interactions is driving the development of novel therapeutic agents[2,44]. Despite the efforts made, the complex relationship between bacteria and urothelial cells (UC) needs to be further elucidated to find novel practice-changing strategies.

Urothelial cells lining the urinary tract play an important role in the defense against intruding pathogens. This epithelium, with the outermost umbrella cell layer, serves as a high-resistance barrier and acts as a first responder upon recognition of bacterial virulence factors[34]. UPEC are equipped with a variety of virulence factors including toxins, fimbrial adhesins, iron-acquisition systems and flagella, which enable them to overcome the urothelial defense systems resulting in colonization, adherence and invasion of the bladder wall[9]. The activation of urothelial cells by virulence factors causes a plethora of downstream effects, resulting in a balanced immune response to pathogens and toxins, in order to maintain the structural integrity of the barrier[19]. This is an intriguing equilibrium, as severe acute inflammatory responses early in infection predisposes to chronic and recurrent infections in mice[43]. This study aims to further characterize the initial responses of urothelial cells to intruding bacteria.

To study these responses, previous research has focused on the interaction between host and pathogen, using specific bacterial components. For example, lipopolysaccharide (LPS), an endotoxin located on the outer membrane of Gram-negative bacteria, is known to activate the Toll-like receptor 4 (TLR4) signaling pathway, which results in the activation of the transcriptional factor nuclear factor kappa B (NF-ƙB), and thereby the regulation of immunomodulatory cytokines[49]. Additionally, LPS has been identified as a direct activator of the cation channel TRPV4, causing a rise in intracellular Ca^{2+} concentrations in UC, independently of the canonical TLR4 signaling pathway[93]. In addition to TLR4 and TRP channels, urothelial cells express purinergic (P2) receptors, including ionotropic P2X and the G-protein coupled

P2Y receptors. P2Y receptors have been considered in the context of detecting damage, with ATP as a crucial damage-associated molecular pattern (DAMP). In addition, recent findings point to a more active role of P2 receptors in the response to infections, as they have been implicated in regulating host immunity and modulating phagocytosis, chemotaxis, efferocytosis and cytokine production[78,130]. On the side of the pathogen, an important role in the establishment of a successful infection was attributed to the adhesin FimH on type 1 pili of UPEC. FimH interacts with uroplakins (UP) expressed on the umbrella cells, which results in a rise in intracellular calcium levels[37].

Despite the various studies that identified bacterial toxins and their molecular targets on urothelial cells, their contribution to acute responses of the urothelial layer to intact bacteria remained poorly understood. Here, we investigated acute Ca^{2+} responses in UC to suspensions of viable UPEC, and evaluated potential molecular pathways involved in these responses.

MATERIALS & METHODS

All experiments using animals were approved by the KU Leuven Ethical Committee Laboratory Animals under project number P158/2018 (*in vivo*) or P184/2021 (*in vitro*).

Cell culture

Primary urothelial cells were isolated from 10 to 12 week old C57Bl/6 mice and cultured as previously described[42]. Briefly, after euthanasia, bladders were removed, cut open, and stretched out on a Sylgard-coated dish containing MEM (Invitrogen) with 2.5 mg/ml Dispase (Invitrogen) for 2-3 h at room temperature. Next, the urothelium was gently scraped from the tissue, treated with trypsin-EDTA (Invitrogen), and resuspended in defined keratinocyte serum-free medium (Invitrogen). The cell suspension was plated on type IV collagen-coated coverslips and incubated overnight at 37°C and 5% CO_2 to ensure attachment.

Calcium imaging

For intracellular Ca^{2+} measurements, cells were incubated with 2 µM Fura-2 acetoxymethyl (AM) ester for 30 min at 37°C. The intracellular Ca^{2+} concentration ($[Ca^{2+}]_i$) was monitored through the ratio of fluorescence measured upon alternating

illumination at 340 and 380 nm, using an MT-10 illumination system and cell^{M} software (Olympus). Absolute calcium concentrations were calculated from the ratio of the fluorescence signals at both wavelengths (F_{340}/F_{380}) after correction for the individual background fluorescence signals, using the Grynkiewicz equation[111]

$$[Ca^{2+}] = K_{eff}\,\frac{R - R_0}{R_1 - R}$$

where the calibration constants R_0, R_1 and K_{eff} were determined from *in vitro* calibrations using droplets of Fura-2AM-containing solution with known calcium concentrations.

The cells were perfused using a gravity-based perfusion system with solutions containing (in mM) 150 NaCl, 6 KCl, 2 $CaCl_2$, 1.5 $MgCl_2$, 10 HEPES, and 10 Glucose and titrated to pH 7.4 with NaOH. Calcium free solution contained (in mM) 150 NaCl, 6 KCl, 1.5 $MgCl_2$, 10 HEPES, 10 Glucose and 1 EGTA. All compounds were obtained from Sigma-Aldrich and were dissolved in the bath solution containing 0 or 2 mM Ca^{2+} as indicated in the individual experiments.

Bacterial culture

The bioluminescent UPEC strain, UTI89-*lux,* was cultured statically overnight at 37°C in an incubator, in Luria-Bretani (LB) broth supplemented with 50 µg/mL kanamycin sulfate, before being diluted 1/100 into fresh LB broth without antibiotics and grown statically for an additional 24h at 37°C. Subsequently, cultures were centrifuged, and the bacterial pellet was resuspended until a concentration of 4 x 10^8 CFU per mL was reached. For each experiment, a fresh bacterial culture was obtained.

Bioluminescence imaging

Bioluminescence imaging was performed as described previously[131]. Briefly, Isoflurane (5% induction and 1.5% maintenance) was used to anesthetize C57BL/6 mice. The animals were placed in the IVIS spectrum® system (Perkin Elmer, Waltham, USA) in supine position and were imaged before instillation, immediately after instillation and various hours or days post-infection. All images were acquired using the IVIS Spectrum with an exposure time of 30-60 seconds, F/stop of 1, field of view D, medium binning, and a subject height of 1 cm. The exposure time was reduced when image saturation occurred. Images were acquired in triplicate. The total photon

flux (photons/s/cm^2/sr) in defined regions of interest was quantified using the Living Image software package (Xenogen) and was used as a read-out for the bacterial load.

Error! Not a valid link. Statistics

Statistical analysis and graphing was performed in OriginPro 9.0. Results were considered significant if the two-sided p-value was smaller than 0.05. Tests used for statistical comparison between groups are indicated in the in the text and legends. Except where indicated otherwise, all summary data are reported as mean ± SEM.

RESULTS

First, we determined the responses of urothelial cells to a viable suspension UPEC (UTI89-*lux*, 4 x 10^8 CFU /mL) by performing intracellular Ca^{2+} recordings in UC isolated from wild type (WT) mice. We observed a rapid and transient rise in intracellular Ca^{2+} levels in the UC exposed to UPEC (fig. 1a). In these experiments, ATP was used to confirm viability of the cells whereas the TRPV4 agonist GSK1016790A (GSK) was used to determine TRPV4-expressing cells. Most cells responded to UPEC, GSK and ATP (37.1%). Interestingly, 18.2% of the cells responded to UPEC and ATP but not GSK. And the minority of the cells (9.8%) responded to GSK and ATP but not to UPEC. Taken together, these results indicated that viable bacteria can induce a calcium response in UC.

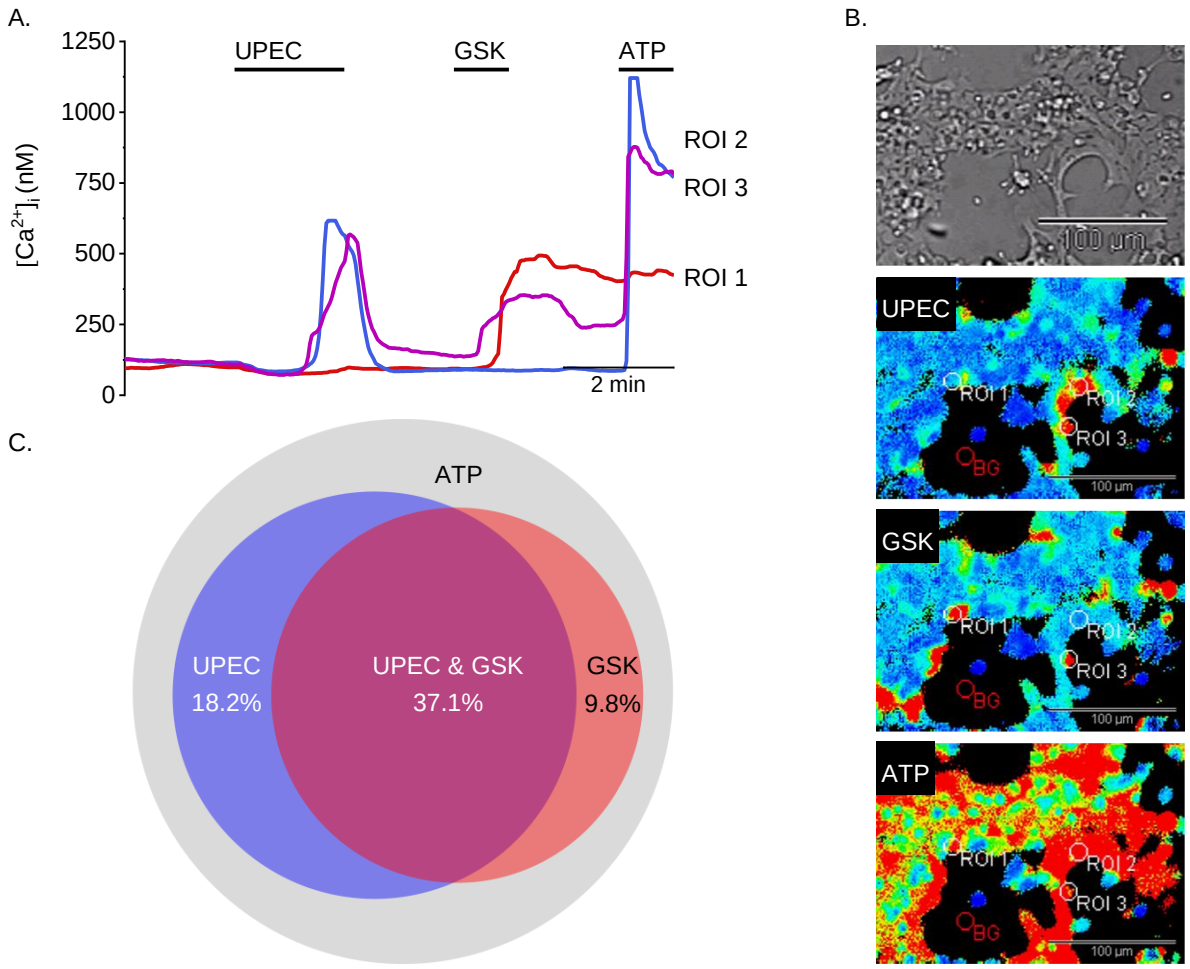

Figure 1. Urothelial cells respond to a bacterial suspension of uropathogenic E. coli (UPEC). (a) *Representative traces of intracellular Ca^{2+} recordings in urothelial cells, in response to UPEC (4 x 10^8 CFU /mL of UTI89-lux), GSK1016790A (10 nM) a potent TRPV4 agonist and ATP (100 µM). Responses to ATP were used to identify viable cells.* ***(b)*** *Microscopic image of a primary urothelial cell culture taken with the objective 40x, scale bar is 100 µm. The next three images represent fluorescence. Pseudo-color image (low calcium (blue), high calcium (red)) of the ratio of 340/380 during stimulation with UPEC, GSK and ATP. The indicated region of interests (ROI) correspond to the traces in panel a. The background (BG) fluorescence is subtracted. (c) Proportional Venn diagram demonstrating the proportion of cells responding to different stimuli. Only cells responsive to ATP were included in the analysis (n = 132).*

The bacterial toxin LPS has previously been demonstrated to evoke urothelial responses, through activation of the metabotropic receptor TLR4 as well as the ion channel TRPV4. Therefore, we evaluated their role in the responses to UPEC using cells harvested from *Trpv4*- or *Tlr4*-deficient animals. Notably, responses to UPEC were preserved in both *Trpv4*-deficient UC (fig. 2a,f) and *Tlr4*-deficient UC. Moreover, robust calcium responses were observed in *Tlr4*-deficient UC treated with the TRPV4 antagonist HC-0674047 or the non-selective cation channel inhibitor ruthenium red (RR). Moreover, responses to UPEC were preserved in the presence of polymyxin B, a compound that sequesters free LPS. Taken together, these data indicate that UC can respond to UPEC independent of LPS-mediated mechanism.

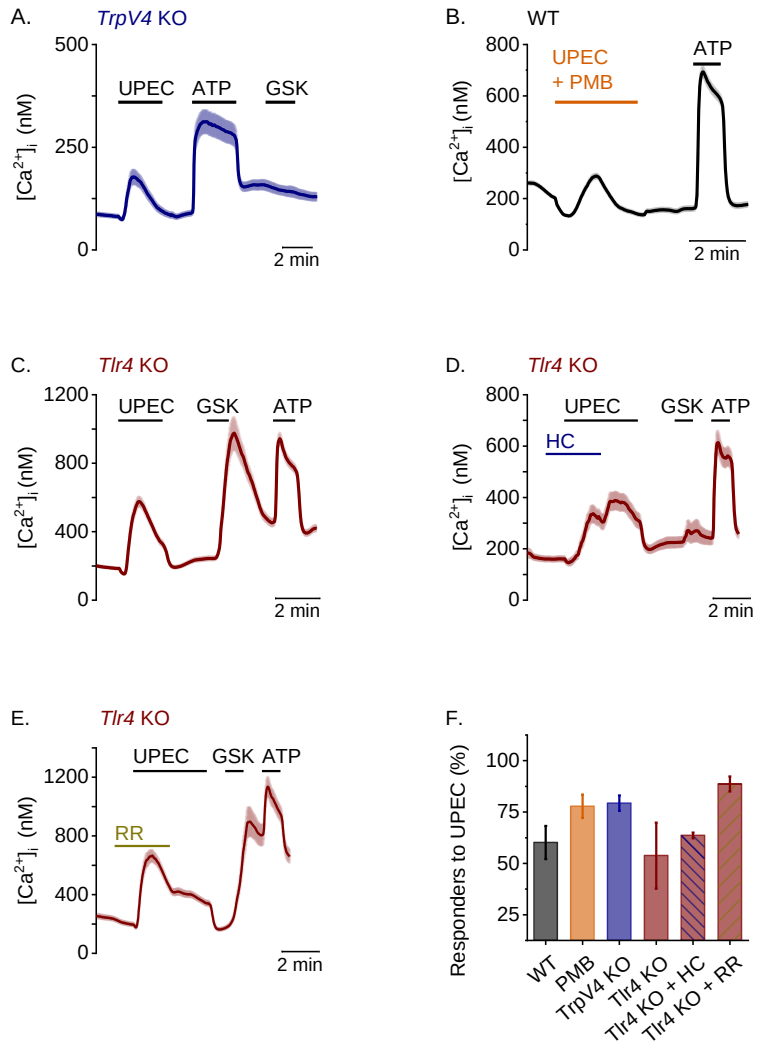

***Figure 2**. **Acute calcium responses evoked by UPEC in TrpV4 and Tlr4-deficient UC. (a-e)** Representative averaged trace of intracellular Ca^{2+} recordings in UC cultured from (**a**) Trpv4 KO **(b)** WT, **(c-e)** Tlr4 KO mice in response UPEC (4 x 10^8 CFU /mL of UTI89-lux), GSK1016790A (10 nM) and ATP (100 µM). **(b)** Polymyxin B (PMB, 300 µg/mL) was added to the bacterial suspension at least 30 min prior to application to sequester all the LPS. The blocking capacities of (**d**) HC-067047 (10 µM), **(e)** ruthenium red (2 µM) were assessed during UPEC (4 x 10^8 CFU /mL of UTI89-lux) stimulation. **(f)** Percentage of responders to UPEC in WT UC (60.2% ± 8.0%; n = 132), Trpv4 KO UC (79% ± 3.8%; n = 362), WT UC in the presence of PMB (78% ± 5.7%; n 443), Tlr4 KO UC (54% ± 16%; n 336), Tlr4 KO UC in the presence of HC-067047 (63.6% ± 1.4%; n 142) and Tlr4 KO UC in the presence of ruthenium red (89% ± 3.7%; n 111). Unpaired student t-test was used to compare the percentage of responders of the KO UC to WT. Data is represented as mean ± SEM.*

Given the indispensable role attributed to TLR4 in pathogen recognition and initiation of immune responses[132], and the altered voiding pattern seen in *TrpV4*-deficient mice, we sought to investigate differences in UTI kinetics *in vivo*. We used bioluminescence imaging to measure the total photon flux emitted after intravesical administration of UTI89-*lux* (50 µL containing 2 x 10^7 CFU) to determine the bacterial load in WT, *TrpV4*- and *Tlr4*-deficient mice. First, we followed both WT and *Trpv4*-deficient animals longitudinally: the animals were imaged at multiple time points post infection, with the latest time point at 6 days. An initial rise in total photon flux was seen after induction of the infection, followed by a rapid decrease, which we attribute to voiding (fig 3a). Subsequently, the bacteria were able to replicate in the bladder and afterwards a slow spontaneous resolution occurred. Overall, the course of the infection was indistinguishable between WT and *TrpV4*-deficient mice (fig. 3a). Likewise, the area under the curve, a global quantification of bacterial load during the entire period, was not significantly different between both groups (fig 3b).

To determine the effect of *Tlr4*-deficiency on UTI kinetics, WT and *Tlr4*-deficient animals were infected twice, at day 0 and day 1, to model a chronic infection. Again, the course of the infection was similar for the WT and *Tlr4*-deficient animals throughout the follow-up period (fig. 3c,d). Taken together, these findings do not provide support for the hypothesis that TRPV4 or TLR4 play a key role in the defense mechanism against bladder infection in mice. However, the findings are consistent with our in vitro results showing the existence of TRPV4- and TLR4-independent acute responses to UPEC in UC, pointing at the existence of alternative pathways leading to rapid urothelial response signals to bacteria.

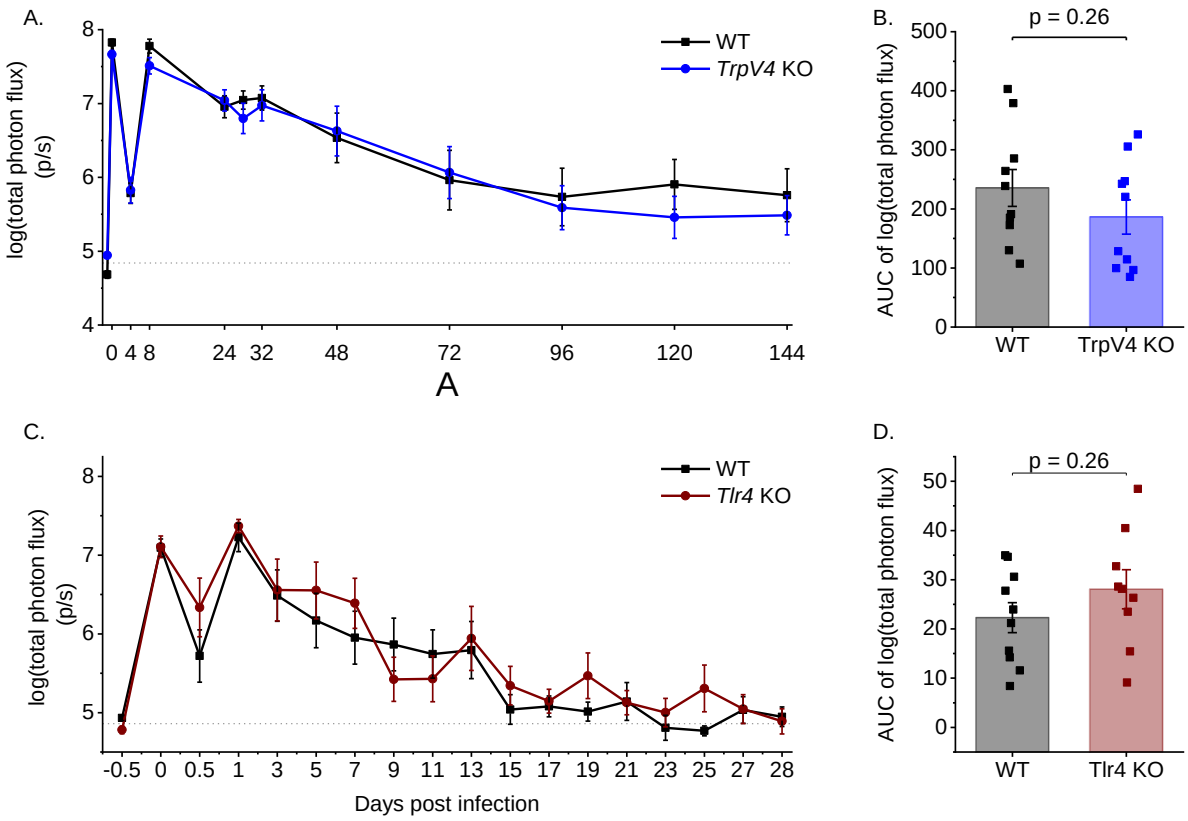

Figure 3. The role of TRPV4 and TLR4 in UTI kinetics. ***(a, c)*** *Imaging of mice was performed using the IVIS Spectrum® system. Traces represent the mean ± SEM of the log(total photon flux) in a region of interest placed over the bladders of animals at various time points post infection (intravesical instillation of 50 µL containing 2 x 10^7 CFU of UTI89-lux). Imaging was performed pre-instillation and the mean background value is shown as the dotted line, as a reference.* ***(a)*** *WT (black) and Trpv4-deficient (blue) mice were infected at day 0 and followed for 144 hours post infection.* ***(b)*** *AUC of the traces in graph A, n = 10 per group. Bars represent mean ± SEM, unpaired t-test p = 0.26* ***(c)*** *WT (black) and Tlr4-deficient (red) mice were infected at both day 0 and day 1 and were followed for 28 days post infection.* ***(d)*** *AUC of the traces in graph C, n = 10 per group. Bars represent mean ± SEM, unpaired t-test p = 0.26*

As a first step to identify the nature of this alternative pathway, we analyzed responses of UC to UPEC in the absence of extracellular calcium (fig. 4a-c). A significant increase in intracellular Ca^{2+} was observed upon UPEC stimulation in a calcium-free environment (fig. 4a), indicating the UPEC response does not critically rely on Ca^{2+} influx. Moreover, the calcium response was fully abrogated upon prior depletion of the intracellular Ca^{2+} stores by the application of the SERCA pump inhibitor thapsigargin (fig. 4b), indicating that the responses represent Ca^{2+} release from intracellular stores. To test the involvement of calcium release via phospholipase C (PLC) coupled receptors, we tested UPEC responses in the presence of the PLC antagonist U73122 or its inactive analog U73343. Notably, U73122 fully suppressed the UPEC-evoked calcium increase, whereas U73343 was ineffective. Taken together, these findings indicate that UPEC causes a rise in intracellular calcium in UC via activation of a PLC-coupled membrane receptor, leading to calcium release from IP_3-sensitive intracellular stores.

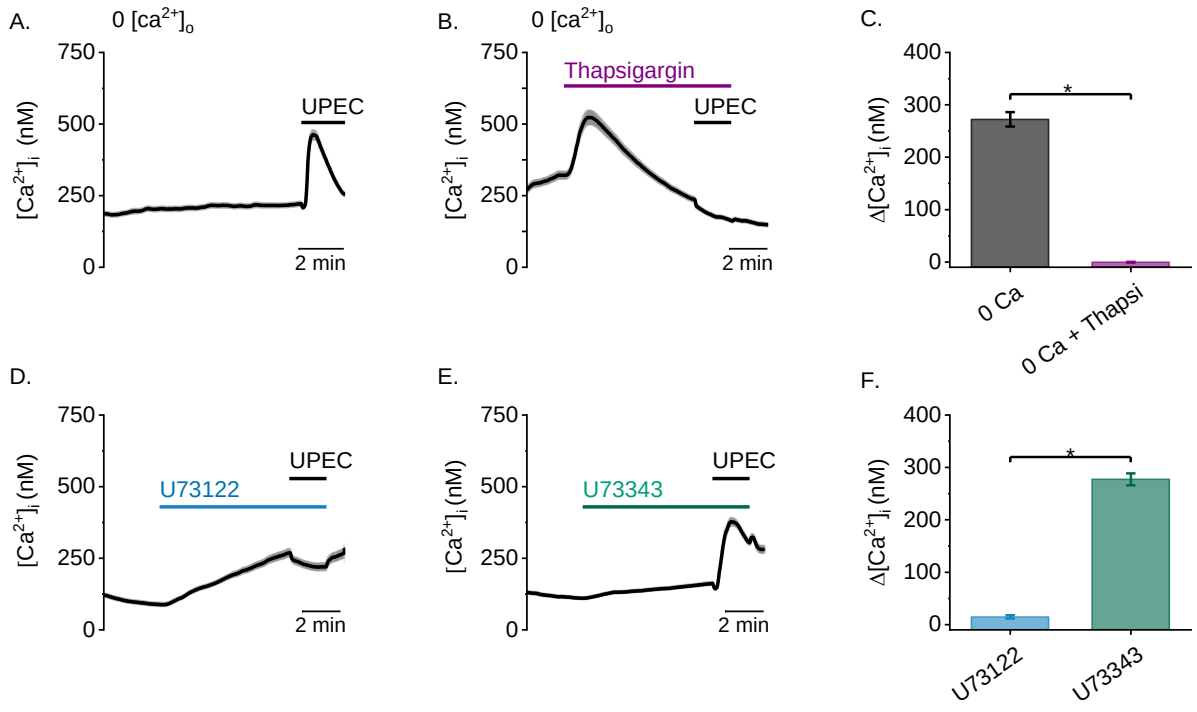

***Figure 4. The UPEC-induced responses originate from Ca^{2+} release from intracellular Ca^{2+} stores**. **(a-b-d-e)** Representative average intracellular Ca^{2+} signals recorded in UC isolated from wild type mice. **(a)** The responses to UPEC (4 x 10^8 CFU /mL of UTI89-lux) stimulation, were assessed in an extracellular calcium-free environment. **(b)** Representative average trace of intracellular Ca^{2+} signals recorded upon application of Thapsigargin (2 µM) in an extracellular Ca^{2+}-free environment. **(c)** Mean amplitudes of intracellular Ca^{2+} responses evoked by UPEC in the absence of extracellular Ca^{2+} (272 ± 14 nM; n = 170,) and during application of 2 µM Thapsigargin (-0.53 ± 0.65 nM; n = 626). **(d)** U73122 (10µM), a phospholipase C inhibitor, was applied in the presence of extracellular calcium (2 mM). **(e)** U73343 (10µM), the inactive analog of U73122, was used as a negative control for PLC inhibition. **(f)** Mean amplitudes of intracellular Ca^{2+} responses evoked by UPEC during application of 10 µM U73122 (15 ± 3.1 nM; n= 219) and application of 10µM U73343 (277 ± 11 nM; n = 189). The bars represent mean ± SEM, unpaired t-test, * p < 0.0001.*

Urothelial cells abundantly expressed the G-protein coupled P2Y receptors, including P2Y1, P2Y2, P2Y4, P2Y6 and P2Y11, which can mediate rapid calcium responses to ATP. To investigate the possible role of P2Y receptors in the UPEC response in UC, we used a cocktail of the potent antagonists of P2Y subtypes, MRS 2279 (500 nM), AR-C118925XX (10 µM), MRS 2578 (1 µM) and NF157 (4 µM) to inhibit P2Y1, P2Y2, P2Y6, and P2Y11, respectively. In the presence of this inhibitor cocktail, responses to UPEC remained intact, whereas the ATP responses were fully abrogated (fig. 5a-d). In summary, these results indicate that P2Y receptors are not the main target of UPEC and allow us to exclude a crucial role for bacterial ATP in evoking UPEC-induced calcium release in UC.

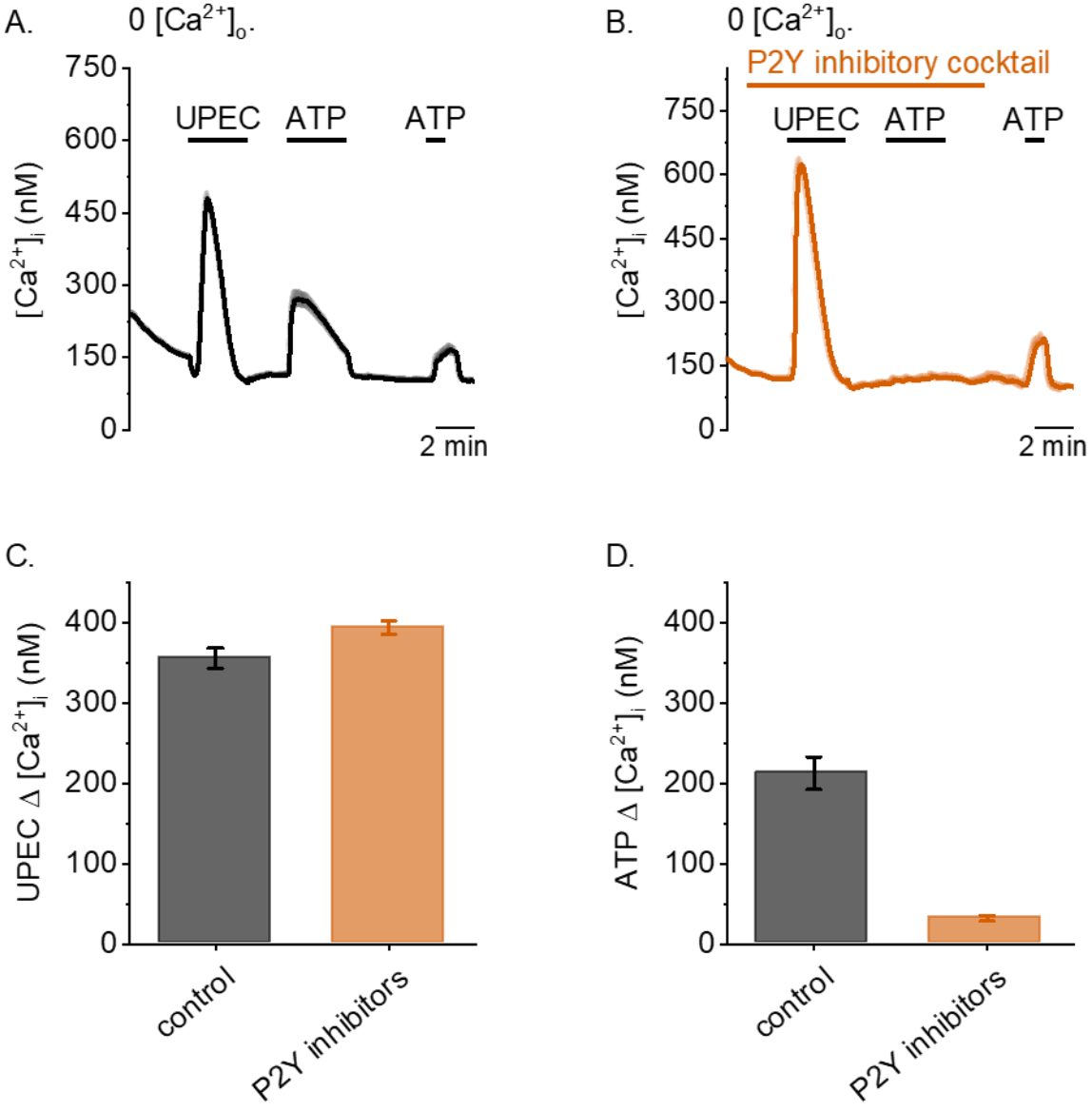

Figure 5. The UPEC induced responses are not P2Y-receptor dependent. (A-B) *Representative average intracellular Ca^{2+} signals recorded in UC in the absence of Ca^{2+}excellularly.* ***(a)*** *Urothelial cells respond to the application of UPEC (4 x 10^8 CFU /mL of UTI89-lux) and ATP (10µM).* ***(b)*** *MRS 2279 (500 nM), AR-C118925XX (10 µM), MRS 2578 (1 µM) and NF157 (4 µM) were combined to inhibit P2Y1, P2Y2, P2Y6 and P2Y11 respectively. UPEC responses were unaltered in the presence of the P2Y inhibitors.* ***(c)*** *Mean amplitudes of intracellular Ca^{2+} responses evoked by UPEC (355 ± 13 nM; n = 198) and during application of the P2Y inhibitory cocktail (393 ± 8.7 nM; n = 768).* ***(d)*** *Mean amplitudes of intracellular Ca^{2+} responses evoked by ATP (213 ± 20 nM; n = 198) and during application of the P2Y inhibitors (32 ± 3.5 nM; n = 768). Data are represented as mean ± SEM.*

DISCUSSION

We have demonstrated that a bacterial suspension triggers rapid, transient calcium responses in urothelial cells. These responses remained intact in *Trpv4*- or *Tlr4*-deficient UC. One of the most used models to study UTIs is the intravesical instillation of LPS as a substitute for bacterial infection. Despite the crucial role of TLR4 in sensing LPS[132], our results indicate that, in the case of live bacterial infection, the lack of TLR4 does not alter UTI clearance kinetics. This indicates that other pathways are involved in the recognition of uropathogens and host-pathogen responses. Recently, TLR4-independent pathways were shown to sense LPS, such as TRPV4 and Caspase-4/5[49]. Besides the role for TRPV4 as an LPS sensor, the channel contributes to mechanosensation of the urothelium and plays an important role in normal bladder function. Mice lacking *TrpV4* have an altered voiding pattern, with increased intercontractile intervals (ICI)[79]. We hypothesized that a longer ICI reduces the expulsion of bacteria infested urine and therefore increases the UTI susceptibility. However, using our longitudinal murine UTI model, we did not observe any alteration in UTI clearance kinetics in *TrpV4*-deficient animals.

In order to elucidate mechanisms underlying the observed UPEC-induced responses, we differentiated between extracellular Ca^{2+} influx and Ca^{2+} release from intracellular stores. These experiments clearly indicated that UPEC induced calcium-release from intracellular stores, via a PLC-dependent pathway. The molecular nature of the PLC-coupled receptor remains unknown, but we were able to exclude a major contribution of the abundantly expressed P2Y purinergic receptors.

Several bacterial toxins and virulence factors have been implicated in the induction of calcium responses in other epithelial cell types. In renal epithelial cells, α-Hemolysin (HlyA) from UPEC induced calcium oscillations and the release of interleukin-6 (IL-6). Both the oscillations and release of pro-inflammatory cytokines were dependent on ATP-mediated P2 receptor signaling, and more specifically $P2Y_2$ played a crucial role[133]. From our data, in urothelial cells a central role for P2Y receptors or ATP signaling could be excluded. A pathway similar to the proposed pathway in our study was found for *Salmonella typhimurium* in colonic epithelial cells. The flagellin fliC of *S. typhimurium* increased $[Ca^{2+}]_i$ via IP_3, which was followed by an activation of nuclear factor kappa B (NF-ƙB) and cytokine production. The chelation of intracellular Ca^{2+} or inhibition of PLC (U73122) resulted in an inhibition NF-ƙB activation[134]. Additionally, in airway and urothelial cells, LPS from gram-negative bacteria has been shown to

increase $[Ca^{2+}]_i$ and trigger protective responses, such as nitric oxide (NO) production and nuclear translocation of NF-ƙB[82,93,94]. Indeed, it would be of interest to investigate whether the UPEC-induced calcium increase in UC leads to similar downstream effects, such as nuclear translocation of NF-ƙB and NO production, as previously demonstrated for LPS.

Previous research has been performed on immortalized urothelial cell lines or using a single bacterial component such as HlyA, FimH or LPS[37,94,133]. These studies have unraveled crucial pathways involving individual bacterial components important in UTIs. However, the clinical disease always results from live bacterial colonization, which was mimicked in the present study using an approach using live bacterial cultures. A potential drawback of this approach is that intrinsic variations in the bacterial preparations may affect the responses[66]. Nevertheless, in our experiments we were able to reproducibly evoke robust calcium signals in a large number of urothelial cell preparations and bacterial cultures, making this approach suitable for future studies aimed at identifying the molecular target underlying the observed acute UPEC responses.

CONCLUSION

We have demonstrated that a live bacterial suspension triggers calcium responses in UC. These responses were independent of the TRPV4 and TLR4 pathways and are mediated by intracellular calcium release via a PLC-dependent pathway. Further research is required to identify the molecular nature of the PLC-coupled receptors that initiate this acute cellular response to pathogenic bacteria.

CHAPTER 3

Inhibition of TRPM8 by the urinary tract analgesic drug phenazopyridine

Noémie Luyts, Jan Daniluk, Annelies Janssens, Ana Nogueira Freitas Peigneur, Marie Mulier, Wouter Everaerts, Thomas Voets

3. Inhibition of TRPM8 by the urinary tract analgesic drug phenazopyridine

submitted to the British Journal of Pharmacology – June 2022

ABSTRACT

Background and purpose: Phenazopyridine hydrochloride (PAP) is an over-the-counter drug that is widely used to provide symptomatic relief of bladder pain in conditions such as cystitis or bladder pain syndrome (BPS). Whereas the analgesic effect of PAP has been attributed to a local effect on the mucosa of the lower urinary tract (LUT), the molecular targets of PAP responsible for the observed pain relief remain unknown. Here, we investigated the effect of PAP on pain-related Transient Receptor Potential (TRP) channels expressed in sensory neurons that innervate the bladder wall.

Experimental approach: The effects of PAP on the activity of relevant TRP channels (TRPV1, TRPA1, TRPM8, TRPM3) expressed in HEK293 or CHO cells was investigated using Fura-2-based calcium measurements and whole-cell patch-clamp recordings. Activity of PAP on TRPM8 in afferent neurons was further analysed using Fura-2-based calcium imaging on sensory neurons isolated from lumbosacral dorsal root ganglia (DRG) of mice.

Key results: PAP rapidly and reversibly inhibits responses of TRPM8 expressed in HEK293 cells to cold and menthol, with IC_{50} values between 5 and 10 µM. It acts by shifting the voltage dependence of channel activation towards positive potentials, opposite to the effect of menthol. PAP also inhibits TRPM8-mediated, menthol-evoked calcium responses in lumbosacral DRG neurons. At a concentration of 10 µM, PAP did not significantly affect TRPA1, TRPV1, or TRPM3.

Conclusion and implications: PAP exerts an inhibitory effect on TRPM8, in a concentration range consistent with PAP levels in the urine of treated patients. Considering that TRPM8 is expressed in bladder afferent neurons and upregulated in patients with painful bladder disorders, local TRPM8 inhibition may contribute to the analgesic activity of PAP.

INTRODUCTION

Phenazopyridine hydrochloride (PAP) is an over-the-counter available urinary analgesic that provides symptomatic relief of pain caused by irritation of the lower urinary tract (LUT)[26,109,135]. It is clinically used in the context of urinary tract infections (UTIs)[26,136], bladder pain syndrome (BPS)[135] or as peri-operative urinary analgesic[137] to reduce symptoms of frequency, urgency or pain. Phenazopyridine was first synthesized by Chichibabin and Zeide in 1914 and was subsequently introduced into the American medical pharmacopoeia in 1928 as a urinary tract antiseptic, before the arrival of the first antibiotics[138]. It is now generally accepted that PAP has no significant bactericidal activity[139,140] and, despite the long and extensive use, the mechanisms underlying the analgesic effects of PAP are largely elusive, and its molecular targets in the LUT remain unknown.

The Transient Receptor Potential (TRP) channel superfamily represents a group of cation-permeable ion channels that respond to a wide variety of physical and chemical stimuli, allowing them to function as polymodal cellular sensors and making them indispensable for many homeostatic and sensory processes[65]. Several TRP channels have been described to participate in sensory processes in the urinary bladder. In particular, TRPA1, TRPV1, TRPM8, and TRPM3 are expressed on sensory neurons innervating the bladder wall and have been implicated in bladder sensation and pain[5,42,102]. The goal of this study was therefore to explore the effects of PAP on these TRP channels, as a possible mechanism for PAP-induced analgesia.

MATERIALS AND METHODS

Cell culture

We used Chinese Hamster Ovary cells (CHO) stably expressing TRPA1, HEK 293 cells stably expressing human TRPM8 or human TRPM3, as well as HEK293 cells transiently transfected with 2 μg of pCAGGS/IRES-GFP vector encoding mouse TRPM8 or human TRPV1, linked to expression of GFP allowing identification of transfected cells. Cells were transfected using TransIT-293 transfection reagent (BioMirus) 24h before the measurement. All cells were cultured in DMEM high glucose (Thermo Fisher) supplemented with 50 mL foetal bovine serum (Gibco), 10 mL penicillin/streptomycin (Gibco), 10 mL glutamax (Thermo Fisher) and 5 mL non-

essential-amino-acids (Thermo fisher). In addition to this, 1 mL hydromycin and 500 µL blasticidin were added to the culture medium of the CHO cells. Cells were kept at 37°C in 10% (HEK293 cells) or 5% (CHO cells) CO_2.

DRG culture

Bilateral L5-S1 DRGs were isolated as described previously[110]. In brief, the spinal column was isolated, cleaned, and split sagittal. The spinal cord, meninges covering the DRG, and the distal axon bundles were removed. DRGs were washed in neurobasal A medium (Invitrogen) supplemented with 10% fetal calf serum (basal medium), and then incubated for 1 h at 37°C in a mix of 1.5 mg /mL collagenase and 2.5 mg /mL dispase (Gibco). Digested ganglia were gently washed twice with basal medium and subsequently washed twice in neurobasal A medium supplemented with B27 (Invitrogen), 2 ng /mL GDNF (Invitrogen), 10 ng /mL NT4 (Peprotech), 1% (v/v) Glutamax (Gibco) and penicillin 50 units /mL—streptomycin 50 µg /mL (Gibco) (complete medium). 1 mL of complete medium plus 1 mL of bovine serum albumin (BSA) solution (16% w/v in PBS) were added to the ganglia. Cells were mechanically dissociated by passage through syringes fitted with increasing needle gauges. The cell suspension was added on top of a 3 mL BSA solution (16% w/v in PBS) and centrifuged at 500 × g for 6 min. The supernatant was discarded, and the pellet was resuspended in complete medium. Neurons were seeded on poly-L-lysine/laminin coated glass-bottom chambers (Fluorodish, WPI) and cultured overnight at 37°C in 5% CO_2 in complete medium.

Measurement of intracellular Ca^{2+} concentration.

For intracellular Ca^{2+} measurements, cells were incubated with 2 µM Fura-2 acetoxymethyl (AM) ester for 30 min at 37°C. The intracellular Ca^{2+} concentration ($[Ca^{2+}]_i$) was monitored through the ratio of fluorescence measured upon alternating illumination at 340 and 380 nm, using an MT-10 illumination system and cell^M software (Olympus). Absolute calcium concentrations were calculated from the ratio of the fluorescence signals at both wavelengths (F_{340}/F_{380}) after correction for the individual background fluorescence signals, using the Grynkiewicz equation[111]

$$[\mathrm{Ca}^{2+}] = K_{eff}\,\frac{R - R_0}{R_1 - R}$$

where the calibration constants R_0, R_1 and K_{eff} were determined from *in vitro* calibrations using droplets of Fura-2AM-containing solution with known calcium concentrations

Patch-clamp experiments.

Membrane currents were measured in the whole-cell mode of the patch-clamp technique using an EPC-10 amplifier and Patchmaster software (HEKA Elektronik). Patch electrodes had a direct current (DC) resistance between 2 and 4 MΩ when filled with intracellular solution. Currents were sampled at 20 kHz and digitally filtered at 2.9 kHz. Between 50 and 70% of the series resistance was electronically compensated to minimize voltage errors. The holding potential in all experiments was 0 mV. A ramp protocol was applied consisting of 500-ms linear voltage ramps, applied at 0.5 Hz, from -100 mV to +100 mV (TRPM8), -100 mV to +150 mV (TRPM3), or -100 mV to +160 mV (TRPV1). For TRPM8, we also used a voltage step protocol, consisting of 100-ms steps to voltages ranging from -120 to +160 mV, followed by a 50-ms step to +60 mV. The standard extracellular solution for electrophysiological measurements contained (in mM) 150 NaCl, 1 $MgCl_2$ 10 HEPES (pH 7.4 with NaOH). Depending on the type of investigated channel, the pipette solution was composed of (in mM) 100 CsAsp, 45 CsCl, 10 EGTA, 10 HEPES, 1 $MgCl_2$ (pH 7.2 with CsOH) (TRPM3), 150 NaCl, 1 $MgCl_2$, 10 HEPES, 5 EGTA (pH 7.2 with NaOH) (TRPV1), or 150 NaCl, 5 $MgCl_2$, 5 EGTA, 10 HEPES (pH 7.2 with NaOH) (TRPM8). All measurements were carried out at room temperature (22–25°C).

Statistical analysis

Statistical analysis and graphing were performed in OriginPro. Results were considered significant if the two-sided p-value was smaller than 0.05. Except where indicated otherwise, all summary data are reported as mean ± SEM.

RESULTS

Several studies have demonstrated an increased expression of TRPM8 on bladder sensory neurons in patients with BPS, suggesting a correlation between TRPM8 and bladder pain[101,102]. To investigate whether PAP affects TRPM8 activity, we performed intracellular Ca^{2+} imaging experiments on HEK293 cells expressing murine TRPM8. We observed a concentration-dependent and reversible inhibition of menthol-induced TRPM8 responses by PAP, with an IC_{50} value of 9.5 ± 0.7 µM (fig. 1a-b). Similarly, PAP (30 µM) strongly suppressed TRPM8-dependent calcium responses to cold stimulation (normalized response: 16 ± 4%) (fig. 1c-d).

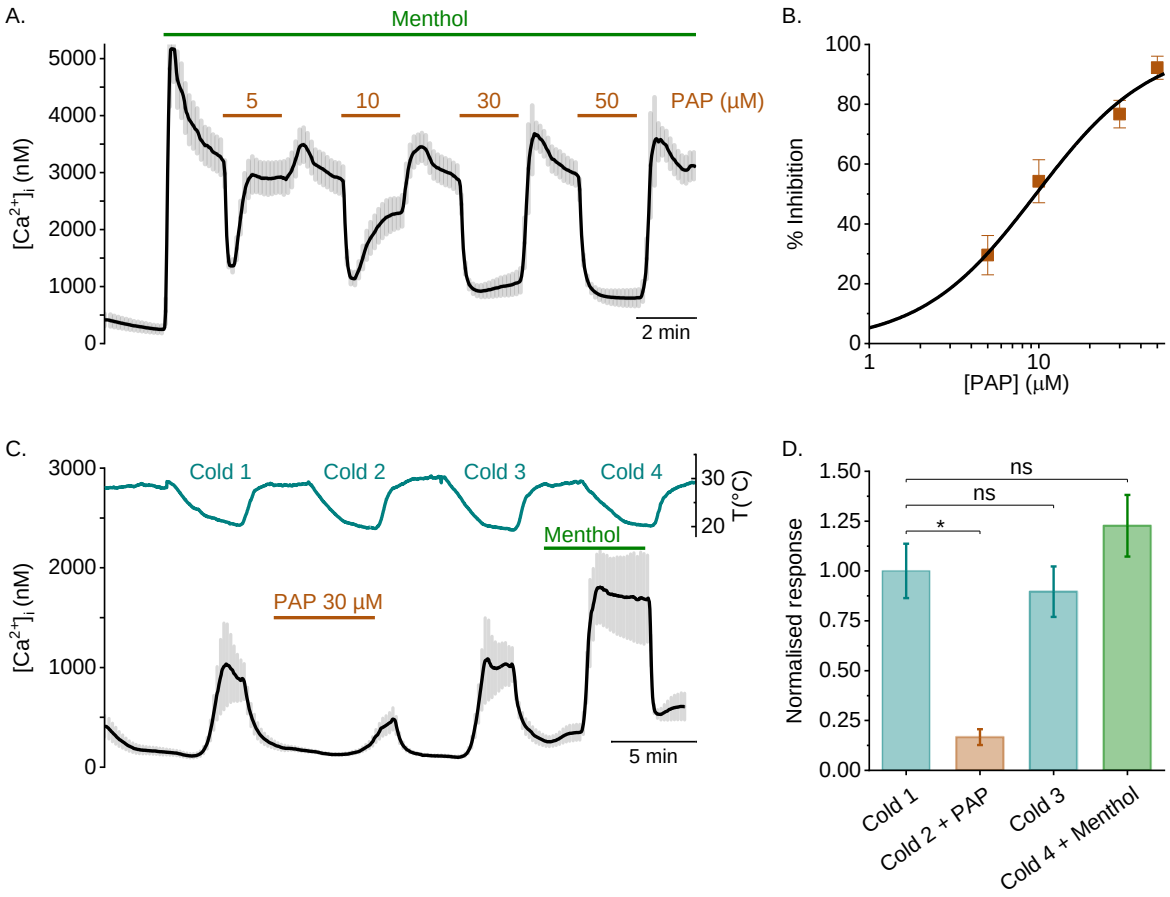

Figure 1. PAP inhibits menthol and cold-induced TRPM8-mediated calcium responses. ***(a)*** *Representative average trace of mTrpm8 HEK293 cells during continuous stimulation with menthol (50 μM) and upon application of increasing PAP concentrations.* ***(b)*** *Concentration dependences of the percentage of inhibition of PAP on menthol (50 μM)-evoked intracellular Ca^{2+} responses in mTRPM8 HEK293 cells. The solid line represents the fit using the Hill equation (n = 23).* ***(c)*** *Representative average trace of mTrpm8 HEK293 cells, stimulated with cold solution (20 °C) in the absence or presence of either PAP (30 μM) or menthol (50 μM).* ***(d)*** *Calcium amplitudes normalised to the first cold application. Upon application of PAP (30 μM) the responses were significantly reduced. Repeated Measures One-Way ANOVA, Dunnett test pairwise comparison of the first cold stimulus compared to cold + PAP, cold and cold + menthol ($p < 0.0001$, $p = 0.69$, $p = 0.13$. respectively, n= 40).*

In patch-clamp recordings, currents on HEK293 cells expressing human *TRPM8*, application of PAP caused a rapid and reversible inhibition of the whole-cell currents in response to voltage-ramps (fig. 2a-b). The inhibitory effect of PAP was more pronounced for inward than for outward currents, with IC_{50} values of 5.7 ± 0.7 µM and 13.7 ± 0.4 µM at -80 mV and +80mV, respectively (fig. 2c).

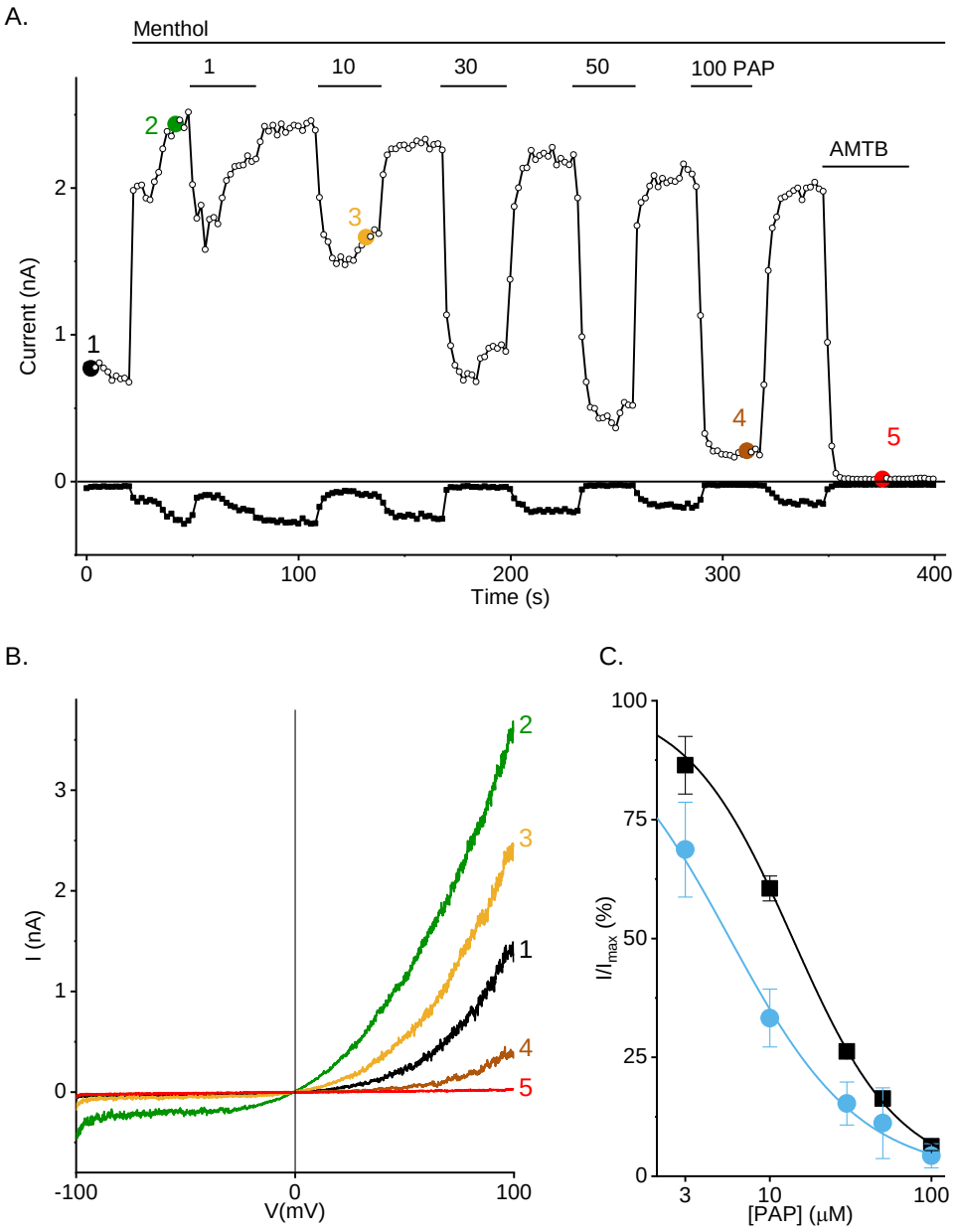

Figure 2. Inhibitory effect of PAP on whole-cell TRPM8 currents. (a) *Representative trace of the whole cell TRPM8 current recorded in HEK293 cells expressing human TRPM8. Shown are currents at +80 mV and –80 mV measured during 500-ms linear voltage ramps from -100 to +100 mV upon application of menthol (50 μM) and subsequent treatment with increasing concentrations of PAP (1, 10, 30, 50, and 100 μM). AMTB (10 μM) was used as positive control.* ***(b)*** *Current-voltage relationship at the time points indicated in (a).* ***(c)*** *Dose response relationship of PAP for TRPM8. Data points are represented as mean current values ± SEM at +80 mV (black) and –80 mV (blue), fitted to a Hill curve (n = 5).*

TRPM8 is a voltage-dependent, depolarization-activated channel, and stimuli such as cold and menthol activate the channel by shifting the voltage dependence of activation towards more negative potentials[141,142]. To analyse the effects of PAP on voltage-dependent gating, we measured whole-cell currents during voltage steps ranging from -120 mV to +160 mV in the absence or presence of menthol (50 µM) and various concentrations of PAP. These experiments revealed that PAP shifts the voltage dependence of TRPM8 towards more positive potentials in a concentration-dependent manner, thus opposing the effects of menthol (fig. 3a-c). Taken together, these findings reveal that PAP is an antagonist of TRPM8.

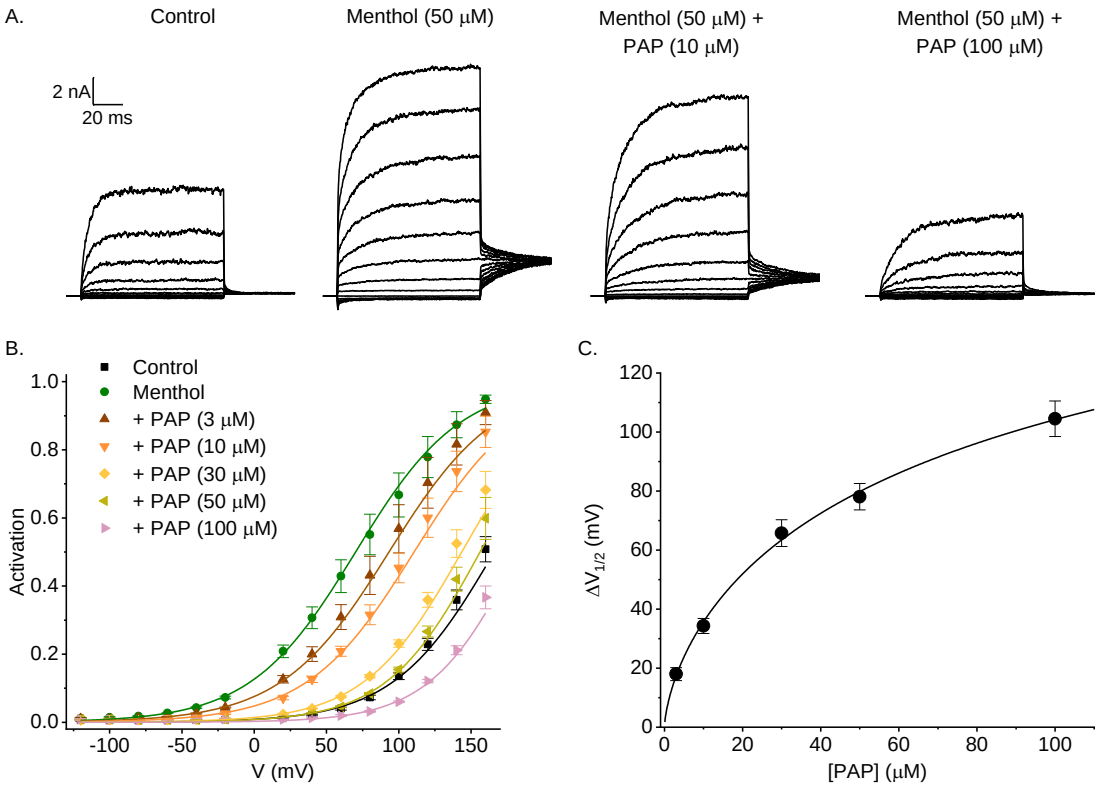

***Figure 3. Effect of PAP on the voltage dependence of TRPM8 activation**. **(a)** TRPM8 currents in response to a step protocol, consisting of 100-ms steps to potentials ranging from -120 to +160 mV followed by a step to +60 mV, illustrating the effect of menthol and PAP on voltage-dependent gating. **(b)** Voltage-dependent activation curves in the indicated conditions (n=5), determined as the steady-state conductance from traces as in (a), normalised to the maximal conductance. Solid lines indicate fits using the Boltzmann equation. **(c)** Concentration dependence of the PAP-induced shift of the midpoints of the voltage-dependent activation curves presented in (b).*

Next, we evaluated the effects of PAP on other TRP channels that are expressed in bladder-innervating sensory neurons. In whole-cell recordings on HEK293 cells expressing human *TRPM3*, PAP (10 µM) did not noticeably affect currents activated by the neurosteroid agonist pregnenolone sulphate, whereas full inhibition was observed with the flavonoid antagonist Isosakuranetin (fig. 4a-c). Similarly, capsaicin-activated whole-cell currents in HEK293 cells expressing human *TRPV1* were unaffected by PAP (10 µM) but fully abolished by the TRPV1 antagonist AMG517 (fig. 4d-f).

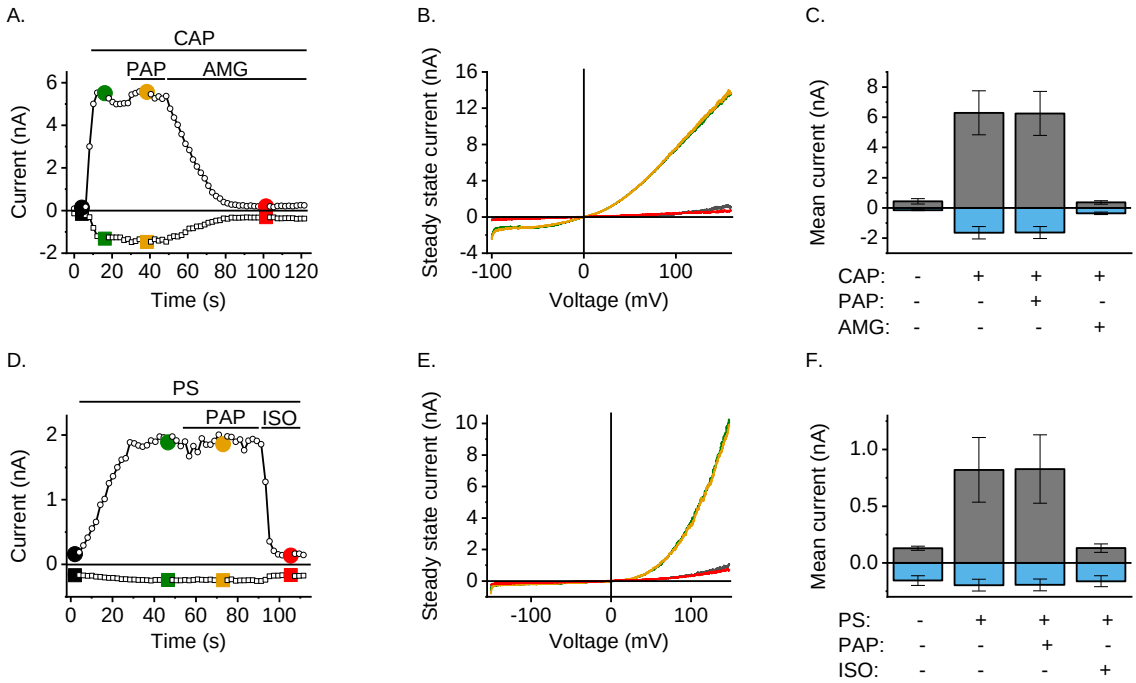

Figure 4. The effects of PAP on other sensory TRP channels. (a) *Representative time course of whole cell TRPV1 current at +80 mV and –80 mV upon application of capsaicin (CAP, 50 nM) and subsequent treatment with 10 µM of PAP. AMG 517 (10 nM) was used as positive control.* ***(b)*** *Current-voltage relationship at the time points indicated in (a).* ***(c)*** *Mean whole cell TRPV1 current at +80 mV (grey) and –80 mV (blue). Data are represented as mean ± SEM (n = 5).* ***(d)*** *Representative time course of whole cell TRPM3 current at +80 mV and –80 mV upon application of pregnenolone sulfate (PS, 40 µM) and subsequent treatment with 10 µM of PAP. Isosakuranetin (ISO, 5 µM) was used as positive control.* ***(e****) Current-voltage relationship at the time points indicated in (d).* ***(f)*** *Mean whole cell TRPM3 current at +80 mV (grey) and –80 mV (blue). Data are represented as mean ± SEM (n = 5).*

Intracellular Ca^{2+} imaging experiments on TRPA1-expressing CHO cells further showed that application of PAP at a concentration of 10 µM did not inhibit the response to the TRPA1 agonist AITC (100 µM) (fig. 5a). In contrast, we observed a small increase in intracellular Ca^{2+} when PAP was applied following stimulation with AITC (fig. 5a), suggesting that it may have an agonistic effect on the channel. Indeed, when applying PAP to TRPA1-expressing CHO cells, we observed sizeable and concentration-dependent increases in cytosolic calcium at concentrations ≥30 µM (fig. 5b-c). However, at the highest test concentration of PAP (100 µM), the amplitude of the calcium response amounted to only 42.4 ± 8.1% of the response to AITC (50 µM), suggesting that PAP is a relatively weak TRPA1 agonist.

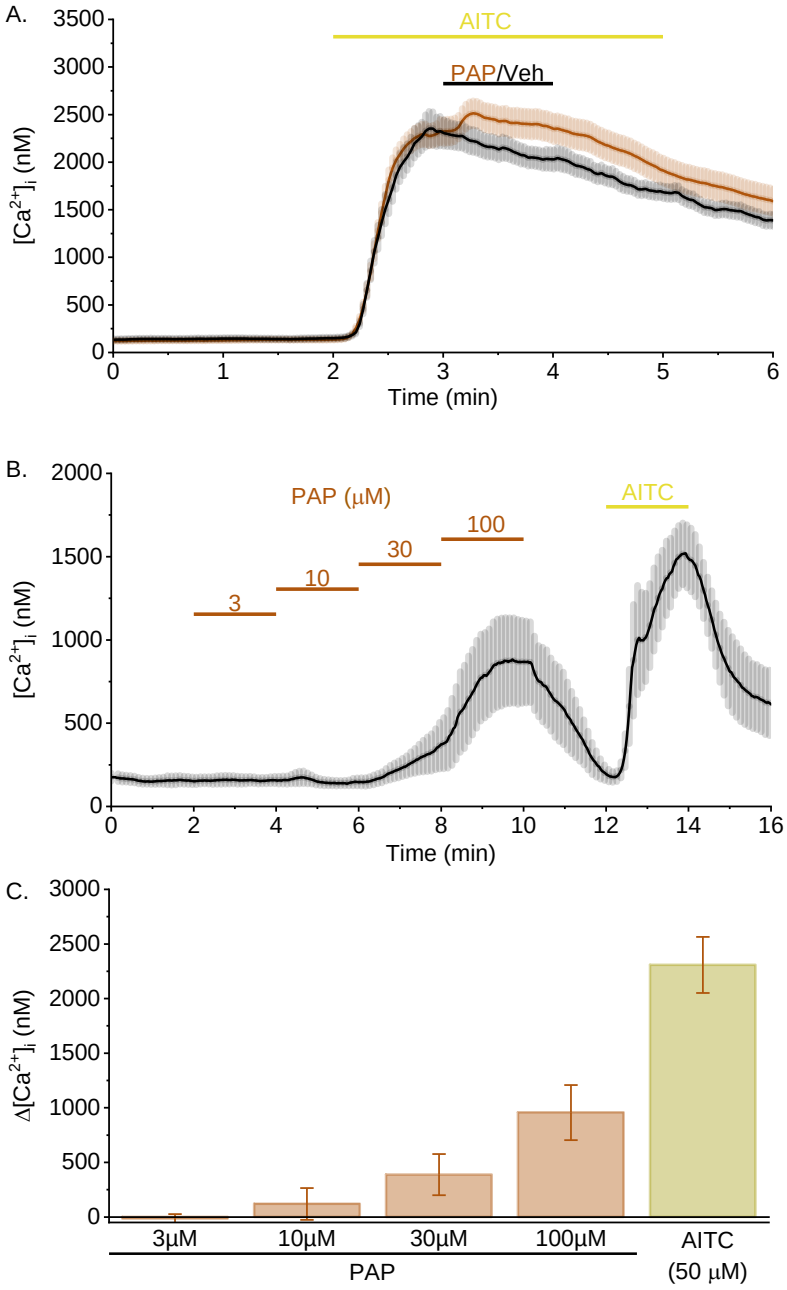

Figure 5. PAP has a small agonistic effect on TRPA1. (a) *Representative average trace of intracellular Ca^{2+} responses upon application of AITC (100 μM) alone (black trace), or upon application of AITC (100 μM) and PAP (10 μM) (brown trace).* ***(b)*** *Representative average trace of CHO cells stably expressing TRPA1 upon application of increasing PAP concentrations (3, 10, 30, 100 μM) and application of AITC (50 μM), as a positive control.* ***(c)*** *Calcium amplitudes upon application of PAP (3, 10, 30, 100 μM) and AITC (50 μM). Bars represent mean ± SEM (n = 20).*

Finally, we evaluated the effect of PAP in isolated dorsal root ganglion neurons (DRGs) from mice, harvested from the spinal levels that innervate the bladder (L5-S1). In line with earlier studies, we detected menthol responses in a small subset of these neurons (9.4%, n = 596). Since menthol can act as an activator, not only of TRPM8 but also of TRPA1, we used allyl isothiocyanate (AITC) to differentiate between TRPM8- and TRPA1-mediated menthol responders (fig. 6a-b). In the AITC-negative, menthol responsive neurons (7.7%), which we identify as *Trpm8* expressing neurons, 50 µM PAP caused a rapid and robust reversal of the calcium signal (79 ± 5 % inhibition), which only partially recovered upon wash-out (fig. 6c). The menthol responses in AITC-positive neurons, which we identify as TRPA1 neurons, were mostly transient in nature and not affected by PAP. In conclusion, our results demonstrate that PAP acts as an inhibitor of TRPM8 activity, both in a heterologous expression system and in primary sensory neurons.

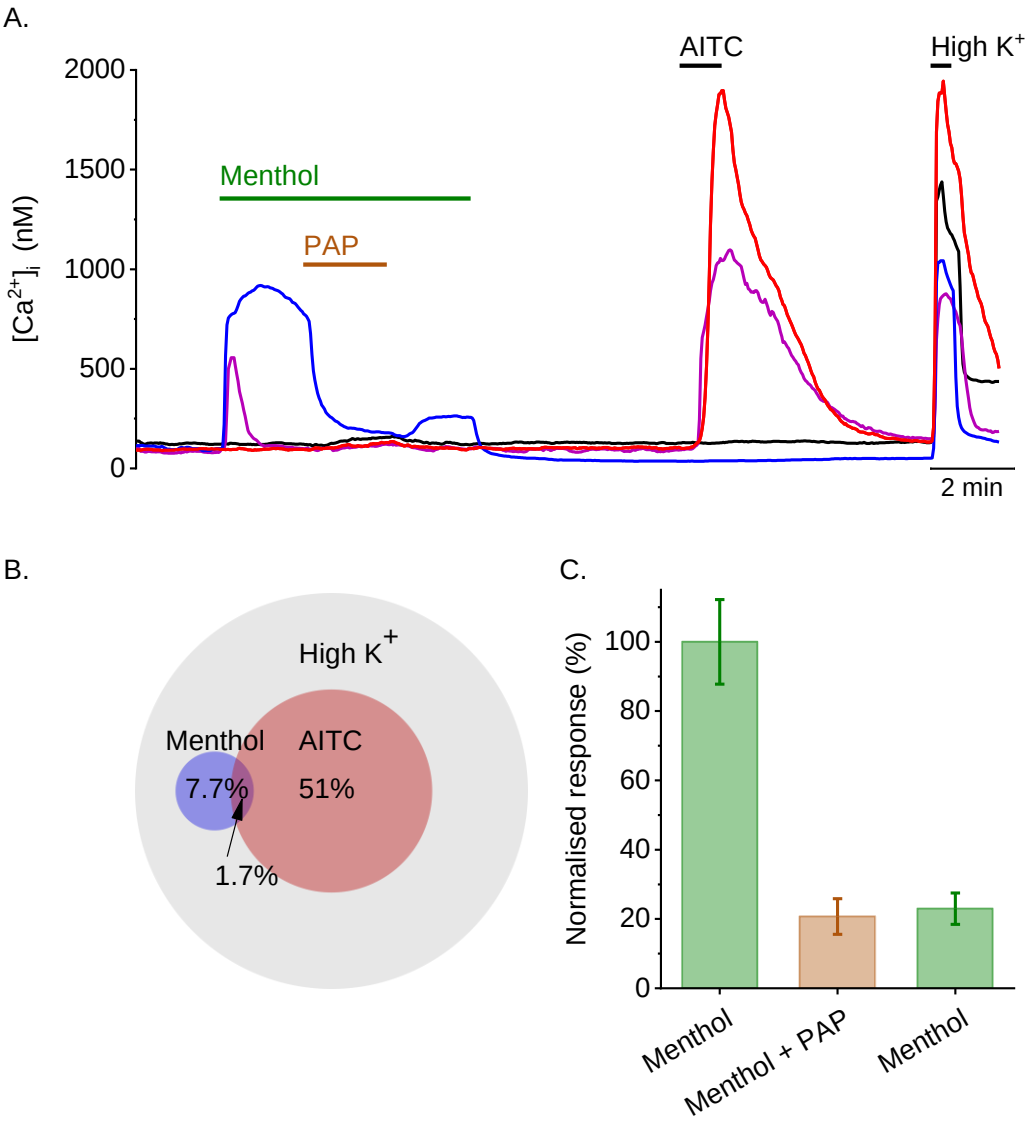

Figure 6. PAP inhibits menthol-induced TRPM8 responses in DRG neurons. (a) *Representative time course of the intracellular calcium concentration in murine DRGs from vertebral levels L5-S1, showing responses to menthol (50 µM) and AITC (100 µM), and inhibition of the menthol induced response by PAP (50 µM). A high K^+-solution (50 mM) was used to distinguish neurons from non-neuronal cells.* ***(b)*** *The percentages of cells responding to Menthol (blue), AITC (red) or both (purple) were 7.7%, 51% and 1.7% respectively (n = 596).* ***(c)*** *Responses normalised to the initial menthol response. PAP inhibits 79 ± 5 % of the menthol-induced Ca^{2+} responses. (menthol 100 ± 12%, menthol + PAP 21 ± 5%, menthol after washout 23 ± 5%; n = 36, only TRPM8-like responders, mean ± SEM).*

DISCUSSION

In this study, we have demonstrated that PAP has an inhibitory effect on the sensory ion channel TRPM8, with an IC_{50} value of approximately 10 μM. This inhibitory effect was observed for menthol- and cold-induced responses in cells heterologously expressing TRPM8 as well as in TRPM8-positive sensory DRG neurons. Furthermore, this effect showed specificity for TRPM8 amongst sensory TRP channels expressed in bladder-innervating sensory neurons: TRPM3 and TRPV1 were not noticeably affected by PAP at 10 μM, whereas PAP had a mild agonistic effect on TRPA1 at concentrations >10 μM.

Several selective TRPM8 antagonists have been developed for clinical testing as analgesic drugs or to treat bladder dysfunction. In preclinical studies, such compounds were found to efficiently inhibit TRPM8-dependent responses such as icilin-induced wet-dog shakes and cold-induced urinary frequency in rats[72,143,144]. However, clinical development of one of the most advanced antagonists, PF-05105679[145], was halted after phase 1 studies revealed significant adverse effects as periorally hot sensations and dysgeusia (NCT01393652)[146]. Most likely, the adverse effects of hot sensations are related to the recently identified role of TRPM8 in warmth sensation, where reduced activity of TRPM8-positive sensory neurons is perceived as warming. Since these adverse effects are likely to be on-target and were observed at free plasma concentrations of only three times the IC_{50}, levels that are also required for analgesic efficacy, it appears that systemically available TRPM8 antagonists may have a relatively low therapeutic index, hampering their clinical implementation[146,147]. In this respect, PAP has a favourable safety profile: the maximal plasma levels of PAP after oral dosing of a therapeutic dose of 200 mg in health male volunteers amounted to only ~300 nM[148], well below the concentrations needed to have a systemic effect on TRPM8 activity. The low plasma exposure can be explained by the highly efficient excretion via the urine, of which a large fraction (41%) as the unchanged drug, resulting in high micromolar to millimolar concentrations in the bladder[138,140]. As such, PAP can act as a topical TRPM8 antagonist in the bladder wall, without the unwanted side effects of systemic TRPM8 inhibition.

Earlier research had demonstrated inhibition of Aδ fibre activity by PAP, but the molecular PAP target on these nerve endings was not identified[149]. Based on molecular modelling experiments, Preynat-Seauve and colleagues identified PAP as

a kinase inhibitor, with high affinity for PIP4K2C, a crucial enzyme for phosphatidylinositol 4,5-bisphosphate (PIP_2) synthesis[150]. PIP_2 is a known TRPM8 modulator, so it can be envisaged that inhibition of PIP4K2C could decrease TRPM8 activity due to PIP_2 depletion[151,152]. However, it appears unlikely that this is the primary underlying mechanism of TRPM8 inhibition in our experiments, since we observed a rapid and reversible inhibition, unlike the slower time course of activity for PIP_2 depletion and resynthesis upon kinase inhibition[153]

PAP is often prescribed to treat bladder pain syndrome (BPS)[154] and was found to improve the symptoms in 61% of all patients[109,135]. BPS is defined as “the complaint of suprapubic pain related to bladder filling, accompanied by other symptoms such as increased day and night-time frequency, in the absence of proven urinary infection or other obvious pathology”[99]. There is a lack of knowledge about the underlying disease mechanism[154]. Wu et al. have found a higher relative density of nerve fibres and an increased expression of TRPM8 mRNA and protein in bladder tissues from patients with BPS, compared to control biopsies[102]. Other groups have confirmed the increased TRPM8 expression and the correlation with clinical symptoms[101,103]. Our finding that PAP at therapeutically relevant concentrations inhibits TRPM8 in these afferent pathways thus provides a straightforward explanation for the local analgesic effect on the lower urinary tract.

CONCLUSION

PAP, at therapeutically relevant concentrations, exerts an inhibitory effect on TRPM8. Considering that TRPM8 is expressed in bladder afferent neurons and upregulated in patients with painful bladder disorders, local TRPM8 inhibition may contribute to the analgesic activity of PAP.

GENERAL DISCUSSION

V. General discussion

Urinary tract infections (UTIs) are amongst the most common bacterial infections in humans, requiring millions of antibiotic prescriptions annually. The three main symptoms of a lower urinary tract infection are frequency, urgency and dysuria. The molecular basis of these symptoms and their role in UTI susceptibility remained to be studied. The general aim of this dissertation was to obtain a better understanding of urothelial and bladder function in response to a bacterial UTI. To this end, we optimized an *in vivo* model with longitudinal follow-up of the bacterial load and looked at the cellular and molecular responses of the urothelium to bacteria. Moreover, we investigated the mechanism of action a urinary analgesic frequently used in UTI patients, leading to new insights in its efficacy against pain-related symptoms.

In **chapter 1**, we optimized a murine UTI model and validated bioluminescent imaging as a technique to longitudinally follow up the bacterial load. At the early stages of this PhD project, it became clear that, in order to investigate UTI susceptibility and kinetics in an animal model, a reproducible, non-invasive, animal-sparing assay to study the course of UTI was indispensable.

For years, the gold standard for the enumeration of bacterial load has been the determination of Colony Forming Units (CFU). This technique requires post-mortem organ homogenates, making it impossible to obtain real-time data and follow the animals longitudinally. Furthermore, serial dilutions of the homogenates need to be plated, resulting in futile work, and limiting reproducibility. In other fields, bioluminescence imaging was gaining popularity. Using pathogens labeled with a *lux*-operon allows for sensitive detection and quantification of the bacterial load in a non-invasive and longitudinal manner[116,117]. However, adoption of BLI in the UTI research field remained limited[112], possibly due to the lack of solid validation of this technique for UTIs.

In this study, we demonstrated for the first time a linear correlation between CFU and BLI *in vivo,* immediately post-instillation of a bacterial suspension in the bladder. At later time points, discrepancies between the two methods were encountered[124,125].

However, this does not indicate the superiority of one technique above the other. Instead, the discrepancies are likely resulting from the fact that bioluminescence and viable counts measure different aspects of cell physiology, and should be regarded as complementary methods to determine the bacterial load[125]. Indeed, bioluminescence provides a measure of the metabolic activity of bacteria in the LUT, whereas CFU counts the number of individual viable bacterial cells (or clumps of cells) that survive the homogenization and isolation procedures. Most importantly, we have shown that the longitudinal model can be used to identify differences in bacterial load in a group of infected animals that were untreated *versus* animals that were treated with antibiotics.

Compared to the golden standard, BLI enables the acquisition of longitudinal and real-time data during UTI, strongly reducing the number of animals needed to obtain statistically relevant results and can easily be implemented thanks to the detailed protocol and instruction video provided in chapter 1.

In **chapter 2**, we have demonstrated that a viable bacterial suspension triggers acute calcium responses in urothelial cells. Previous research has been focusing on the interaction between host and pathogen with the use of specific bacterial components, leading to the identification of key bacterial toxins and their targets on urothelial cells. However, the relevance of these mechanistic insights on actual interactions between bacteria and urothelial cells *in vitro* and *in vivo* remained unclear.

The aim of our study was therefore to investigate the host-pathogen responses under more realistic, clinically relevant conditions, by directly applying bacterial suspension instead of isolated bacterial toxins to urothelial cells. Urothelial cells are believed to detect the presence of pathogens in the urine, resulting in a cellular signal that induces a defense response. We observed a robust rise in intracellular calcium upon application of UPEC to urothelial cells and investigated possible signaling pathways that could underlie these responses, as summarized in figure 6.

Figure 6. Cellular responses to UPEC

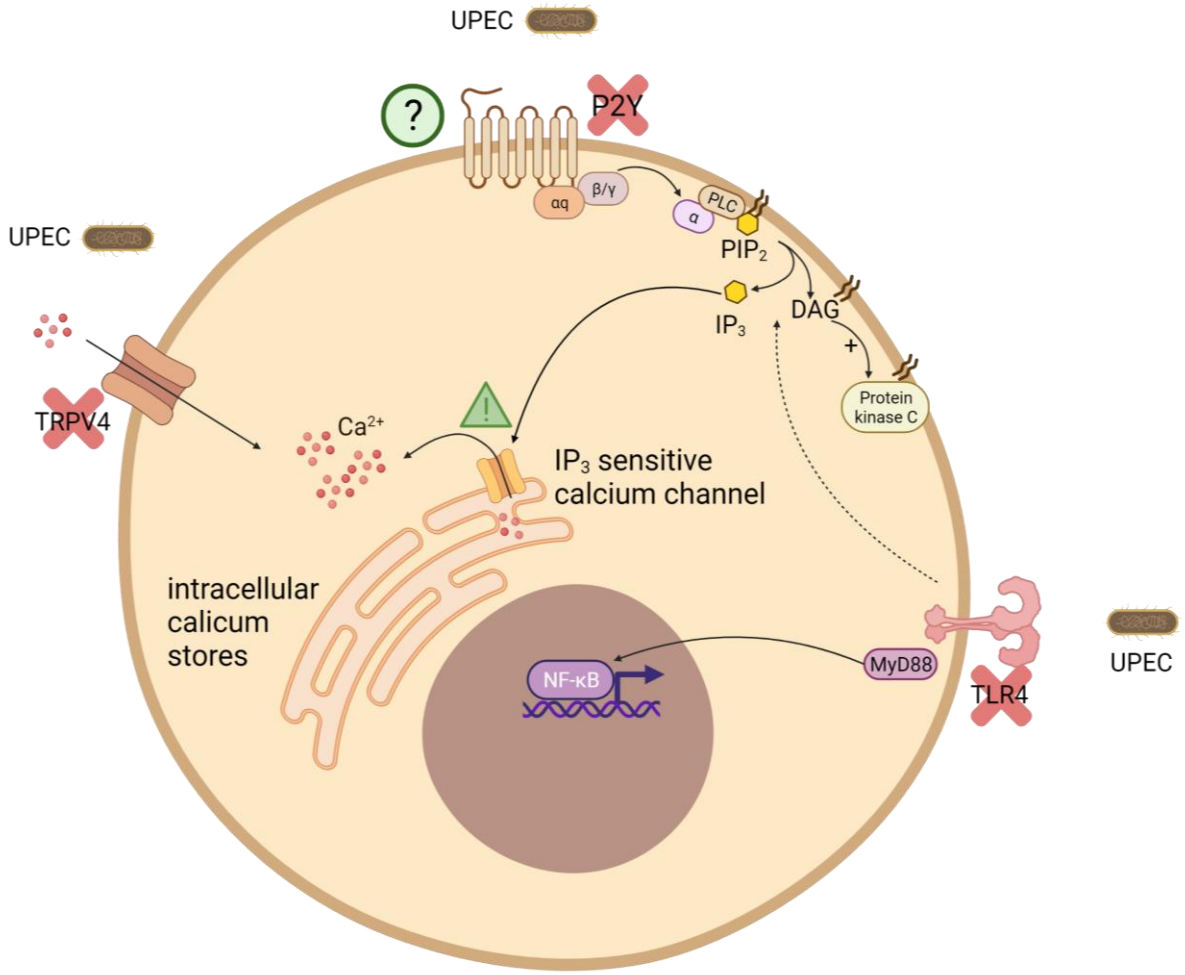

The calcium-permeable plasma membrane cation channel TRPV4 was the first molecular target to be investigated. This was based on earlier research from our research team showing that TRPV4 is highly expressed in urothelial cells, where it plays a role in sensing the filling state of the bladder, and that *E. coli* LPS directly activates urothelial TRPV4[93,94,79]. However, the calcium response to UPEC was unaltered in urothelial cells form *TrpV4*-deficient mice, and these animals also showed normal UTI clearance (measured using our BLI model). Next, given the indispensable role attributed to TLR4 in pathogen recognition and initiation of immune responses[132], we investigated the contribution of this metabotropic receptor to the observed calcium responses and UTI kinetics. Previous research has shown that, besides activation of MyD88, the NF-ƙB pathway and inflammasome formation, activation of the TLR4 pathway can lead to an increase in intracellular calcium concentration. Upon activation by LPS, CD14 induces the hydrolysis of phosphatidylinositol 4,5-bisphosphate (PIP_2)

and thereby the production of diacylglycerol (DAG) and IP3, leading to activation of the calcium-permeable ion channel TRPC6 and IP3-mediated calcium release[82,155]. However, like for TRPV4, our data demonstrated that TLR4 was dispensable for the urothelial calcium response to UPEC and for normal bacterial clearance in the *in vivo* UTO model.

We see two possible explanations for the fact that we did not observe any significant difference in UTI clearance between wild type mice and mice lacking either TRPV4 or TRL4 using the BLI model *in vivo*. First, these KO-animals may indeed have unaltered UTI kinetics. This conclusion is in line with our *in vitro* findings showing that TRPV4 and TLR4 are not involved in the acute urothelial response to UPEC and suggest the existence of alternative signaling pathways for the early detection of bacteria and their clearance. Alternatively, the BLI method may be not sensitive enough to detect differences under the mild infectious conditions used in our experiments, as indeed all animals in our study were able to fully clear the UTI. Therefore, our findings do not exclude the possibility of important contributions of TRPV4 and/or TLR4 to UTI clearance under more stringent conditions.

Differences in UTI susceptibility have been the focus of intense investigation by many research teams. The variability in the induction and resolution of UTIs in genetically distinct mice inoculated with the same *E. coli* strain indicates that genetic makeup is an important factor in determining host susceptibility and defense against infection[122]. In mice, UTIs will spontaneously resolve in most cases, as seen in our data for wild type, *TrpV4* and *Tlr4*-deficient mice in a C57Bl/6 background. However, UTIs were shown to persist for an extended length of time in mice with specific other genetic backgrounds, suggesting a strong contribution of specific genetic factors[122]. For example, C3H/HeJ mice, lacking LPS responsiveness genes, were found to be more susceptible. However, Hopkins et al. contradicted these findings, by showing equal rates of UTI susceptibility and ability to resolve the UTI between LPS-responder and nonresponder C3H mice. They stated that factors other than LPS responsiveness are important in determining host resistance to UTI[156]. Our data of *Tlr4* and *TrpV4*-deficient mice support this finding.

Since TRPV4 and TLR4 could be excluded as essential molecular sensors, we set out to identify alternative pathways to explain the acute response of urothelial cells to intact UPEC. We found that the calcium responses to UPEC do not require calcium influx,

but rather depend on IP_3-mediated release of calcium from the intracellular stores downstream of activation of phospholipase C (PLC). We hypothesized that a PLC-coupled metabotropic receptor in the urothelial cells is the target for UPEC. P2Y receptors, which are abundantly expressed in urothelial cells[78,157] and can provoke PLC-dependent calcium responses, were obvious candidates. However, our findings using a cocktail of P2Y inhibitors allowed us to exclude a central role for P2Y receptors as the main target for UPEC. Thus, the specific molecular target for this UPEC-mediated Ca^{2+} release remains to be identified. Single cell RNA-sequencing data, such as those available via Tabula Muris[157], may be used in future work to identify candidate PLC-coupled receptors that are highly expressed in urothelial cells. One of those candidates of interest is the protease-activated receptor 2 (PAR2). PAR2 is highly expressed on urothelial cells and plays an important role in inflammation and pain[157,158].

The inflammatory response to a bacterial infection may be seen as a double-edged sword. On one hand, it is beneficial as it will aid in combatting the pathogen and help the clearance of the infection. On the other hand, excessive inflammation can lead to tissue damage, which in turn can predispose the host to a worse outcome or chronic infection[159]. This was illustrated by the contrasting role of TRPA1 in acute versus chronic airway inflammation mouse models, where TRPA1 protects against LPS-induced acute pneumonitis, but enhances respiratory deterioration in the long term[39]. Additionally, Ingersoll et al have reported that granulocyte colony-stimulating factor (G-CSF), a cytokine that attracts neutrophils, is being released upon UPEC infection. However, neutralization of G-CSF led to a paradoxical found reduction of bacterial burden[160]. This unexpected result may be in part explained by upregulation of alternative pathways promoting the production of macrophage-activating cytokines[160]. Overall, these findings illustrate how delicately the host inflammatory responses are regulated. Therefore, instead of targeting a single pathway, based on knowledge obtained with a single bacterial toxin, the interplay between all UPEC targets should be investigated and understood before a rational treatment can be developed.

In **chapter 3**, we have investigated the mechanism of action of the urinary analgesic Phenazopyridine (PAP). PAP has been on the market for over 100 years, for symptomatic treatment of bladder pain, for instance during UTI. However, the

molecular targets of PAP responsible for the observed pain relief remained unknown. Randomized controlled trials with PAP have focused on the antiseptic effect or post-surgery pain relief [161,162], but did not provide convincing evidence to promote the usage of PAP. Therefore, PAP has been taken of the Belgian market in June 2021. The scope of our paper was to identify a possible mode of action, by investigating a possible role for TRP channels in PAP-induced analgesia, and to improve our understanding of the patient populations that could benefit from use of PAP.

Considering the utilization of PAP as a urinary analgesic, bladder pain syndrome (BPS) has gained our attention due to its association with increased TRP channel expression. BPS is defined as "the complaint of suprapubic pain related to bladder filling, accompanied by other symptoms such as increased daytime and night- time frequency, in the absence of proven urinary infection or other obvious pathology"[99]. Patient's charts of women enrolled in the retrospective Interstitial Cystitis Data Base study show a large variety of treatments for BPS. The authors suggest that this variety reflects the absence of effective treatment options and the lack of knowledge about the underlying disease mechanism[154]. Despite the lack of evidence, PAP is often used for pain relief in patients with BPS, taking a third place after hydro-distention and amitriptyline[154]. PAP improved the symptoms in 61% of all patients in a study that compares evidence-based efficacy and patient-reported treatment effectiveness[109,135]. This percentage is especially high when considering the difficulties that physicians encounter when treating patients with BPS.

In search of the cellular mechanisms driving BPS, a number of potential pathways have been proposed, including upregulation of the activity of ion channels from the TRP superfamily. Here, TRPM8 has been identified as a sensory channel that functions role in the activation of bladder afferent pathways. Wu et al have found that the expression of TRPM8 mRNA and protein was significantly increased in bladder tissues from patients with BPS, compared to control biopsies. Additionally, they reported an increased relative density of the nerve fibers in these patients[102]. Other groups have confirmed the increased TRPM8 expression and even the correlation with clinical symptoms[101,103]. We found that PAP, at concentrations that are easily attained in the bladder of patients taking the medication, causes inhibition of TRPM8 activity, providing a straightforward rationale for the local analgesic effect of PAP on the urinary tract mucosa, particularly under conditions where the TRPM8 expression is higher,

such as in BPS patients. Note that the expression of TRPM8 reportedly very low in DRG neurons innervating healthy bladder, which has been used as an argument to question a role for TRPM8 in human bladder sensory function[163,164]. Our data show that approximately 10% of cultured DRG neurons from mice responded to menthol, which includes both TRPM8-dependent and TRPA1-dependent responses. Interestingly, PAP (30 µM) inhibited the TRPM8-mediated menthol responses by about 80%. Currently, our lab is using single-cell RNA-seq to investigate alterations in the transcriptome of DRG neurons innervating the bladder after induction of inflammation. It will be of interest to determine if inflammation increases TRPM8 expression and function, and, if so, whether this increased activity can be normalized by PAP.

Selective TRPM8 antagonists have been developed for clinical use as analgesic drugs or to treat bladder dysfunction. In preclinical studies, such compounds were found to efficiently inhibit TRPM8-dependent processes such as icilin-induced wet-dog shakes and cold-induced urinary frequency in rats[72,143,144] . However, due to adverse effects in phase 1 clinical trials, which included severe perioral burning sensations likely representing an on target effect, the clinical development of TRPM8 antagonists was halted[146]. Typical contemporary drug development goes from *in vitro* discoveries over preclinical *in vivo* work to clinical trials. In case of PAP, however, which has been on the market for several decades and shows a favorable safety profile and patient-reported treatment effectiveness, these steps have not been followed, and a clear molecular target has never been identified. Based on our findings, we speculate that the particular pharmacokinetic properties of PAP contribute to its efficacy and favorable safety profile. The rapid clearance prevents PAP to reach plasma levels that would lead to substantial systemic TRPM8 inhibition and the concurrent unwanted side effects such as thermal dysesthesias. At the same time, PAP excretion leads to high intravesical concentrations that are sufficient to cause substantial TRPM8 inhibition on sensory neurons in the bladder wall. Future clinical research may involve controlled trails evaluating hyperalgesia and LUT symptoms in patients with BPS before and after treatment of PAP, correlating the efficacy of PAP action with TRPM8 expression in the bladder-innervating sensory neurons. Such clinical studies may be more useful than *in vivo* animal studies, since bladder pain and its perceptions are difficult to assess in animal models[35,97].

CONCLUSION AND FUTURE STEPS

VI. Conclusion and future steps

1. Longitudinal follow-up of urinary tract infections and their treatment in mice using bioluminescence imaging

We have established a model for the longitudinal follow-up of urinary tract infections in mice using a bioluminescent UPEC strain and the BLI acquisition software. The linear correlation between CFU and BLI *in vivo* and the effect of a known treatment (enrofloxacin) were demonstrated, validating the use of BLI. Considerations such as the changing bladder volume and discrepancies between CFU counts and BLI have been addressed. All steps of the protocol were filmed and are available at the JoVE website.

The cumbersome method of enumeration of CFU was limiting the reproducibility and efficacy of research in the UTI field. The experimental setup with BLI will advance *in vivo* UTI research by enabling noninvasive, longitudinal follow-up, while reducing the number of animals needed for these types of studies. The future applications of BLI are multifold, first it can be used to elucidate the influence of different host and/or pathogen characteristics that affect the infection risk. Secondly, it can be used for preclinical testing of new compounds for the prevention or treatment of UTIs. BLI facilitates the evaluation of dose-dependent effects on the bacterial load *in vitro* and provides longitudinal follow-up in *vivo*.

2. Urothelial cells respond to a viable bacterial solution with release of calcium from the intracellular stores in an PLC-dependent manner

We have demonstrated that a viable bacterial suspension triggers calcium responses in urothelial cells. These responses were independent of TRPV4 and TLR4 but are mediated by intracellular calcium release via a PLC-dependent pathway.

To better understand the exact mechanisms underlying the urothelium's response to UPEC, further research is required to identify which receptor in the urothelial cells is activated by these bacteria and initiated the PLC-pathway. Additionally, the downstream effects of PLC activation and subsequent calcium release needs further elucidation. Currently it is unclear whether this cascade results in the release of second messengers like NO or ATP by the urothelial cells, or whether it initiates immune responses via the NF-ƙB pathway. Therefore, additional experiments are needed; a

screen of multiple PLC-coupled receptors could help to identify the specific receptor that detects bacterial compounds. Secondly, further research is needed to untangle the downstream effects of bacteria-induced Ca^{2+} influx, including fluorescence based NO monitoring and luciferase-based ATP measurements, before proceeding to clinical studies.

3. Inhibition of TRPM8 by the urinary tract analgesic drug phenazopyridine

We have shown that PAP, at therapeutically relevant concentrations, inhibits TRPM8 in afferent pathways, which provides a straightforward explanation for the well-established local analgesic effect of this drug on the lower urinary tract.

In conclusion, our data and the patient self-reported effectiveness data by Hill et al. suggest that patients with bladder pain syndrome could benefit from a treatment with PAP and further clinical investigation is thus warranted. Since PAP is a known drug with long term efficacy data, used in routine clinical practice, the clinical efficacy of this drug for bladder pain syndrome should be more specifically addressed. To this end, a randomized controlled trial comparing PAP versus placebo in patients with BPS is warranted. The primary endpoint of this study would be patient perceived pain relief, using validated questionnaires. A secondary goal of the study would be to analyze the TRPM8 expression in bladder biopsies and to investigate a possible correlation between an increased TRPM8 expression and pain relief in response to PAP. The results of this study could help guide the treatment of patients with BPS in the future and/or to identify which patient population will benefit from PAP therapy. Furthermore, by improving our understanding about the mechanisms underlying bladder pain syndrome, we hope to be able to translate these findings to other diseases related to the LUT, including chronic prostatitis.

ABSTRACT

VII. Abstract

Urinary tract infections (UTIs) are amongst the most common bacterial infections in humans, requiring millions of antibiotic prescriptions annually. Available therapies have not evolved significantly in recent years, do not prevent recurrences, and are challenged by rising antibiotic resistance. The field lacks a thorough understanding of the protective host immunity and the impact of bladder function on UTI susceptibility[39]. As such, there is an urgent need for novel strategies for the treatment and prevention of UTIs[10]. The general aim of this dissertation is to obtain a better understanding of the interaction between the host and the pathogen, the urothelium and uropathogenic *Escherichia coli* (UPEC).

To this end, we have optimized a murine UTI model, using bioluminescence imaging to enable the non-invasive, longitudinal follow up of the bacterial load. In a next step, this model was used to investigate UTI clearance kinetics in vivo in *Tlr4* and *TrpV4*-deficient mice. *In vivo* and *in vitro* results did not confirm the role of these receptors in the responses to a UPEC challenge.

We have demonstrated that a viable bacterial suspension triggers calcium responses in urothelial cells. The origin of the observed calcium responses was an IP_3-mediated release of calcium from the intracellular stores via the PLC-pathway. The precise target and downstream effects of the calcium responses remain to be investigated.

Finally, we have investigated the local analgesic effect of phenazopyridine (PAP) on the lower urinary tract. We have shown that PAP at therapeutically relevant concentrations inhibits TRPM8 in afferent pathways, and can thus provide pain relief, especially under pathological conditions such as bladder pain syndrome or chronic inflammation.

In conclusion, we have investigated UTI susceptibility, urothelial responses and the involvement of TRP channels by challenging cells and animals with UPEC.

DUTCH SUMMARY

VIII. Dutch summary

Urineweginfecties behoren tot de meest voorkomende bacteriële infecties bij de mens en zijn jaarlijks verantwoordelijk voor een enorme hoeveelheid antibiotica die wordt voorgeschreven. Door een toenemende resistentie tegen antibiotica, wordt de behandeling van urineweginfecties met conventionele antibiotica moeilijker en krijgen infecties steeds meer een chronisch of recurrent karakter. Om alternatieve strategieën te kunnen ontwikkelen, moet de interactie tussen de uropathogene bacteriën en het urotheel verder ontrafeld worden. Het doel van dit project was dan ook om de aangeboren immuniteit van de urotheelcellen tegen uropathogene bacteriën te onderzoeken en de impact van blaasfunctie op de vatbaarheid voor infecties te doorgronden.

Om dit te verwezenlijken, hebben we een muis model van een urineweginfectie geoptimaliseerd. Hiervoor werd de techniek 'bioluminescence imaging' gebruikt, waarbij aan de hand van bioluminescente bacteriën de ernst van de infectie op een niet-invasieve, longitudinale manier kan worden opgevolgd. In een volgende stap, hebben we het model gebruikt om de kinetiek van urineweginfecties in muizen zonder *Tlr4*- of *TrpV4*-receptoren te onderzoeken. Zowel onze *in vitro* als onze *in vivo* data konden geen belangrijke rol voor deze receptoren aantonen in de reactie op uropathogene bacteriën.

Verder hebben we aangetoond dat bacteriën calcium responsen in urotheel cellen kunnen veroorzaken. De oorsprong van deze calcium responsen is een IP_3-gemedieerde vrijzetting van calcium uit de intracellulaire 'stores' via de PLC-pathway. Verder onderzoek zal de exacte receptor en downstream effecten nog moeten uitwijzen.

Tenslotte hebben we het werkingsmechanisme van phenazopyridine, een geneesmiddel dat wordt gebruikt voor lokale pijnstilling in de blaas, onderzocht. We hebben aangetoond dat phenazopyridine TRPM8 in de afferente zenuwuiteinden kan inhiberen. Onder pathologische omstandigheden, waarbij de TRPM8 expressie hoger is, zoals bij patiënten met blaas pijn syndroom of chronische inflammatie, kan deze inhibitie dus het lokale analgetisch effect verklaren.

Ter conclusie, we onderzochten de kinetiek van urineweginfecties, de urotheliale responsen en de rol van TRP kanalen, door celculturen en muizen aan uropathegene bacteriën bloot te stellen.

ACADEMIC CV



NOÉMIE LUYTS

noemie.luyts@kuleuven.be | +324 94 22 40 06 | 3000, Leuven Belgium

EXPERIENCE

08/2018 – Current KU LEUVEN Leuven

PhD Candidate

- Conducted data collection and analysis.
- Managed project timelines and coordinated research tasks.
- Attended national and international conferences.
- Prepared and presented academic papers and abstracts.

08/2018 – Current UZ LEUVEN Leuven

Urologist in Training

- Engaged in active listening to provide accurate diagnoses and care.
- Enhanced patient outcomes by performing treatments and surgical procedures.
- Prioritized and organized tasks to efficiently accomplish goals.
- Worked closely with team members.

PUBLICATIONS

JOURNAL ARTICLES

Luyts, N. et al. (2021) Longitudinal Follow-Up of Urinary Tract Infections and Their Treatment in Mice using Bioluminescence Imaging. J. Vis. Exp. (172), e62614, doi:10.3791/62614.

Luyts, N. et al. Inhibition of TRPM8 by the urinary tract analgesic drug phenazopyridine (submitted)

Luyts, N et al. Urothelial cells respond to a viable bacterial solution with release of calcium from the intracellular stores in an PLC-dependent manner (manuscript in preparation)

ABSTRACTS AND POSTERS

Luyts N, De Bruyn H, Vanneste M, Vande Velde G, Voets T, Everaerts W. The role of TRP channels in the defense against UTIs. Establishing a murine model; VIB congress 2019, poster **Genk**

Luyts N, De Bruyn H, Vanneste M, Vande Velde G, Voets T, Everaerts W. Bioluminescence Imaging (BLI) enables the study of functional changes

during Urinary Tract Infections (UTIs); 36th Annual EAU Congress 2021, abstract presentation **Milan (virtual)**

Luyts N, De Bruyn H, Vanneste M, Voets T, Everaerts W. Inhibition of TRPM8 by Phenazopyridine; The 4th International TRP Meeting 2021, abstract presentation **Leuven**

Luyts N. Inhibitie van TRPM8 verklaart het analgetisch effect van fenazopyridine; Elautprijs 2022, oral presentation **Gent**

Luyts N. mechanism of action of Phenazopyridine; 37th Annual EAU Congress 2022, abstract presentation, **Amsterdam**

BOOK CONTRIBUTIONS

Alhasso A. et al. (2020) Treatment of Storage LUTS. In: Drake M., Cocci A., Pereira e Silva R. (eds) Lower Urinary Tract Symptoms in Adults. Springer, Cham. doi:10.1007/978-3-030-27747-5_6

EDUCATION

2005 – 2011 Vita-et-pax Schoten

Summa cum laude graduate

2011 – 2018 KU Leuven, Master of Medicine Leuven

Magna cum laude graduate

CERTIFICATIONS

- Tropical Medicine & Biomedical development cooperation
- Medical French
- Radioprotection
- Research integrity
- Felasa B
- Biostatistics
- Presentation skills for biomedical researchers
- Writing skills for biomedical researchers

EXTRACURRICULAR ACTIVITIES

- National communication officer (NCO) and chairman-elect of European Society of Residents in Urology (ESRU) Belgium
- Medical Volunteer work in Uganda (NUVHOP)
- Internship abroad in Paris & La Réunion
- 'Wetenschap op stap'

KEY TERMS

X. Key terms

Urinary tract infections

Urothelium

Uropathogenic *Escherichia coli*

Bladder physiology

Transient receptor potential channels

- TRPV4
- TRPM8
- TRPA1
- TRPV1
- TRPM3

Toll-like receptor

- TLR4

Bioluminescent imaging

Phenazopyridine hydrochloride

Bladder pain syndrome

Calcium responses

SCIENTIFIC ACKNOWLEDGEMENTS

PERSONAL CONTRIBUTIONS

CONFLICT OF INTEREST

XI. Scientific acknowledgements & personal contributions

All figures in the introduction and discussion were made by NL using Biorender, when they were adapted from previous publications, the references were given.

Chapter 1

This section is accepted for publication in the Journal of Visualized Experiments and was published as an original article.

Longitudinal follow-up of urinary tract infections and their treatment in mice using bioluminescence imaging

Noémie Luyts, Greetje Vande Velde, Matthias Vanneste, Helene De Bruyn, Annelies Janssens, Natalie Verstraeten, Thomas Voets, Wouter Everaerts.

Data collection and technical optimization was performed by NL, GVdV, HDB, AJ. NL performed data analysis. NL, GVdV, TV and WE contributed to study design and interpretation. NL, MV, NV and WE wrote the first draft of the manuscript and all authors commented on the manuscript. Final version was read and approved by all authors.

The strain UTI89-lux was a generous gift from Prof. Seed's Laboratory.

Chapter 2

This section will be submitted as an original article.

Urothelial cells respond to a viable bacterial solution with release of calcium from the intracellular stores in an PLC-dependent manner

Noémie Luyts, Brett Boonen, Annelies Janssens, Silvia Pinto, Thomas Voets, Wouter Everaerts.

NL is the first author and contributed to study design, experiments, data analysis and interpretation, figure layout and manuscript preparation. BB contributed to data interpretation, figure layout and commented on the manuscript. AJ contributed to calcium imaging experiments and optimization of experimental design. SP contributed to in vivo experimental design and maintained KO animal lines. TV and WE added to the design of the study, data interpretation and preparation of the manuscript.

Chapter 3

This section will be submitted as an original article in the British Journal of Pharmacology.

Inhibition of TRPM8 by the urinary tract analgesic drug phenazopyridine

Noémie Luyts, Jan Daniluk, Annelies Janssens, Ana Nogueira Freitas Peigneur, Marie Mulier, Wouter Everaerts, Thomas Voets

NL is the first author. NL, TV and WE designed the experiments. NL performed the calcium imaging experiments and analyzed the data. Patch clamp data was obtained by JD, AJ and TV and they analyzed the data (fig 2-4). DRG neurons were cultured by ANFP and calcium imaging experiments with DRG neurons were performed by NL with the assistance of ANFP, together they interpreted the data (fig 6). The manuscript was drafted by NL and JD. Final manuscript was written by TV. All authors critically revised the manuscript before submission.

XII. Conflict of interest statement

All authors and co-authors declare no conflict of interest for the work presented in this doctoral thesis manuscript.

This work was supported by grants from the Research Foundation — Flanders (FWO; G0B4718N to WE and TV; G066322N to WE), the Research Council of KU Leuven (C2-Tackling the Roots of Pain; to TV and WE), the Queen Elisabeth Medical Foundation for Neurosciences (to TV) and the VIB (to TV). WE is a senior clinical researcher and MM and AF are post-doctoral researchers of the Research Foundation — Flanders (FWO).

REFERENCES

XIII. References

1 Foxman, B. The Epidemiology of Urinary Tract Infection. *Nature Reviews Urology.* **7** (12), 653-660, (2010).

2 O'Brien, V. P., Hannan, T. J., Nielsen, H. V. & Hultgren, S. J. Drug and vaccine development for the treatment and prevention of urinary tract infections. *Microbiology spectrum.* **4** (1), (2016).

3 Hooton, T. M. *et al.* Effect of Increased Daily Water Intake in Premenopausal Women With Recurrent Urinary Tract Infections: A Randomized Clinical Trial. *JAMA Internal Medicine.* **178** (11), 1509-1515, (2018).

4 Nilius, B. & Flockerzi, V. Mammalian Transient Receptor Potential (TRP) cation channels. *Handbook of experimental Pharmacology.* **222** (), (2014).

5 Vanneste, M., Segal, A., Voets, T. & Everaerts, W. Transient Reeptor Potential Channels in Sensory Mechanisms of the Lower Urinary Tract. *Nature Reviews Urology.* **18** (3), 139-159, (2021).

6 Pezzlo, M. Laboratory Diagnosis of Urinary Tract Infections: Guidelines, Challenges, and Innovations. *Clinical Microbiology Newsletter.* **36** (12), 87-93, (2014).

7 Hooton, T. M., Roberts, P. L., Cox, M. E. & Stapleton, A. E. Voided midstream urine culture and acute cystitis in premenopausal women. *N Engl J Med.* **369** (20), 1883-1891, (2013).

8 Foxman, B. Epidemiology of urinary tract infections: incidence, morbidity, and economic costs. *American Journal of Medicine.* **113** (1A), 5-13, (2002).

9 Terlizzi, M. E., Gribaudo, G. & Maffei, M. E. UroPathogenic *Escherichia coli* (UPEC) Infections: Virulence Factors, Bladder Responses, Antibiotic, and Non-antibiotic Antimicrobial Strategies. *Frontiers in Microbiology.* **8** 1566, (2017).

10 Silverman, J. A., Schreiber, H. L. t., Hooton, T. M. & Hultgren, S. J. From physiology to pharmacy: developments in the pathogenesis and treatment of recurrent urinary tract infections. *Current Urology Reports.* **14** (5), 448-456, (2013).

11 Bonkat, G. *et al.* EAU Guidelines on Urological infections. (2021).

12 Geerlings, S. E. Clinical Presentations and Epidemiology of Urinary Tract Infections. *Microbiol Spectr.* **4** (5), (2016).

13 Gupta, K., Hooton, T. M., Roberts, P. L. & Stamm, W. E. Short-Course Nitrofurantoin for the Treatment of Acute Uncomplicated Cystitis in Women. *Archives of Internal Medicine.* **167** (20), 2207-2212, (2007).

14 Lee, D. S., Lee, S. J. & Choe, H. S. Community-Acquired Urinary Tract Infection by *Escherichia coli* in the Era of Antibiotic Resistance. *Biomed Res Int.* **2018** 7656752, (2018).

15 Paul, R. State of the Globe: Rising Antimicrobial Resistance of Pathogens in Urinary Tract Infection. *J Glob Infect Dis.* **10** (3), 117-118, (2018).

16 Gupta, K. *et al.* International clinical practice guidelines for the treatment of acute uncomplicated cystitis and pyelonephritis in women: A 2010 update by the Infectious Diseases Society of America and the European Society for Microbiology and Infectious Diseases. *Clin Infect Dis.* **52** (5), e103-120, (2011).

17 Lee, D. S. *et al.* Antimicrobial Susceptibility Pattern and Epidemiology of Female Urinary Tract Infections in South Korea, 2010-2011. *Antimicrobial Agents and Chemotherapy.* **57** (11), 5384-5393, (2013).

18 Melekos, M. D. & Naber, K. G. Complicated urinary tract infections. *International Journal of Antimicrobial Agents.* **15** (4), 247-256, (2000).
19 Abraham, S. N. & Miao, Y. The nature of immune responses to urinary tract infections. *Nature Reviews Immunology.* **15** (10), 655-663, (2015).
20 Brannon, J. R. *et al.* Invasion of vaginal epithelial cells by uropathogenic Escherichia coli. *Nature Communications.* **11** (1), 2803, (2020).
21 Anger, J. *et al.* Recurrent Uncomplicated Urinary Tract Infections in Women: AUA/CUA/SUFU Guideline. *J Urol.* **202** (2), 282-289, (2019).
22 Huttner, A. *et al.* Nitrofurantoin revisited: a systematic review and meta-analysis of controlled trials. *Journal of Antimicrobial Chemotherapy.* **70** (9), 2456-2464, (2015).
23 Nicolle, L. E. Pivmecillinam in the treatment of urinary tract infections. *Journal of Antimicrobial Chemotherapy.* **46** (suppl_1), 35-39, (2000).
24 Bader, M. S., Loeb, M., Leto, D. & Brooks, A. A. Treatment of urinary tract infections in the era of antimicrobial resistance and new antimicrobial agents. *Postgrad Med.* **132** (3), 234-250, (2020).
25 EMA. Vol. 175398/2019 (ed European medicines agency) (2019).
26 Hooton, T. M. Uncomplicated Urinary Tract Infection. *The New England Journal of Medicine.* **366** (11), 1028-1037, (2012).
27 Beerepoot, M. A., Geerlings, S. E., van Haarst, E. P., van Charante, N. M. & ter Riet, G. Nonantibiotic prophylaxis for recurrent urinary tract infections: a systematic review and meta-analysis of randomized controlled trials. *Journal of Urology.* **190** (6), 1981-1989, (2013).
28 Kranjcec, B., Papes, D. & Altarac, S. D-mannose powder for prophylaxis of recurrent urinary tract infections in women: a randomized clinical trial. *World J Urol.* **32** (1), 79-84, (2014).
29 Jepson, R. G., Williams, G. & Craig, J. C. Cranberries for preventing urinary tract infections. *Cochrane Database Systematic Reviews.* **10** (10), Cd001321, (2012).
30 Lüthje, P. *et al.* Estrogen Supports Urothelial Defense Mechanisms. *Science Translational Medicine.* **5** (190), 190ra181-197, (2013).
31 Chen, Y. Y., Su, T. H. & Lau, H. H. Estrogen for the prevention of recurrent urinary tract infections in postmenopausal women: a meta-analysis of randomized controlled trials. *Int Urogynecol J.* **32** (1), 17-25, (2021).
32 Khandelwal, P., Abraham, S. N. & Apodaca, G. Cell biology and physiology of the uroepithelium. *American journal of physiology. Renal physiology.* **297** (6), F1477-1501, (2009).
33 Apodaca, G., Balestreire, E. & Birder, L. A. The uroepithelial-associated sensory web. *Kidney International.* **72** (9), 1057-1064, (2007).
34 Merrill, L., Gonzalez, E. J., Girard, B. M. & Vizzard, M. A. Receptors, channels, and signalling in the urothelial sensory system in the bladder. *Nature Reviews Urology.* **13** (4), 193-204, (2016).
35 Birder, L. A. & Klumpp, D. J. Host Responses to Urinary Tract Infections and Emerging Therapeutics Sensation and Pain within the Urinary Tract. *Microbiology spectrum.* **4** (5), 0023, (2016).
36 Negrete, H. O., Lavelle, J. P., Berg, J., Lewis, S. A. & Zeidel, M. L. Permeability properties of the intact mammalian bladder epithelium. *American Journal of Physiology* **271** (4 Pt 2), F886-894, (1996).

37 Thumbikat, P. *et al.* Bacteria-induced uroplakin signaling mediates bladder response to infection. *PLoS Pathogens.* **5** (5), e1000415, (2009).
38 Wyndaele, J. J. J. *et al.* GAG replenishment therapy for bladder pain syndrome/interstitial cystitis. *Neurourology Urodynamics.* **38** (2), 535-544, (2019).
39 McLellan, L. K. & Hunstad, D. A. Urinary Tract Infection: Pathogenesis and Outlook. *Trends in Molecular Medicine.* **22** (11), 946-957, (2016).
40 Yoshimura, N. *et al.* Therapeutic receptor targets for lower urinary tract dysfunction. *Naunyn-Schmiedeberg's Archives of Pharmacology.* **377** (4), 437-448, (2008).
41 Araki, I. *et al.* Roles of mechanosensitive ion channels in bladder sensory transduction and overactive bladder. *International Journal of Urology.* **15** (8), 681-687, (2008).
42 Everaerts, W. *et al.* Functional Characterization of Transient Receptor Potential Channels in Mouse Urothelial Cells. *American Journal of Physiology - Renal Physiology.* **298** (3), F692-701, (2010).
43 Hannan, T. J., Mysorekar, I. U., Hung, C. S., Isaacson-Schmid, M. L. & Hultgren, S. J. Early severe inflammatory responses to uropathogenic E. coli predispose to chronic and recurrent urinary tract infection. *PLoS Pathogens.* **6** (8), e1001042, (2010).
44 Nielubowicz, G. R. & Mobley, H. L. Host-pathogen interactions in urinary tract infection. *Nature Reviews Urology.* **7** (8), 430-441, (2010).
45 Miao, Y., Li, G., Zhang, X., Xu, H. & Abraham, S. N. A TRP Channel Senses Lysosome Neutralization by Pathogens to Trigger Their Expulsion. *Cell.* **161** (6), 1306-1319, (2015).
46 Chan, C. Y., St John, A. L. & Abraham, S. N. Mast cell interleukin-10 drives localized tolerance in chronic bladder infection. *Immunity.* **38** (2), 349-359, (2013).
47 Wiles, T. J., Kulesus, R. R. & Mulvey, M. A. Origins and virulence mechanisms of uropathogenic Escherichia coli. *Experimental and Molecular Pathology.* **85** (1), 11-19, (2008).
48 Cohen-Poradosu, R. & Kasper, D. L. in *Mandell, Douglas, and Bennett's Principles and Practice of Infectious Diseases* 10.1016/b978-1-4557-4801-3.00244-7 2736-2743.e2731 (2015).
49 Mazgaeen, L. & Gurung, P. Recent Advances in Lipopolysaccharide Recognition Systems. *International Journal of Molecular Sciences.* **21** (2), (2020).
50 Bäckhed, F., Söderhäll, M., Ekman, P., Normark, S. & Richter-Dahlfors, A. Induction of innate immune responses by Escherichia coli and purified lipopolysaccharide correlates with organ- and cell-specific expression of Toll-like receptors within the human urinary tract. *Cellular Microbiology.* **3** (3), 153-158, (2001).
51 Martinez, J. J., Mulvey, M. A., Schilling, J. D., Pinkner, J. S. & Hultgren, S. J. Type 1 pilus-mediated bacterial invasion of bladder epithelial cells. *The EMBO journal.* **19** (20), 2803-2812, (2000).
52 Hultgren, S. J., Porter, T. N., Schaeffer, A. J. & Duncan, J. L. Role of type 1 pili and effects of phase variation on lower urinary tract infections produced by Escherichia coli. *Infection and Immunity.* **50** (2), 370-377, (1985).
53 Nakamura, S. & Minamino, T. Flagella-Driven Motility of Bacteria. *Biomolecules.* **9** (7), (2019).
54 Ulett, G. C. *et al.* Uropathogenic Escherichia coli virulence and innate immune responses during urinary tract infection. *Current Opinion in Microbiology.* **16** (1), 100-107, (2013).

55 Nagamatsu, K. *et al.* Dysregulation of *Escherichia coli* α-hemolysin expression alters the course of acute and persistent urinary tract infection. *Proceedings of the National Academy of Sciences.* **112** (8), E871-E880, (2015).
56 Uhlén, P. *et al.* Alpha-haemolysin of uropathogenic E. coli induces Ca2+ oscillations in renal epithelial cells. *Letters to Nature.* **405** (6787), 694-697, (2000).
57 Rosen, D. A., Hooton, T. M., Stamm, W. E., Humphrey, P. A. & Hultgren, S. J. Detection of intracellular bacterial communities in human urinary tract infection. *PLoS Med.* **4** (12), e329, (2007).
58 Song, J. *et al.* A novel TLR4-mediated signaling pathway leading to IL-6 responses in human bladder epithelial cells. *PLoS Pathogens.* **3** (4), e60, (2007).
59 Hung, C. S., Dodson, K. W. & Hultgren, S. J. A Murine Model of Urinary Tract Infection. *Nature Protocols.* **4** (8), 1230-1243, (2009).
60 Justice, S. S., Hunstad, D. A., Seed, P. C. & Hultgren, S. J. Filamentation by Escherichia coli subverts innate defenses during urinary tract infection. *Proc Natl Acad Sci U S A.* **103** (52), 19884-19889, (2006).
61 Blango, M. G., Ott, E. M., Erman, A., Veranic, P. & Mulvey, M. A. Forced resurgence and targeting of intracellular uropathogenic Escherichia coli reservoirs. *PLoS One.* **9** (3), e93327, (2014).
62 Mysorekar, I. U. & Hultgren, S. J. Mechanisms of uropathogenic Escherichia coli persistence and eradication from the urinary tract. *Proc Natl Acad Sci U S A.* **103** (38), 14170-14175, (2006).
63 Mulvey, M. A., Schilling, J. D. & Hultgren, S. J. Establishment of a persistent Escherichia coli reservoir during the acute phase of a bladder infection. *Infection and Immunity.* **69** (7), 4572-4579, (2001).
64 Leatham-Jensen, M. P. *et al.* Uropathogenic Escherichia coli Metabolite-Dependent Quiescence and Persistence May Explain Antibiotic Tolerance during Urinary Tract Infection. *mSphere.* **1** (1), (2016).
65 Nilius, B., Owsianik, G., Voets, T. & Peters, J. A. Transient receptor potential cation channels in disease. *Physiology Review.* **87** (1), 165-217, (2007).
66 TranVan Nhieu, G., Clair, C., Grompone, G. & Sansonetti, P. Calcium signalling during cell interactions with bacterial pathogens. *Biology of the Cell.* **96** (1), 93-101, (2004).
67 Montell, C. The TRP Superfamily of Cation Channels. *Science's STKE.* **22** (272), re3, (2005).
68 Everaerts, W., Gevaert, T., Nilius, B. & De Ridder, D. On the origin of bladder sensing: Tr(i)ps in urology. *Neurourology and Urodynamics.* **27** (4), 264-273, (2008).
69 Andersson, K. E. TRP Channels as Lower Urinary Tract Sensory Targets. *Medical Sciences* **7**(5), (2019).
70 Andersson, K. E., Gratzke, C. & Hedlund, P. The role of the transient receptor potential (TRP) superfamily of cation-selective channels in the management of the overactive bladder. *BJU International.* **106** (8), 1114-1127, (2010).
71 Gees, M., Owsianik, G., Nilius, B. & Voets, T. TRP channels. *Comprehensive Physiology.* **2** (1), 563-608, (2012).
72 Uvin, P. *et al.* Essential role of transient receptor potential M8 (TRPM8) in a model of acute cold-induced urinary urgency. *European Urology.* **68** (4), 655-661, (2015).
73 Mukerji, G. *et al.* Pain during ice water test distinguishes clinical bladder hypersensitivity from overactivity disorders. *BMC Urology.* **6** 31, (2006).

74 Aizawa, N. *et al.* KPR-2579, a novel TRPM8 antagonist, inhibits acetic acid-induced bladder afferent hyperactivity in rats. *Neurourology and Urodynamics.* **37** (5), 1633-1640, (2018).
75 Gardiner, J. C. *et al.* The role of TRPM8 in the Guinea-pig bladder-cooling reflex investigated using a novel TRPM8 antagonist. *European Journal of Pharmacology.* **740** 398-409, (2014).
76 Ito, H. *et al.* Functional role of the transient receptor potential melastatin 8 (TRPM8) ion channel in the urinary bladder assessed by conscious cystometry and ex vivo measurements of single-unit mechanosensitive bladder afferent activities in the rat. *BJU International.* **117** (3), 484-494, (2016).
77 Mochizuki, T. *et al.* The TRPV4 cation channel mediates stretch-evoked Ca2+ influx and ATP release in primary urothelial cell cultures. *Journal of Biological Chemistry.* **284** (32), 21257-21264, (2009).
78 Chess-Williams, R., Sellers, D. J., Brierley, S. M., Grundy, D. & Grundy, L. Purinergic receptor mediated calcium signalling in urothelial cells. *Scientific Reports.* **9** (1), 16101, (2019).
79 Gevaert, T. *et al.* Deletion of the transient receptor potential cation channel TRPV4 impairs murine bladder voiding. *the Journal of Clinical Investigation.* **117** (11), 3453-3462, (2007).
80 Everaerts, W. *et al.* Inhibition of the cation channel TRPV4 improves bladder function in mice and rats with cyclophosphamide-induced cystitis. *Proc Natl Acad Sci U S A.* **107** (44), 19084-19089, (2010).
81 Deruyver, Y. *et al.* Intravesical Activation of the Cation Channel TRPV4 Improves Bladder Function in a Rat Model for Detrusor Underactivity. *European Urology.* **74** (3), 336-345, (2018).
82 Boonen, B., Alpizar, Y. A., Meseguer, V. M. & Talavera, K. TRP Channels as Sensors of Bacterial Endotoxins. *Toxins (Basel).* **10** (8), (2018).
83 Cyril, A. C., Jan, R. K. & Radhakrishnan, R. Pain in chronic prostatitis and the role of ion channels: a brief overview. *British Journal of Pain.* **16** (1), 50-59, (2021).
84 Andersson, D. A., Gentry, C., Moss, S. & Bevan, S. Transient receptor potential A1 is a sensory receptor for multiple products of oxidative stress. *Journal of Neuroscience.* **28** (10), 2485-2494, (2008).
85 Nicholas, S., Yuan, S. Y., Brookes, S. J., Spencer, N. J. & Zagorodnyuk, V. P. Hydrogen peroxide preferentially activates capsaicin-sensitive high threshold afferents via TRPA1 channels in the guinea pig bladder. *Br J Pharmacol.* **174** (2), 126-138, (2017).
86 Oyama, S. *et al.* Pathophysiological Role of Transient Receptor Potential Ankyrin 1 in a Mouse Long-Lasting Cystitis Model Induced by an Intravesical Injection of Hydrogen Peroxide. *Frontiers in Physiology.* **8** 877, (2017).
87 Charrua, A., Cruz, C. D., Cruz, F. & Avelino, A. Transient receptor potential vanilloid subfamily 1 is essential for the generation of noxious bladder input and bladder overactivity in cystitis. *Journal of Urology.* **177** (4), 1537-1541, (2007).
88 Charrua, A. *et al.* Co-administration of transient receptor potential vanilloid 4 (TRPV4) and TRPV1 antagonists potentiate the effect of each drug in a rat model of cystitis. *BJU International.* **115** (3), 452-460, (2015).
89 Perraud, A. L., Schmitz, C. & Scharenberg, A. M. TRPM2 Ca2+ permeable cation channels: from gene to biological function. *Cell Calcium.* **33** (5-6), 519-531, (2003).

90 Quintana, A., Griesemer, D., Schwarz, E. C. & Hoth, M. Calcium-dependent activation of T-lymphocytes. *Pflugers Archieve.* **450** (1), 1-12, (2005).
91 Scheraga, R. G., Southern, B. D., Grove, L. M. & Olman, M. A. The Role of TRPV4 in Regulating Innate Immune Cell Function in Lung Inflammation. *Frontiers in Immunology.* **11** 1211, (2020).
92 Scheraga, R. G. *et al.* TRPV4 Protects the Lung from Bacterial Pneumonia via MAPK Molecular Pathway Switching. *Journal of Immunology.* **204** (5), 1310-1321, (2020).
93 Alpizar, Y. A. *et al.* TRPV4 Mediates Acute Bladder Responses to Bacterial Lipopolysaccharides. *Frontiers in Immunology.* **11** 799, (2020).
94 Alpizar, Y. A. *et al.* TRPV4 activation triggers protective responses to bacterial lipopolysaccharides in airway epithelial cells. *Nature Communications.* **8** (1), 1059, (2017).
95 Meseguer, V. *et al.* TRPA1 channels mediate acute neurogenic inflammation and pain produced by bacterial endotoxins. *Nat Commun.* **5** 3125, (2014).
96 Kamei, J. *et al.* Attenuated lipopolysaccharide-induced inflammatory bladder hypersensitivity in mice deficient of transient receptor potential ankilin1. *Scientific Reports.* **8** (1), 15622, (2018).
97 Rosen, J. M. & Klumpp, D. J. Mechanisms of pain from urinary tract infection. *International Journal of Urology.* **21 Suppl 1** 26-32, (2014).
98 Rudick, C. N. *et al.* O-antigen modulates infection-induced pain states. *PLoS One.* **7** (8), e41273, (2012).
99 van de Merwe, J. P. *et al.* Diagnostic criteria, classification, and nomenclature for painful bladder syndrome/interstitial cystitis: an ESSIC proposal. *Eur Urol.* **53** (1), 60-67, (2008).
100 Voets, T., Vriens, J. & Vennekens, R. Targeting TRP Channels - Valuable Alternatives to Combat Pain, Lower Urinary Tract Disorders, and Type 2 Diabetes? *Trends in Pharmacological Sciences.* **40** (9), 669-683, (2019).
101 Mukerji, G. *et al.* Cool and menthol receptor TRPM8 in human urinary bladder disorders and clinical correlations. *BMC Urology.* **6** 6, (2006).
102 Wu, L., Zhang, J., Zhou, F. & Zhang, P. Increased Transient Receptor Potential Melastatin 8 Expression in the Development of Bladder Pain in Patients With Interstitial Cystitis/Bladder Pain Syndrome. *Urology.* **146** 3011-3016, (2020).
103 Homma, Y. *et al.* Increased mRNA expression of genes involved in pronociceptive inflammatory reactions in bladder tissue of interstitial cystitis. *Journal of Urology.* **190** (5), 1925-1931, (2013).
104 Liu, B. L. *et al.* Increased severity of inflammation correlates with elevated expression of TRPV1 nerve fibers and nerve growth factor on interstitial cystitis/bladder pain syndrome. *Urologia Internationalis.* **92** (2), 202-208, (2014).
105 Payne, C. K. *et al.* Intravesical resiniferatoxin for the treatment of interstitial cystitis: a randomized, double-blind, placebo controlled trial. *Journal of Urology.* **173** (5), 1590-1594, (2005).
106 Meotti, F. C., Forner, S., Lima-Garcia, J. F., Viana, A. F. & Calixto, J. B. Antagonism of the transient receptor potential ankyrin 1 (TRPA1) attenuates hyperalgesia and urinary bladder overactivity in cyclophosphamide-induced haemorrhagic cystitis. *Chemico-Biological Interactions.* **203** (2), 440-447, (2013).

107 Maggi, C. A. *et al.* Cystometric Evidence that Capsaicin-Sensitive Nerves Modulate the Afferent Branch of Micturition Reflex in Humans. *Journal of Urology.* **142** (1), 150-154, (1989).
108 Andersson, K. E. Agents in early development for treatment of bladder dysfunction - promise of drugs acting at TRP channels? *Expert Opin Investig Drugs.* **28** (9), 749-755, (2019).
109 Hill, J. R., Isom-Batz, G., Panagopoulos, G., Zakariasen, K. & Kavaler, E. Patient perceived outcomes of treatments used for interstitial cystitis. *Urology.* **71** (1), 62-66, (2008).
110 Mulier, M. *et al.* Upregulation of TRPM3 in nociceptors innervating inflamed tissue. *Elife.* **9**, (2020).
111 Grynkiewicz, G., Poenie, M. & Tsien, R. Y. A new generation of Ca2+ indicators with greatly improved fluorescence properties. *J Biol Chem.* **260** (6), 3440-3450, (1985).
112 Balsara, Z. R. *et al.* Enhanced Susceptibility to Urinary Tract Infection in the Spinal Cord-Injured Host with Neurogenic Bladder. *Infection and Immunity.* **81** (8), 3018-3026, (2013).
113 Barber, A. E., Norton, J. P., Wiles, T. J. & Mulvey, M. A. Strengths and limitations of model systems for the study of urinary tract infections and related pathologies. *Microbiology and Molecular Biology Reviews.* **80** (2), 351-367, (2016).
114 Carey, A. J. *et al.* Urinary tract infection of mice to model human disease: Practicalities, implications and limitations. *Crititical Reviews in Microbiology.* **42** (5), 780-799, (2016).
115 Contag, C. H. *et al.* Photonic detection of bacterial pathogens in living hosts. *Molecular Microbiology.* **18** (4), 593-603, (1995).
116 Contag, P. R., Olomu, I. N., Stevenson, D. K. & Contag, C. H. Bioluminescent indicators in living mammals. *Nature Medicine.* **4** (2), 245-247, (1998).
117 Doyle, T. C., Burns, S. M. & Contag, C. H. *In vivo* bioluminescence imaging for integrated studies of infection. *Cellular Microbiology.* **6** (4), 303-317, (2004).
118 Hutchens, M. & Luker, G. D. Applications of bioluminescence imaging to the study of infectious diseases. *Cellular Microbiology.* **9** (10), 2315-2322, (2007).
119 Avci, P. *et al. In-vivo* monitoring of infectious diseases in living animals using bioluminescence imaging. *Virulence.* **9** (1), 28-63, (2018).
120 Huang, Y. Y. *et al.* Antimicrobial photodynamic therapy mediated by methylene blue and potassium iodide to treat urinary tract infection in a female rat model. *Scientific Reports.* **8** (1), 7257, (2018).
121 Hannan, T. J. & Hunstad, D. A. A murine model for *E. coli* urinary tract infection. *Methods in Molecular Biology.* **1333** 83-100, (2016).
122 Hopkins, W. J., Gendron-Fitzpatrick, A., Balish, E. & Uehling, D. T. Time course and host responses to *Escherichia coli* urinary tract infection in genetically distinct mouse strains. *American Society for Microbiology.* **66** (6), 2798-1802, (1998).
123 Vanherp, L. *et al.* Sensitive bioluminescence imaging of fungal dissemination to the brain in mouse models of cryptococcosis. *Disease Models & Mechanisms.* 10.1242/dmm.039123, (2019).
124 Keyaerts, M., Caveliers, V. & Lahoutte, T. Bioluminescence imaging: looking beyond the light. *Trends in Molecular Medicine.* **18** (3), 164-172, (2012).
125 Marques, C. N., Salisbury, V. C., Greenman, J., Bowker, K. E. & Nelson, S. M. Discrepancy between viable counts and light output as viability measurements,

following ciprofloxacin challenge of self-bioluminescent *Pseudomonas aeruginosa* biofilms. *Journal of Antimicrobial Chemotherapy.* **56** (4), 665-671, (2005).

126 Vande Velde, G., Kucharikova, S., Van Dijck, P. & Himmelreich, U. Bioluminescence imaging increases in vivo screening efficiency for antifungal activity against device-associated *Candida albicans* biofilms. *International Journal of Antimicrobial Agents.* **52** (1), 42-51, (2018).

127 Oliver, J. D. Recent findings on the viable but nonculturable state in pathogenic bacteria. *FEMS Microbiology Reviews.* **34** (4), 415-425, (2010).

128 Kucharikova, S., Vande Velde, G., Himmelreich, U. & Van Dijck, P. *Candida albicans* biofilm development on medically-relevant foreign bodies in a mouse subcutaneous model followed by bioluminescence imaging. *Journal of Visualized Experiments.* 10.3791/52239 (95), 52239, (2015).

129 Vande Velde, G., Kucharikova, S., Schrevens, S., Himmelreich, U. & Van Dijck, P. Towards non-invasive monitoring of pathogen-host interactions during *Candida albicans* biofilm formation using *in vivo* bioluminescence. *Cellular Microbiology.* **16** (1), 115-130, (2014).

130 Säve, S. & Persson, K. Extracellular ATP and P2Y Receptor Activation Induce a Proinflammatory Host Response in the Human Urinary Tract. *Infection and Immunity.* **78** (8), 3609-3615, (2010).

131 Luyts, N. *et al.* Longitudinal Follow-Up of Urinary Tract Infections and Their Treatment in Mice using Bioluminescence Imaging. *Journal of Visualized Experiments.* 10.3791/62614 (172), e62614, (2021).

132 Kawasaki, T. & Kawai, T. Toll-Like Receptor Signaling Pathways. *Frontiers in Immunology.* **5**, (2014).

133 Christensen, M. G. *et al.* [Ca2+]i Oscillations and IL-6 Release Induced by α-Hemolysin from *Escherichia coli* Require P2 Receptor Activation in Renal Epithelia*. *Journal of Biological Chemistry.* **290** (23), 14776-14784, (2015).

134 Takahashi, A. *et al.* Production of β-defensin-2 by human colonic epithelial cells induced by Salmonella enteritidis flagella filament structural protein. *FEBS Letters.* **508** (3), 484-488, (2001).

135 Lusty, A., Kavaler, E., Zakariasen, K., Tolls, V. & Nickel, J. C. Treatment effectiveness in interstitial cystitis/bladder pain syndrome: Do patient perceptions align with efficacy-based guidelines? *Can Urol Assoc J.* **12** (1), E1-E5, (2018).

136 Davidov, M. I. *et al.* Phenazopyridine and fosfomycin for the acute cystitis treatment: results of multicenter randomized study. *Urologiia.* (3), 20-27, (2021).

137 Stewart, L. E., Siddique, M., Jacobs, K. M., Raker, C. A. & Sung, V. W. Oral Phenazopyridine vs Intravesical Lidocaine for Bladder OnabotulinumtoxinA Analgesia: A Randomized Controlled Trial (OPIL). *Am J Obstet Gynecol.* 10.1016/j.ajog.2022.05.025, (2022).

138 Johnson, W. J. & Chartrand, A. The metabolism and excretion of Phenazopyridine Hydrochloride in animals and man. *Toxicology and applied pharmacology.* **37** 371-376, (1976).

139 Zelenitsky, S. & Zhanel, G. Phenazopyridine in urinary tract infections. *The Annals of Pharmacotherapy.* **30** 866-868, (1996).

140 Amabile-Cuevas, C. F. & Arredondo-Garcia, J. L. Nitrofurantoin, phenazopyridine, and the superoxide-response regulon *soxRS* of *Escherichia coli*. *Journal of Infection and Chemotherapy.* **19** (6), 1135-1140, (2013).

141 Voets, T. *et al.* The principle of temperature-dependent gating in cold- and heat-sensitive TRP channels. *Nature.* **430** (7001), 748-754, (2004).
142 Voets, T., Owsianik, G., Janssens, A., Talavera, K. & Nilius, B. TRPM8 voltage sensor mutants reveal a mechanism for integrating thermal and chemical stimuli. *Nat Chem Biol.* **3** (3), 174-182, (2007).
143 Kobayashi, J. I. *et al.* Identification of N-acyl-N-indanyl-alpha-phenylglycinamides as selective TRPM8 antagonists designed to mitigate the risk of adverse effects. *Bioorganic & Medicinal Chemistry.* **30** 115903, (2021).
144 Aizawa, N. & Fujita, T. The TRPM8 channel as a potential therapeutic target for bladder hypersensitive disorders. *Journal of Smooth Muscle Research.* **58** (0), 11-21, (2022).
145 Paricio-Montesinos, R. *et al.* The Sensory Coding of Warm Perception. *Neuron.* **106** (5), 830-841.e833, (2020).
146 Winchester, W. J. *et al.* Inhibition of TRPM8 Channels Reduces Pain in the Cold Pressor Test in Humans. *Journal of Pharmacology and Experimental Therapeutics.* **351** (2), 259-269, (2014).
147 Weyer, A. D. & Lehto, S. G. Development of TRPM8 Antagonists to Treat Chronic Pain and Migraine. *Pharmaceuticals (Basel).* **10** (2), (2017).
148 Li, K. *et al.* Determination of Phenazopyridine in Human Plasma by GC--MS and its Pharmacokinetics. *Journal of chromatographic science.* **46** 686-689, (2008).
149 Aizawa, N. & Wyndaele, J. J. Effects of phenazopyridine on rat bladder primary afferent activity, and comparison with lidocaine and acetaminophen. *Neurourology and Urodynamics.* **29** (8), 1445-1450, (2010).
150 Preynat-Seauve, O. *et al.* Novel Mechanism for an Old Drug: Phenazopyridine is a Kinase Inhibitor Affecting Autophagy and Cellular Differentiation. *Frontiers in Pharmacology.* **12** 664608, (2021).
151 Liu, L., Yudin, Y. & Rohacs, T. PIP2 Depletion Contributes to Inhibition of TRPM8 Activity by GQ Protein Coupled Receptors. *Biophysical Journal.* **114** (3, Supplement 1), 642a-643a, (2018).
152 Liu, L. & Rohacs, T. Regulation of the cold-sensing TRPM8 channels by phosphoinositides and G(q)-coupled receptors. *Channels.* **14** (1), 79-86, (2020).
153 Liu, B. & Qin, F. Functional control of cold- and menthol-sensitive TRPM8 ion channels by phosphatidylinositol 4,5-bisphosphate. *Journal of Neuroscience.* **25** (7), 1674-1681, (2005).
154 Rovner, E. *et al.* Treatments used in women with interstitial cystitis: the intersitial cystatis data base (ICDB) study experience. . *Urology.* **56** 940-945, (2000).
155 Tauseef, M. *et al.* TLR4 activation of TRPC6-dependent calcium signaling mediates endotoxin-induced lung vascular permeability and inflammation. *J Exp Med.* **209** (11), 1953-1968, (2012).
156 Hopkins, W., Gendron-Fitzpatrick, A., McCarthy, D. O., Haine, J. E. & Uehling, D. T. Lipopolysaccharide-responder and nonresponder C3H mouse strains are equally susceptible to an induced Escherichia coli urinary tract infection. *Infection and Immunology.* **64** (4), 1369-1372, (1996).
157 Schaum, N. *et al.* Single-cell transcriptomics of 20 mouse organs creates a Tabula Muris. *Nature.* **562** (7727), 367-372, (2018).
158 Cottrell, G. S., Amadesi, S., Schmidlin, F. & Bunnett, N. Protease-activated receptor 2: activation, signalling and function. *Biochemal Society Transactions.* **31** (Pt 6), 1191-1197, (2003).

159 Hajna, Z. *et al.* Complex Regulatory Role of the TRPA1 Receptor in Acute and Chronic Airway Inflammation Mouse Models. *International Journal of Molecular Sciences.* **21** (11), (2020).
160 Ingersoll, M. A., Kline, K. A., Nielsen, H. V. & Hultgren, S. J. G-CSF induction early in uropathogenic Escherichia coli infection of the urinary tract modulates host immunity. *Cellullar Microbiology.* **10** (12), 2568-2578, (2008).
161 Duenas-Garcia, O. F. *et al.* The Effect of Oral Phenazopyridine on Perioperative Voiding After Midurethral Slings (EPIPhANy Study). *Female Pelvic Medicine & Reconstructive Surgery.* **24** (2), 95-99, (2018).
162 Sierra, T., Taylor, D. L., Leung, K., Hall, C. D. & Flynn, M. K. The Effect of Phenazopyridine on Immediate Postoperative Voiding After Prolapse Surgery: A Randomized Controlled Trial. *Female Pelvic Medicine & Reconstructive Surgery.* **27** (2), 85-89, (2021).
163 Lashinger, E. S. *et al.* AMTB, a TRPM8 channel blocker: evidence in rats for activity in overactive bladder and painful bladder syndrome. *American Journal of Physiology and Renal Physiology.* **295** (3), F803-810, (2008).
164 Du, S. *et al.* Differential expression profile of cold (TRPA1) and cool (TRPM8) receptors in human urogenital organs. *Urology.* **72** (2), 450-455, (2008).